

Echtzeitvisualisierung von Lawinenrisiko basierend auf einem großräumigen Geodatenatz

DIPLOMARBEIT

zur Erlangung des akademischen Grades

Diplom-Ingenieur

im Rahmen des Studiums

Visual Computing

eingereicht von

Johannes Eschner, BSc

Matrikelnummer 01633402

an der Fakultät für Informatik

der Technischen Universität Wien

Betreuung: Assistant Prof. Dr.in techn. Manuela Waldner

Mitwirkung: Dipl.-Ing. Adam Celarek, BSc

Wien, 4. Mai 2023

Johannes Eschner

Manuela Waldner



Die approbierte gedruckte Originalversion dieser Diplomarbeit ist an der TU Wien Bibliothek verfügbar
The approved original version of this thesis is available in print at TU Wien Bibliothek.



Real-Time Avalanche Risk Visualization on a Large-Scale Geospatial Dataset

DIPLOMA THESIS

submitted in partial fulfillment of the requirements for the degree of

Diplom-Ingenieur

in

Visual Computing

by

Johannes Eschner, BSc

Registration Number 01633402

to the Faculty of Informatics

at the TU Wien

Advisor: Assistant Prof. Dr.in techn. Manuela Waldner

Assistance: Dipl.-Ing. Adam Celarek, BSc

Vienna, 4th May, 2023

Johannes Eschner

Manuela Waldner



Die approbierte gedruckte Originalversion dieser Diplomarbeit ist an der TU Wien Bibliothek verfügbar
The approved original version of this thesis is available in print at TU Wien Bibliothek.

Erklärung zur Verfassung der Arbeit

Johannes Eschner, BSc

Hiermit erkläre ich, dass ich diese Arbeit selbständig verfasst habe, dass ich die verwendeten Quellen und Hilfsmittel vollständig angegeben habe und dass ich die Stellen der Arbeit – einschließlich Tabellen, Karten und Abbildungen –, die anderen Werken oder dem Internet im Wortlaut oder dem Sinn nach entnommen sind, auf jeden Fall unter Angabe der Quelle als Entlehnung kenntlich gemacht habe.

Wien, 4. Mai 2023

Johannes Eschner



Die approbierte gedruckte Originalversion dieser Diplomarbeit ist an der TU Wien Bibliothek verfügbar
The approved original version of this thesis is available in print at TU Wien Bibliothek.

Danksagung

Zuallererst möchte ich mich bei meiner Betreuerin Manuela Waldner und bei meinem Betreuer Adam Celarek bedanke, die mich während meiner Arbeit an diesem Projekt allgegenwärtig unterstützt haben. All die langen, spannenden Gespräche und Diskussionen, die sich nicht selten in lebhaftem Bericht über unsere eigenen Tourenerfahrungen verwandelten, haben meine Leidenschaft für dieses Projekt am Leben erhalten.

Weiters möchte ich mich auch bei meinen Kolleginnen und Kollegen vom Forschungsbereich Computergraphik bedanken, die mich herzlich in ihrem Umfeld aufgenommen haben und immer für meine Fragen zur Verfügung standen.

Ein besonderer Dank geht an Christoph Mitterer vom Lawinenwarndienst Tirol, der mir mit seinem Fachwissen den wichtigen Unterschied zwischen Lawinengefahr und Lawinenrisiko näher gebracht hat. Außerdem möchte ich mich bei Max Demmelbauer von der Toursprung GmbH bedanken, der nicht nur einen großen Beitrag zur Entwicklung des MapLibre Terrain Renderers geleistet hat, sondern mir auch geholfen hat, das Innenleben dieses Mapping Frameworks kennen zu lernen.

Ich möchte mich auch bei allen Teilnehmerinnen und Teilnehmern meiner User Study bedanken, die nicht nur ihre Zeit zur Verfügung gestellt haben, um meine Implementierung zu testen, sondern auch ihr Fachwissen über Tourenplanung mit mir geteilt haben und mir somit wertvolle Einblicke gewährten.

Schließlich möchte ich mich bei meiner Familie bedanken, die mich während meines gesamten Studiums unterstützte und es mir somit ermöglichte, dieses Vorhaben zu verfolgen.



Die approbierte gedruckte Originalversion dieser Diplomarbeit ist an der TU Wien Bibliothek verfügbar
The approved original version of this thesis is available in print at TU Wien Bibliothek.

Acknowledgements

First and foremost, I want to thank my supervisors Manuela Waldner and Adam Celarek for their ever-present support during my work on this project. All the long, intriguing talks and discussions that more often than not transformed into vivid recounts of our own touring experiences, kept my passion for this project going.

Furthermore, I also want to thank all my colleagues at the Research Unit of Computer Graphics, who warmly welcomed me into their environment and were always here to answer my questions.

Special thanks go out to Christoph Mitterer from the Avalanche Warning Service Tirol, who contributed his expertise, introducing me to the important differentiation between avalanche danger and avalanche risk. Additionally, I want to thank Max Demmelbauer from Toursprung GmbH, who is a MapLibre development hero and helped to get to know the inner workings of this mapping framework.

I also want to thank all the participants of my user study, who not only provided their time to test my implementation but also shared their expertise in tour planning, providing me with valuable insights.

Finally, I want to thank my family who supported me throughout my studies and therefore enabled me to pursue this endeavor.



Die approbierte gedruckte Originalversion dieser Diplomarbeit ist an der TU Wien Bibliothek verfügbar
The approved original version of this thesis is available in print at TU Wien Bibliothek.

Kurzfassung

In jeder Wintersaison sind Berichte über tödliche Lawinenunfälle in den Alpen Teil des Nachrichtenzyklus. Daten für die Tourenplanung mit Lawinenrisikobewertung stehen Freizeitsportlerinnen und Freizeitsportlern in Form von täglichen Lawinenlageberichten und Outdoor-Karten zur Verfügung. Diese Daten sind jedoch über verschiedene Quellen verteilt und müssen manuell integriert werden, um eine Risikobewertung für eine bestimmte Tour zu erstellen. Reduktionsmethoden bieten eine Hilfestellung für diesen Integrationsprozess und ermöglichen es Bergsteigerinnen und Bergsteigern, das Gesamtrisiko zu beurteilen und potenzielle Schlüsselstellen im Voraus zu bestimmen.

Wir stellen ein integriertes Risikovisualisierungstool zur Unterstützung einer risikoaversen Tourenplanung für Skitouren vor. Basierend auf einem hochauflösenden digitalen Höhenmodell zeigt unsere Visualisierung das Lawinenrisiko in Echtzeit auf einer webbasierten 2.5D-Kartenanwendung an. Verschiedene statische und dynamische Lawinenrisikolayer, die die alpinen Regionen Österreichs abdecken, werden auf der Grafikkarte ausgewertet und gerendert.

Durch die Implementierung einer Prototyp-Anwendung zeigen wir, dass mit Hilfe von existierenden Reduktionsmethoden das Höhenmodell und der Lawinenlagebericht für die Region Österreich in Echtzeit ausgewertet und dargestellt werden können. Diese Darstellung erlaubt es uns das lokale Lawinenrisiko großflächig zu visualisieren. Um unseren Visualisierungsprototyp zu evaluieren, führten wir eine Pilot User Study durch. Die Ergebnisse dieser Studie zeigen, dass das Vertrauen der Benutzer in eine integrierte Risikovisualisierung gering ist, wenn sie mit der zugrunde liegenden Risikoreduktionsmethode nicht vertraut sind. Die Ergebnisse zeigen jedoch auch, dass die Kombination einer 2.5D-Karte mit unserem integrierten Risikolayer die Identifizierung potenziell risikoreicher Stellen erleichtert. Wir kommen zu dem Schluss, dass unsere Arbeit eine wertvolle Grundlage für eine integrierte Lawinenrisikovisualisierung darstellt, jedoch noch weitere Validierungsschritte notwendig sind.



Die approbierte gedruckte Originalversion dieser Diplomarbeit ist an der TU Wien Bibliothek verfügbar
The approved original version of this thesis is available in print at TU Wien Bibliothek.

Abstract

Every winter season reports of fatal avalanche accidents in the Alps are part of the news cycle. Data for tour planning with avalanche risk evaluation is available to recreationists in the form of daily avalanche reports and outdoor maps. These data are, however, distributed across different sources and have to be manually integrated by the end user to arrive at a risk value for a given tour. Risk reduction methods provide a framework for this integration process and thereby allow mountaineers to judge the overall risk and determine potential high-risk areas beforehand.

We present an integrated risk visualization tool to support risk-averse tour planning for backcountry skiing. Based on a high-resolution Digital Elevation Model (DEM), our visualization displays avalanche risk levels in real-time as a web-based 2.5D map application. Different static and dynamic avalanche risk layers are rendered on the Graphics Processing Unit (GPU) covering the alpine regions of Austria.

By implementing a prototype application, we show that reduction methods can be evaluated in real-time based on existing data sources consisting of a Digital Elevation Model (DEM) and the per-region avalanche report for Austria. This evaluation allows us to visualize localized avalanche risk for a large area. To evaluate our prototype visualization, we conducted a pilot user study. The results of the study show that users have low trust in an integrated risk visualization when they are not familiar with the underlying risk reduction method. However, results also indicate that the combination of a 2.5D map with our integrated risk layer facilitates the identification of potential high-risk areas. We conclude that our work provides a foundation for an integrated risk avalanche risk visualization, however, further validation steps are still necessary.



Die approbierte gedruckte Originalversion dieser Diplomarbeit ist an der TU Wien Bibliothek verfügbar
The approved original version of this thesis is available in print at TU Wien Bibliothek.

Contents

Kurzfassung	xi
Abstract	xiii
Contents	xv
1 Introduction	1
1.1 Motivation and Problem Statement	1
1.2 Aim of the Work	2
1.3 Contribution	3
1.4 Outline	3
2 Background	5
2.1 Avalanche Reports	5
2.2 Reduction Methods	11
2.3 Terrain Rendering	15
2.4 Visualization on 2.5D Terrain	20
3 Related Work	27
3.1 Avalanche Risk Visualization	27
3.2 Risk Visualization and Navigation on 2.5D Maps	33
4 Overview	35
4.1 Requirements	35
4.2 Frameworks for Real-Time Terrain Rendering on the Web	37
4.3 Software Components	38
5 Visualization and Interaction Design	39
5.1 Avalanche Risk Overlays	39
5.2 User Interface	51
6 Implementation	55
6.1 Static Data Preprocessing	55
6.2 Dynamic Data Preprocessing	57
	xv

6.3	Extending the MapLibre Framework with a Custom Shader Pipeline	60
6.4	User Interface and Interaction	63
6.5	Performance	65
7	Pilot User Study	67
7.1	Hypotheses	67
7.2	Tasks	68
7.3	Design	68
7.4	Procedure and Apparatus	69
7.5	Recruiting	71
7.6	Results	71
7.7	Discussion	79
8	Conclusion	81
8.1	Conclusion	81
8.2	Limitations	82
8.3	Future Work	82
	List of Figures	87
	List of Tables	91
	List of Algorithms	93
	List of Listings	95
	Bibliography	97
	Appendix A: Study Materials	103
	Interview Questionnaires	103
	Application Overview	103
	Task Descriptions	103
	Appendix B: Coded Interviews	109
	Interview I: Tour Planning	109
	Interview II: Qualitative Feedback	109

Introduction

1.1 Motivation and Problem Statement

Over the last 70 years, on average, there have been 30 avalanche fatalities per year in Austria, with about 75% of them occurring in backcountry avalanches (also known as *tourist avalanches*) [Hö17]. A study on human-triggered avalanches by Schweizer and Lütschg [SL01] showed that in Switzerland 90% of tourist avalanche fatalities happened in avalanches triggered by recreationists. Although information on the avalanche risk in the Austrian Alps is publicly available, this information is scattered over multiple different sources. Consolidated wide area avalanche danger forecasts are available in the European Avalanche Danger Scale (EADS) format. To compute the on-site risk for a given tour, two additional information sources have to be taken into account: Firstly, the risk is strongly influenced by *terrain features* such as elevation, exposition, slope steepness, and ground cover. Secondly, to arrive at a comprehensive risk rating, additional data on *local features* such as the presence of tracks or wind-drifted snow have to be incorporated into the risk evaluation.

So-called risk reduction methods have been introduced to assist recreationists in their tour planning process. These methods provide simple, concise heuristics for combining the avalanche danger with the terrain features, while additionally offering guidelines for performing the on-site checks. The heuristics used in risk reduction methods can be executed algorithmically and presented visually to users. A risk visualization that combines the avalanche danger rating with terrain features can therefore reduce the users' workload in the risk assessment process, allowing them to concentrate on the on-site checks for which no algorithmic implementation is available. Ideally, the risk visualization either clearly shows whether the tour is safe or not, or guides user attention toward critical areas where further on-site checks are necessary.

Although, with Skitouren guru [Sch22], there exists a service that integrates the available data to compute the risk along pre-defined tours, there is no such service that provides

an integrated risk evaluation for the whole terrain. The large-scale terrain-based risk evaluation is made possible by the availability of high-resolution terrain data in the form of a Digital Elevation Model (DEM) with a resolution of $1\text{ m} \times 1\text{ m}$ that covers Austria. Visualizing the integrated avalanche risk on the whole terrain has two benefits: (i) it allows users to get a better understanding of where the risk comes from and (ii) it does not restrict them to pre-defined tours. While other risk visualizations mostly utilize 2D map representation, having access to a DEM allows for a 3D representation of the terrain itself. Presenting steep, alpine terrain in 3D can potentially help users to better match the map representation with the real terrain, supporting the recognition of critical areas on-site. Finally, an integrated avalanche risk visualization should be interactive, allowing users to view the situation on different days and from different perspectives.

1.2 Aim of the Work

The goal of this master thesis is to build a web-based prototype visualization and preliminarily evaluate whether it facilitates the identification of potential risk areas compared to a traditional tour planning approach, where users consult maps and avalanche reports independently from each other. The two main data sources which we combine for the prototype visualization are: (i) the EADS avalanche forecasts and (ii) a high-resolution DEM of the alpine regions of Austria.

To build an integrated interactive risk visualization we aim to show that the heuristics used by reduction methods can be implemented algorithmically to computationally evaluate and visualize the risk in real-time. A fundamental aim is to design a visualization that facilitates the recognizability of critical areas on the terrain. To this extent, our application will render the terrain in a 3D representation, including small-scale features such as trees. Based on this terrain representation, it is our goal to find and evaluate visual risk encodings that convey the avalanche risk in an understandable and meaningful way to potential users.

Using the integrated risk visualization users should have the ability to judge the overall risk at a glance as well as recognize critical areas at a detail level. Ultimately, we aim to reduce the cognitive load of integrating multiple information sources for risk evaluation, allowing the users to focus on the on-site evaluation of critical areas along their tour.

In summary, the aim of this work is to answer the following research questions:

RQ1: How can we evaluate reduction methods in real-time to determine localized avalanche risk on a terrain model?

RQ2: How can we visually encode the avalanche risk on a 3D terrain visualization to guide attention toward the high-risk areas?

1.3 Contribution

The main contribution of this thesis is that, by implementing our prototype visualization, we show that it is possible to do a real-time reduction method evaluation of the current avalanche report on a DEM. We present a comprehensive pipeline for collecting, parsing, and visualizing avalanche risk data based solely on well-accepted reduction methods and without manual intervention. Our method processes and visualizes the data on demand on the Graphics Processing Unit (GPU) without the need for computationally expensive pre-processing.

As a second contribution, we show that such a real-time avalanche risk visualization has the potential to improve users' risk assessment abilities during tour planning. We do this by conducting a pilot user study in which we let our target audience perform tour planning tasks with our prototype implementation as well as a 2D slope map in combination with an avalanche report as a baseline. Results from the pilot user study show that performance for overview tasks was better using the 2D slope map, however in a more detailed risk area identification task, results were better when users used our visualization. Through qualitative user feedback, we also found that user trust in our visualization was low, indicating that integrating well-accepted methods is not sufficient for building trust in a risk visualization.

1.4 Outline

This thesis is structured as follows: Chapter 2 provides an overview of the background of this thesis. This includes an introduction to avalanche danger and avalanche risk, the structure of avalanche reports, and reduction methods for determining the avalanche risk. Furthermore, we also provide technical details on real-time terrain rendering methods, such as tile pyramids, and formats such as GeoJSON which we utilize in the implementation. In the final background section, visualization methods for map-based data visualization are presented. In Chapter 3, we present related work in the field. Here, we look at current approaches to avalanche risk visualization, covering both static and dynamic methods. Additionally, we also summarize previous work on risk visualization and navigation on 2.5D maps outside of the avalanche context.

In Chapter 4 we provide an overview of our prototype implementation by first gathering requirements and presenting state-of-the-art frameworks for web-based real-time terrain rendering. This is followed by a look into the necessary software components that make up the application. We then formulate a design concept for our avalanche risk visualization in Chapter 5. Based on this design the implementation of our prototype application is then described in Chapter 6, where pre-processing, rendering, and user interaction are explained. In Chapter 7 we present the pilot user study which we conducted for evaluating our prototype evaluation. We provide insights into the study outcome and discuss possible implications of the presented implementation. Chapter 8 concludes the thesis by discussing limitations and providing possibilities for future work.



Die approbierte gedruckte Originalversion dieser Diplomarbeit ist an der TU Wien Bibliothek verfügbar
The approved original version of this thesis is available in print at TU Wien Bibliothek.

Background

This chapter serves as an introduction to some of the background necessary to understand the design decisions that were made in developing our avalanche risk visualization. First, an insight into the current status of avalanche reports is given. This is followed by a presentation of risk reduction methods for tour planning. Then we look at terrain rendering with a special focus on real-time applications that are web-based. Finally, a brief introduction to visualization techniques on 2.5D terrain models is given.

2.1 Avalanche Reports

Avalanche reports (or avalanche bulletins) are the main tool used to communicate the current avalanche situation to recreationists such as backcountry skiers. Although avalanche reports mostly follow international standards, we focus on the format used by the Austrian Avalanche Warning Service. As the prototype we built is limited to the Austrian Alps, this constraint does not impact the applicability of our implementation.

2.1.1 Avalanche Danger vs. Avalanche Risk

In general, the hazard posed by avalanches can be broken down into two parts. The first part, *avalanche danger*, refers to the dynamic conditions or processes which can result in an avalanche event. Avalanche danger is therefore influenced by dynamic, often weather-related, so-called danger patterns (e.g., new snow). The five typical avalanche problems as defined in the glossary of the European Avalanche Warning Services (EAWS) [Ser23a] are the following:

- **New Snow:** Recently fallen snow can cause avalanche activity through additional loading on the existing snowpack or a lack of cohesion in the newly fallen snow.

- **Wind Slab:** Wind transported snow which is typically packed on the leeward side into wind-sheltered locations.
- **Persistent Weak Layers:** Weak layers buried in the old snowpack, which can persist for weeks to months.
- **Gliding Snow:** The entire snowpack glides on the ground, which often occurs in the presence of meltwater or rain.
- **Wet Snow:** The snowpack is infiltrated by water, which weakens the snowpack.

Based on the snowpack condition given by the avalanche problems and the general avalanche situation, the avalanche danger is described with the five-part European Avalanche Danger Scale (EADS) as follows:

- 1 - Low
- 2 - Moderate
- 3 - Considerable
- 4 - High
- 5 - Very high

The five levels of the scale are commonly color encoded in a discrete scale ranging from green (for low) to dark red (for very high). The exact hues do, however, vary for different avalanche reports and are also sometimes accompanied by glyphs, as can be seen in Figure 2.1. The report in Figure 2.2, for example, uses slightly different hues and substitutes the dark red with black. The red-green color scale does not provide great accessibility as persons with a color vision deficiency might have problems distinguishing different levels based on the color. The danger level is provided for regions with an area $>100 \text{ km}^2$ and does therefore not represent the conditions on a specific slope [Ser23a].



Figure 2.1: Glyphs with a typical color scheme for encoding avalanche danger levels. Note that level 5 uses a checkerboard pattern instead of dark red. Images from [Ser23a].

The second part of avalanche hazard is the *avalanche risk*. Avalanche risk refers to the static likelihood of occurrence as a combination of mathematical probability, risk exposure, and possible damages. The avalanche report with a given danger level, therefore, factors into the avalanche risk as the mathematical probability of avalanche release [Ser23a].

As our visualization approach augments the danger rating of the avalanche report with additional data through a reduction method (see Section 2.2), we display the avalanche risk as opposed to the avalanche danger provided by the report.

2.1.2 Standardized Avalanche Reports

Avalanche reports in Austria are published daily during the winter season. Starting with the winter season 2020/2021 the reports are published in a standardized format [SNS⁺20]. As these reports form the baseline for current tour planning methods against which we compare our visualization, we will now break down how such a report is constructed. Each state of Austria (with the exception of Vienna and Burgenland) has its own avalanche warning service providing the reports through its website. Avalanche reports are published in the afternoon for the following day, and in case there is an update an amended version may be published after that.

For each state, the report is subdivided into regions. Inside a region, an EADS danger rating is provided consisting of either one or two danger levels. In case two danger levels are present, the danger rating is divided into two elevation ranges to discern different avalanche danger levels based on elevation. The elevation at which the danger level changes is either indicated by an explicit elevation value in meters or by referencing the forest line. In addition to the danger level, the report also contains information on avalanche problems present in the region. Here, for each problem, the affected expositions are pointed out in the report by listing the orientations where the problem is present. Next to these standardized overview indicators, a textual description of the situation is added which contains additional information on factors such as the weather and critical terrain features.

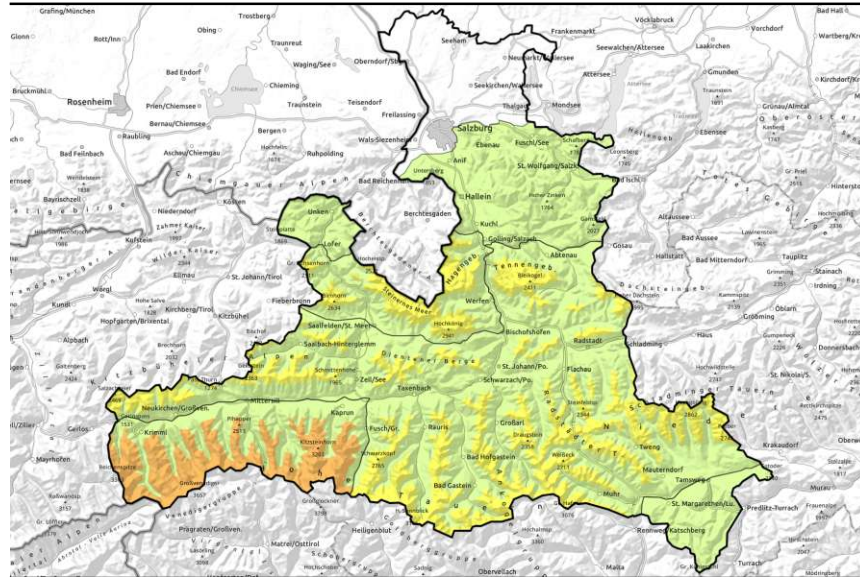
To exemplify how the information is typically displayed in an avalanche report, we will now look at a published report in more detail. The example report depicts the avalanche situation in the state of Salzburg on December 25th 2022. Figure 2.2 shows an overview of the situation in the whole state on the date given. Underneath a map showing all regions of the state, the danger levels as well as the border height between danger levels, if applicable, are given for each region. In addition, next to each region pictograms displaying avalanche problems (see Section 2.1.1) are added. Each pictogram is accompanied by a wind rose indicating the favorable (white) and unfavorable (black) expositions. In this context, an unfavorable exposition implies that the accompanying avalanche problem applies.

More detailed information is then available for each region on a separate page. Figure 2.3 shows an example of such a detailed region view. Apart from a more in-depth explanation of the avalanche problems present next to the map, the main information content consists of text detailing the report. This includes information on the snowpack structure as well as a weather report. The textual information is less structured than the strictly classified danger levels and avalanche problems but adds an option to highlight noteworthy additional information and explanations on how the report came to be.

2. BACKGROUND

published at 24.12.2022, 18:00 h by Matthias Walcher

Avalanche report for Sunday, 25.12.2022



Considerable avalanche danger regionally

	2300 m	Großenedigergruppe Alpenhauptkamm, Glocknergruppe Alpenhauptkamm, Großenedigergruppe Nord, Glocknergruppe Nord		
	2300 m	Kitzbüheler Alpen, Glemmtal, Dientner Grasberge, Pongauer Grasberge, Oberpinzgauer Grasberge, Goldberggruppe Nord, Niedere Tauern Nord, Niedere Tauern Alpenhauptkamm, Niedere Tauern Süd, Ankogelgruppe, Muhr, Goldberggruppe Alpenhauptkamm, Tennengebirge, Gosaukamm		
	2300 m	Steinernes Meer, Hochkönig, Hagengebirge, Göllstock, Loferer und Leoganger Steinberge		
		Nockberge		
		Osterhorngruppe, Gamsfeldgruppe, Untersbergstock, Chiemgauer Alpen, Heutal, Reiteralpe		

Avalanche problems



Danger ratings



Expositions



Figure 2.2: Overview of the avalanche report for the state Salzburg for December 25th 2022 [Wal22].

published at 24.12.2022, 18:00 h by Matthias Walcher

Avalanche report for Sunday, 25.12.2022

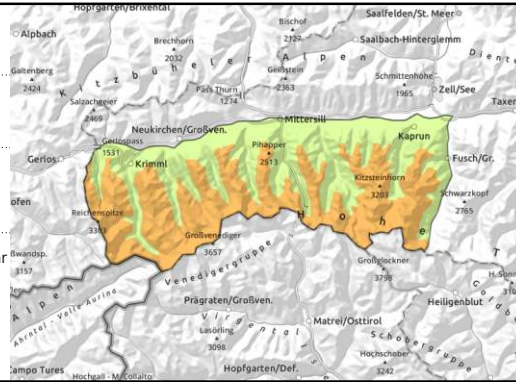


**Großenedigergruppe Alpenhauptkamm,
Glocknergruppe Alpenhauptkamm,
Großenedigergruppe Nord, Glocknergruppe Nord**



unfavourable layering in high alpine regions: faceted, soft layers in the fundament

in gullies and steep bowls, near to and distant from ridgelines



Persistent weak layer in high alpine regions

Avalanche danger above 2300 m is CONSIDERABLE, below that altitude danger is LOW. Weak layers inside the old snowpack can on shady slopes above approximately 2300 m still be triggered, particularly on wind-protected slopes at the foot of rock walls or behind abrupt discontinuities in the terrain. Avalanches can attain medium size. In addition, fresh snowdrift accumulations are prone to triggering, particularly on steep (>30°) N/E facing slopes above 2200 m. Danger zones occur behind abrupt discontinuities in the terrain, in gullies and bowls, the size and trigger-sensitivity increasing with ascending altitude. Fractures down to deeper layers is possible. Small glide-snow avalanches are still possible.

Reports from the relevant regions with regard to the persistent weak layer are few and far between currently (due to the snow situation); for that reason, these estimates are uncertain.

Snowpack structure

There has been 10-15 cm of fresh snow registered, amid strong-to-stormy winds which transported the snow in highly irregular fashion. The snowdrifts were deposited in gullies and bowls; the crests and ridges are snowblown bare. The snowdrifts lie particularly atop soft layers, on shady slopes at high altitudes. On high-alpine north-facing slopes the layer above 2300 m is often unfavourable due to a sequence of melt-freeze crusts and faceted crystals. This applies particularly to wind-protected slopes.

Below 2300 m the precipitation often fell as rain, which is leading to increasingly frequent wet-snow and glide-snow avalanches. Due to the dropping temperature on Saturday, the snowpack has stabilised. On Sunday it will be quite mild, the zero-degree level will ascend to above 3000 m. Thereby the snowdrifts will rapidly consolidate. Below 1800 m there is little snow on the ground.

Weather

Sunday: On Christmas Day, very fine weather with lots of sunshine. Residual cloud and fogbanks will recede, visibility will be unhindered. Winds will be light. It will be very mild. At 2000 m: 2-7 degrees; at 3000 m at midday, 0 degrees.

Monday: Above the layers of fog, visibility on Boxing Day will be very good, only some cirrus clouds far above summit level. Winds will be mostly light except on the Main Tauern Ridge (30-40 km/hr) from the south. Still mild: at 2000 m at midday 4 degrees, at 3000 m 0 degrees.

Avalanche problems



Danger ratings



Expositions



Figure 2.3: Detail view of a single region from the avalanche report for the state of Salzburg for December 25th 2022 [Wal22].

2. BACKGROUND

Next to the human-readable report file, avalanche reports are also published as XML files. These utilize the standardized Canadian Avalanche Association Markup Language (CAAML) profile ‘EAWS Bulletin’, which was established to facilitate information exchange within the EAWS [HHNG20].

```
1 <observations>
2   <Bulletin>
3     <metaDataProperty>
4     </metaDataProperty>
5     <validTime>
6     </validTime>
7     <bulletinResultsOf>
8       <BulletinMeasurements>
9         <dangerRatings>
10          <DangerRating>
11            <validElevation xlink:href="ElevationRange_2300Hi"/>
12            <mainValue>3</mainValue>
13          </DangerRating>
14          <DangerRating>
15            <validElevation xlink:href="ElevationRange_2300Lo"/>
16            <mainValue>1</mainValue>
17          </DangerRating>
18        </dangerRatings>
19        <avProblems>
20          <AvProblem>
21            <type>old snow</type>
22            <validAspect xlink:href="AspectRange_N"/>
23            <validAspect xlink:href="AspectRange_NE"/>
24            <validAspect xlink:href="AspectRange_NW"/>
25          </AvProblem>
26          <AvProblem>
27            <type>drifting snow</type>
28            <validAspect xlink:href="AspectRange_N"/>
29            <validAspect xlink:href="AspectRange_NE"/>
30            <validAspect xlink:href="AspectRange_E"/>
31          </AvProblem>
32        </avProblems>
33        [...]
34      </BulletinMeasurements>
35    </bulletinResultsOf>
36    <locRef xlink:href="AT-05-07"/>
37    <locRef xlink:href="AT-05-06"/>
38    <locRef xlink:href="AT-05-11"/>
39    <locRef xlink:href="AT-05-10"/>
40  </Bulletin>
41  [...]
42 </observations>
```

Listing 2.1: Shortened example CAAML file which contains the avalanche report for the state of Salzburg for December 25th 2022 [Wal22].

A CAAML file, (an example of which can be seen in Listing 2.1) is published per state and contains information on the avalanche situation for regions within that state. The top-level

structure is a collection of observations where each sub-element is of type `<Bulletin>`. The publishing date of the `<Bulletin>`, as well as the issuing authority, are noted in the `<metaDataProperty>`, and the time range for which the reported data is valid is given in the `<validTime>` property. One `<Bulletin>` represents an area of one or more regions, as given by the corresponding `<locRef>` elements. Regions are encoded in an ISO 3166-2 [ISO20] compliant code. For example, the region AT-05-07 is the region 07, in the state of Salzburg (05) in Austria (AT). In the context of our implementation, the main interest in each `<Bulletin>` entry lies in the `<BulletinMeasurements>`, which contains the avalanche danger information (see Section 2.1.1). In case there are different danger ratings depending on the elevation, multiple danger ratings are provided, each with an accompanying elevation range. Apart from the danger rating, information on avalanche problems, including the affected range of expositions, is also given. More details on how we parse and utilize the data from the avalanche report can be found in Section 6.2.

2.2 Reduction Methods

In the context of our visualization, the interaction between avalanche danger ratings and terrain features is especially interesting as it can be used to compute the avalanche risk. Reduction methods are frameworks developed with the intention to help recreationists make better-informed decisions in avalanche terrain [MH04]. Multiple such decision frameworks have been introduced beginning in the 1990s. In very general terms, reduction methods combine environmental factors such as the avalanche danger rating from the avalanche report with terrain features, such as slope steepness. They also provide guidelines for behavior on site. The combination of terrain features with the avalanche report is based on heuristics which essentially form a simple algorithm to determine the avalanche risk. We, therefore, choose two reduction methods, the *SnowCard* [EM01] and the *Stop-or-Go* method [Lar99] which we algorithmically implement in our visualization, forming the core of our risk computation. The decision to implement these two methods is based on the fact that they are the officially recommended methods by the German and Austrian Alpine Associations, respectively.

2.2.1 Elementary Reduction Method and Professional Reduction Method

The Elementary Reduction Method (ERM) and the Professional Reduction Method (PRM) were developed by Werner Munter [Mun97] [Mun01] and represent the first formalization of risk reduction methods. For the ERM, each level of the avalanche danger rating is paired up with a maximum slope steepness. These paired-up values are the basis for deciding which tours are deemed acceptable. Table 2.1 shows which factor combinations are acceptable under the ERM. Higher danger ratings also lead to larger areas of influence. This means that for a danger rating at level 2, only the immediate surroundings have to be taken into account to determine the maximum slope steepness.

Conversely, when the rating is at level 4, the whole slope has to have a steepness below the maximum of 40°. For favorable expositions the ERM allows the avalanche rating to be lowered by one level, effectively increasing the steepness limit.

Avalanche Danger Rating	Slope Steepness
2	<40°
3	<35°
4	<30°

Table 2.1: Acceptable combinations of danger rating and slope steepness for the ERM [Mun01].

In the PRM, the simple rules of the ERM are replaced by a risk factor calculation that is computed using the following equation:

$$\text{residual risk} = \frac{\text{danger potential}}{\text{reduction factor} \times \text{reduction factor}} \leq 1. \quad (2.1)$$

Here, the danger potential is determined through an exponential function based on the avalanche danger rating. A danger rating of 2 equates to a danger potential of 2 and with each step in the danger rating the danger potential doubles leading to a danger potential of 8 for level 4. So-called reduction factors are then applied to reduce the risk posed by the danger potential. Reduction factors are categorized into three classes. First-class reduction factors limit the slope steepness. The lower the slope steepness is, the larger the reduction factor becomes. Limiting the tour to slopes no steeper than 30°, for example, results in a reduction factor of 4. Second-class reduction factors limit the expositions in which the tour can lie, whereas third-class reduction factors limit the group size. Smaller groups and safety distances result in higher reduction factors. Each reduction factor is represented by an integer value and multiple factors can be combined to reduce the residual risk by division. If the residual risk is less than or equal to one, the tour is deemed acceptable [Mun01]. While the ERM forms the basis of other reduction methods, both it and the PRM have been superseded by widely recommended methods such as the SnowCard or Stop-or-Go. Therefore, the ERM and the PRM are not part of our implementation.

2.2.2 SnowCard

The SnowCard was introduced by Engler and Mersch [EM01] in the year 2000. For this method the avalanche danger rating, the slope steepness, and the exposition are combined to compute a risk factor. Similar to the ERM the area of influence for the slope steepness is coupled with the danger rating. At danger level 2 only the perimeter of the track (20 m - 40 m) counts to the steepness while at level 3 the whole slope has to be considered. At level 4 the area of influence expands to the whole hollow. In contrast to the ERM, the SnowCard explicitly differentiates between favorable and unfavorable

expositions by providing two different mappings between slope steepness and danger rating depending on the exposition.

Instead of a numerical value, the risk factor in the SnowCard is encoded graphically using a color gradient. This color gradient ranges from green for generally safe slopes to red for high-risk areas. Between the two extremes, there is a gradual transition to a yellow area, where cautionary measures should be applied. These measures include keeping safety distances while ascending as well as descending slopes individually. The boundaries between the different risk indications are based on Munter's basic reduction method, the personal experience of the developers, and a limited statistical analysis of recorded avalanche incidents [MH04]. According to its developers, the SnowCard should encourage novice backcountry skiers, who were previously discouraged by complicated rules, to perform a proper risk assessment [Eng01].

The SnowCard method is distributed as a physical representation which consists of a single portable card with two graphical representations of avalanche risk in a lenticular print setup. The two multicolored graphics show the avalanche risk depending on the avalanche danger rating and the slope steepness in degrees. One representation depicts the risk for favorable expositions while the other shows the risk for unfavorable conditions. Both representations and the legend for the risk encoding can be seen in Figure 2.4.

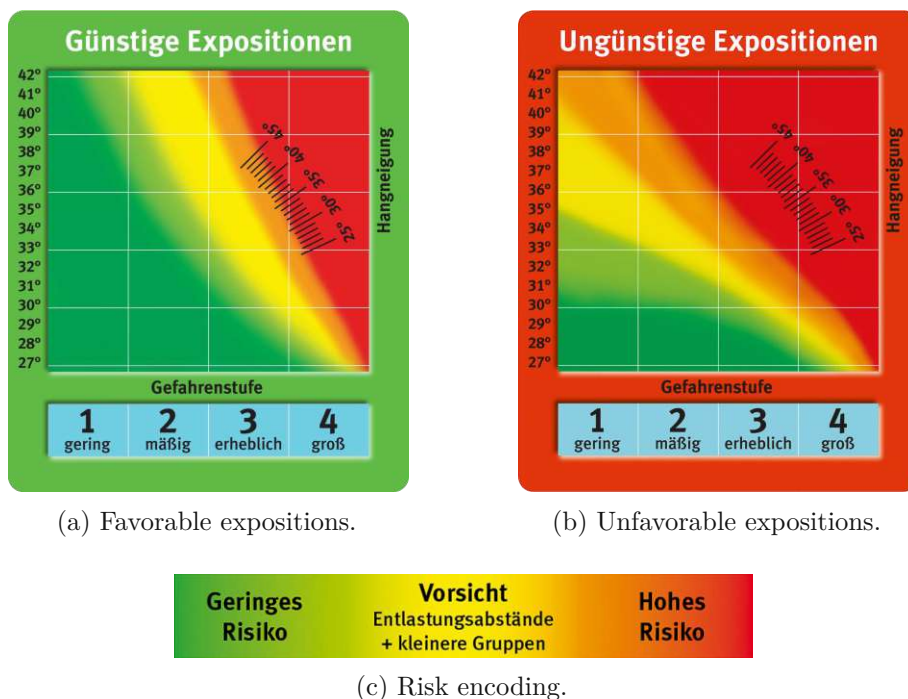


Figure 2.4: Both versions of the SnowCard for different expositions (a) and (b). Legend for the risk encoding (c). Risk values range from “low risk” to “caution” to “high risk”. Images taken from Deutscher Alpenverein [Deu23].

2.2.3 Stop-or-Go

The second standard risk reduction method we choose to implement into our risk visualization is the Stop-or-Go method, which was introduced by Larcher [Lar99] in 1999. In contrast to the SnowCard, this is a decision framework to reach a binary decision: a tour is either “Stop” or “Go” based on a number of conditions that have to be evaluated, both before and after arriving on site. One of the main motivations behind the development of Stop-or-Go was to provide a more accessible decision framework that alleviates the need for calculations as present in PRM and therefore potentially is appealing to a broader audience [Lar99].

Similar to the SnowCard, Stop-or-Go bases its initial decision criteria on the avalanche danger rating in combination with slope steepness. For the terrain-based “Check 1”, Stop-or-Go directly implements the ERM by Munter [MLW22] (albeit extended to the five level EADS scale): If the danger rating is 1, any slope is considered a “Go”. For level 2, slopes above 40° within the area of the track are a “Stop” criterion. For level 3 the cutoff is lowered to 35° and the whole slope has to be taken into consideration. At level 4 the steepness cutoff is at 30°, which concerns the whole hollow. At level 5 tours should generally not be attempted. For slopes in favorable expositions, the danger rating can be lowered by one level. As with the SnowCard, the Stop-or-Go checks are made available as a portable card, a depiction of which can be seen in Figure 2.5.



Figure 2.5: Portable Stop-or-Go card published by Österreichischer Alpenverein [Ö23].

Next to the terrain-based criteria, the Stop-or-Go method also includes an array of on-site factors, which in some circumstances can overrule a terrain-based “Stop” decision in the “Check 1” step. Examples of such factors are a large number of tracks on the slope or

forest areas. Our visualization is primarily concerned with off-site planning and therefore omits these factors for the risk evaluation. However, by identifying critical areas within the terrain model, we aim to facilitate “Check 2” by guiding user attention toward these areas (see also Section 4.1).

2.2.4 Evaluation of Reduction Methods

The viability of utilizing the presented risk reduction methods for preventing avalanche accidents is supported by multiple statistical analyses. McCammon and Hägeli [MH04] compare different decision frameworks by analyzing historical avalanche accident data from the United States. They come to the conclusion that simpler methods are apparently superior to more complex decision methods. Furthermore, they find that the training level of the affected person has no significant impact on the validity of a given decision framework. According to their analysis, all methods perform best when the danger levels are considerable to high, with severely limited effectiveness when the avalanche danger level is low. McCammon and Hägeli also point out that most avalanche accidents in the US happen when the hazard is readily apparent in the avalanche report. Based on this finding they suggest that it is sufficient for decision frameworks to cover these cases in order to prevent the majority of avalanche accidents.

Mersch and Behr [MB21] analyze the effectiveness of the SnowCard based on historic accident data spanning seven winters with a total of 231 fatalities. In their classification, they consider an accident preventable if the conditions lie within the red or orange areas of the SnowCard. Using this metric they conclude that 85% of all fatalities could have been prevented if the SnowCard had been applied as a decision basis. Similar to the conclusion by McCammon and Hägeli they find that for the lower danger level of 2 (which was the case for 30% of all fatalities), the percentage of preventable accidents drops to 59%. If the SnowCard were to be applied in a more conservative manner, i.e. completely abstaining from tours in conditions that are not marked in green, the percentage of theoretically preventable fatalities would rise to 96%.

2.3 Terrain Rendering

Real-time terrain rendering is used in 3D applications ranging from games and simulators to geoinformation systems and digital twins. In all these applications, both interactivity and highly detailed representations are generally desired. In this section, we discuss the technical background of real-time terrain visualization with a focus on the data sources and data structures involved.

2.3.1 Simple Data Structures

A common basis for a terrain model is a *height map*, which encodes an elevation value for each ground point. Height maps can be stored in a greyscale image, where the pixel

intensity encodes the elevation at that location [CR11]. An example of such a height map representation can be seen in Figure 2.6.

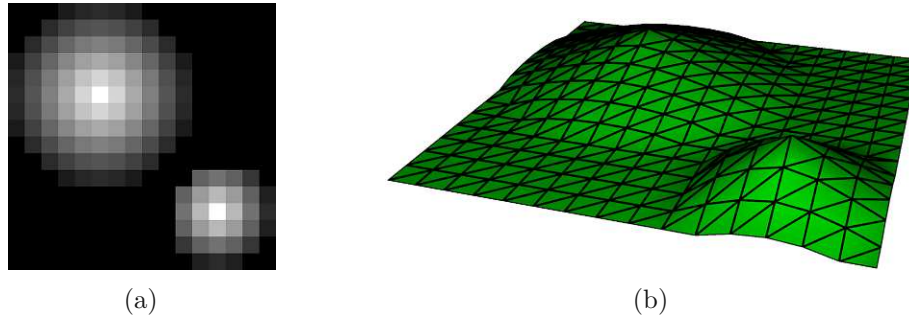


Figure 2.6: (a) A raster image with a resolution of 16×16 pixels with the height encoded in the pixel intensity. (b) The resulting terrain mesh. Images from [CR11].

The surface described by a height map can be represented as a set of points $(x \ y \ z)$ with

$$z = f(x, y). \quad (2.2)$$

As the function f maps the domain $D \subset \mathbb{R}^2$ to one real value, it is not possible to represent an actual 3D terrain using a height map [Pfe02]. Terrain features such as overhangs and caves cannot be reconstructed from a height map. While vertical cliffs can be approximated by increasing the resolution of the height map, fully vertical surfaces cannot be represented. For this reason, this type of terrain representation is also known as 2.5D. Due to its simplicity, in combination with the fact that on a large scale, real-world terrains behave like the 2.5D case [PEH20], this approach is most widely used in terrain rendering. Another advantage of the 2.5D approach is that multiple scales can be represented by an image pyramid of scaled height maps. A more detailed description of this data structure can be found in Section 2.3.2.

Restricting the terrain representation to 2.5D also makes data capture of terrains easier as it is sufficient to record a single height value for every location. Height maps from real-world terrains are commonly generated through photogrammetry methods, such as laser scanning using Light Detection And Ranging (LIDAR) [Pfe02]. Such height maps are generally referred to as Digital Elevation Model (DEM). Specifically, there are two kinds of DEMs: a Digital Surface Model (DSM) is a digital representation of a real world surface including surface features such as foliage and man-made objects. A Digital Terrain Model (DTM), in contrast, only contains the terrain surface at ground level [Hir15] [Pfe02].

Constructing a mesh from a DEM is a straightforward process. For each pixel in the raster image, a vertex is created at the pixel center. The resulting vertices are then connected to form triangles. For a raster image with a resolution of $x \times y$ pixels, this results in $x \times y$ vertices and $2(x-1)(y-1)$ triangles. A visualization of the mesh creation process can be seen in Figure 2.7.

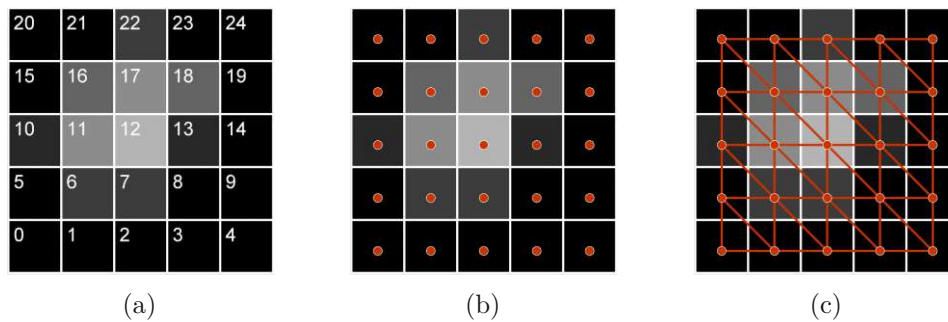


Figure 2.7: Triangle mesh creation from a 5×5 height map (a). (b) Vertices are placed at the center of each pixel. (c) Triangles are obtained by connecting the vertices. Images from [CR11].

In addition to the height information, the terrain model should also differentiate between different surface types, such as rocks and foliage. A simple solution to this is to add a color map to the terrain. Aerial or satellite images can provide the desired surface information for the terrain. This imagery has to be orthorectified in order to allow projection onto our terrain and is therefore also known as *orthoimagery*. An example of an orthoimage can be seen in Figure 2.8. As the terrain mesh already comes with an (x, y) parametrization, texture mapping the terrain is trivial. An image texture with the same aspect ratio as the height map can be applied by linearly mapping the (x, y) parametrization of the terrain mesh into a (u, v) texture parametrization [CR11].



Figure 2.8: Orthoimagery of the Austrian Alps. Image from [Geo23].

2.3.2 Advanced Data Structures

Storing a high-resolution DEM in a single source file is not feasible when the goal is to render the terrain in real-time. A DEM covering Austria at a resolution of 1×1 meters, with the elevation values encoded in 10 cm steps would take up over 200 Gigabytes ($83\,882 \text{ km}^2 \times 18 \text{ Bits per m}^2$). With this amount of data neither downloading the data from a server nor rendering it will be possible in real-time.

In map applications, the concept of tiling is employed to alleviate this problem. As we do not need the full resolution at all zoom levels, the height data can be stored at different resolutions. Furthermore, when zooming into the map only a section of the map data is visible at a certain point in time, therefore only select tiles need to be loaded in order to draw the current view.

Typically, map data is represented by projecting the spherical globe coordinates into a flat, tileable plane. To consistently index the tiles of this plane we need a tiling scheme. The most common map projection for web mapping is the Web Mercator or WGS'84 projection (EPSG:3857) [EPS20], which was developed by Google for the first version of Google Maps [Ste17]. Web Mercator is based on an ellipsoidal model of the earth using the WGS'84 ellipsoid, with a semi-major axis of 6378.137 km and a semi-minor axis of 6356.752 314 245 km [Age14]. Map features are assigned ellipsoidal coordinates, which are then projected using the spherical Mercator projection. The resulting map is cut off at approximately $\pm 85^\circ$, resulting in a perfect square map with properties close to the original Mercator projection. The square map shape helps with tiling as each tile can be equally subdivided into four sub-tiles [Ste17].

With the ability to tile the map, it is possible to pre-compute the tiles at different zoom levels (for both the DEM and the orthoimagery). These pre-computed tiles can then be stored on the server and served to the client on demand. In the tiling scheme developed by Google, which is also known as the *Slippy Map* scheme, each tile has a resolution of 256×256 pixels. As can be seen in Table 2.2, the number of tiles to cover the earth is dependent on the zoom level, with $level^4$ tiles at each zoom level. The first tile in the tile pyramid covers the whole earth. Within a zoom level z , the tiles are indexed by a pair of integers (x, y) , where x represents the longitudinal coordinate starting at 180° heading towards east and y the latitude starting at $+85.051129$ degrees north and heading towards south. This indexing directly translates to the server directory structure where a raster tile is stored as $/z/x/y.png$. An alternative tiling scheme is the *Tile Map Service* (TMS) scheme, where the y value is flipped starting from -85.051129 degrees in the south.

With orthoimagery, displaying the Slippy Map tiles is straightforward as the raster data from each tile can be directly used as a texture in the map. For the DEM data, the elevation in meters is stored as float values with a precision of 16 bits per value or higher. To use this data in a pixel-based rendering pipeline, an additional encoding step has to be performed in order to store the data in raster tiles that use standardized pixel graphics representations such as PNG. A raster tile is a map tile that contains information in a discretized pixel raster. Mapbox [Map23b] provides a format to encode elevation data in RGB raster tiles with a height resolution of 10 cm. In this format, the elevation is represented as a three-digit base-256 number with red, green, and blue each containing one digit. A raster tile containing height data in this format can be seen in Figure 2.9. This allows for $256^3 = 16\,777\,216$ unique elevation values. In addition, the elevation is offset by 10 000 meters to support negative elevation values, such as areas that lie below sea level.

Level	Tiles per Level	m / pixel (on Equator)
0	1	156 543
1	4	78 272
2	16	39 136
3	64	19 568
4	256	9 784
5	1 024	4 892
6	4 096	2 446
7	16 384	1 223
8	65 536	611.496
9	262 144	305.748
10	1 048 576	152.874
11	4 194 304	76.437
12	16 777 216	38.219
13	67 108 864	19.109
14	268 435 456	9.555
15	1 073 741 824	4.777
16	4 294 967 296	2.389
17	17 179 869 184	1.194
18	68 719 476 736	0.597
19	274 877 906 944	0.299
20	1 099 511 627 776	0.149

Table 2.2: Number of tiles and pixel size on equator per zoom level [Ste17].

To decode the elevation data, the RGB base-256 values are decoded into a base-10 floating-point value, which can then be used to displace the mesh as described in Section 2.3.1. For this decoding the following formula is used:

$$\text{elevation} = -10000 + ((\mathbf{R} \cdot 256 \cdot 256 + \mathbf{G} \cdot 256 + \mathbf{B}) \cdot 0.1). \quad (2.3)$$

In addition to raster data, another common type of data is vector based. These vector sources include features such as road networks and text labels. Similar to raster data, vector data may be served via a tile pyramid, containing pre-computed vector data for different zoom levels. This pre-computation is necessary as there is no reliable mechanism for automated map generalization [Ste17]. In contrast to raster tiles, which are directly used as a texture, different visualization techniques for vector tiles exist. Zechmeister [Zec20] provides an overview of these techniques. One visualization technique for vector tiles rasterizes the vector data for each tile and then utilizes the same pipeline as for rendering raster tiles. For this rasterization, a style document containing a description of how to render different vector elements is provided in conjunction with the tiles.

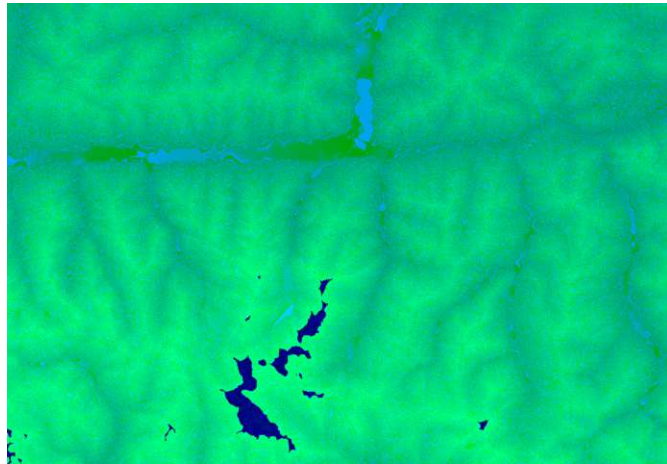


Figure 2.9: Section of Mapbox [Map23a] RGB-encoded elevation data showing the Austrian Alps. Dark blue areas have an elevation beyond 3107.1 meters, at which point the red channel is incremented by one.

Vector data may also be provided in a non-tiled structure, especially for simpler features, such as individual paths or areas. Here, different formats exist, with GeoJSON [BDD⁺16] being widely supported. GeoJSON is based on the JavaScript Object Notation (JSON) and allows for describing geographic features by objects, such as paths and polygons.

2.4 Visualization on 2.5D Terrain

In the context of visualizing geospatial data in 2.5D, specific challenges such as occlusion, visual clutter and an absence of a constant map scale arise. Therefore, a visualization application that uses a 2.5D terrain as its basis has to incorporate strategies to solve these challenges [STJD15].

2.4.1 Hill Shading

Hill shading or relief shading is a widely used method for displaying terrain surface data on 2D and 2.5D maps. In this terrain representation, contour lines are replaced by shading in order to visually convey terrain properties. Horn [Hor81] introduced a method for computing hill-shading based on DEM data.

Horn introduces automatic hill shading as a process of computing the gradient of a DEM and then using the extracted surface orientation at each position for applying diffuse shading to the terrain. An example of this shading can be seen in Figure 2.11. The obtained surface orientation can also be used for determining topographical terrain features such as slope and aspect. In Horn's method the gradient at a position (i, j) in the terrain is computed by retrieving the elevation values in the 8-neighborhood of the elevation value z_{00} at (i, j) , see Figure 2.10.

z_{-+}	z_{0+}	z_{++}
z_{-0}	z_{00}	z_{+0}
z_{--}	z_{0-}	z_{--}

Figure 2.10: Indices of elevations in 8-neighborhood around the elevation value z_{00} . Image adapted from [Hor81].

From the nine elevation values z_{xy} , the two partial derivatives are obtained as

$$\frac{\partial z}{\partial x} = \frac{(z_{++} + 2z_{+0} + z_{+-}) - (z_{-+} + 2z_{-0} + z_{--})}{8\Delta x} \quad (2.4)$$

and

$$\frac{\partial z}{\partial y} = \frac{(z_{++} + 2z_{0+} + z_{-+}) - (z_{+-} + 2z_{0-} + z_{--})}{8\Delta x}, \quad (2.5)$$

with Δx being the grid interval or the pixel size in case of a raster DEM image.

To obtain the principal slope angle from the derivatives, Burrough and McDonnell [BM98] propose to use a second-order finite difference algorithm fitted to the neighborhood window. This defines the slope S as

$$\tan S = \sqrt{(\partial z / \partial x)^2 + (\partial z / \partial y)^2} \quad (2.6)$$

with

$$s = \arctan\left(\sqrt{(\partial z / \partial x)^2 + (\partial z / \partial y)^2}\right) 180 / \pi \quad (2.7)$$

giving the slope angle s in degrees.

The aspect, or exposition, A is given by

$$\tan A = -(\partial z / \partial y) / (\partial z / \partial x) \quad (2.8)$$

or, in degrees

$$a = \arctan2\left((\partial z / \partial y), -(\partial z / \partial x)\right) 180 / \pi. \quad (2.9)$$

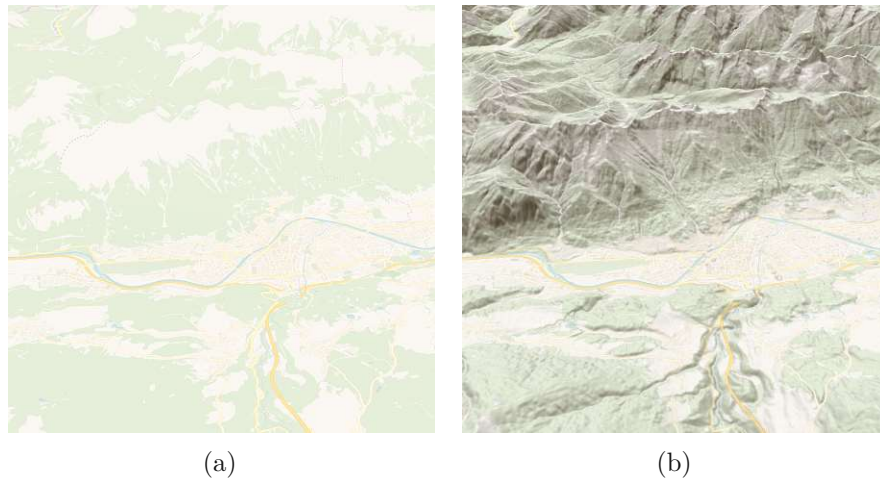


Figure 2.11: 2.5D representation of alpine terrain (a) without and (b) with hill shading enabled.

2.4.2 Visualization Layers

Apart from visualizing terrain properties, one may also want to add data visualization layers to a terrain. In a naive implementation of data visualization on a 2.5D terrain, we can exploit the fact that the terrain model only displaces the ground plane along the z-axis. This allows for rendering a data layer as regular 2D map tiles and then draping the resulting image onto the corresponding terrain tiles as a texture. This approach is, for example, implemented by MapLibre and Mapbox. While conceptually and computationally simple, this approach comes with the disadvantage that the color image draped on the terrain will be distorted, with the distortion being amplified in areas of increased steepness (see Figure 2.12). For visualizing data layers containing features such as lines, points, and polygons, draping color maps over a hill-shaded terrain model is a widely used visualization method [MHW⁺12].

When it comes to visualizing information on a 2.5D terrain representation, some visualization challenges arise. As MacEachren [Mac04] points out, 2.5D or 3D representations unavoidably lead to hidden areas in the map due to occlusion. Another problem that arises when perspective is introduced in the 3D rendering of a map is inconsistencies of scale. As soon as perspective distortion is applied to the map, representation scales within a given map view are no longer comparable. According to MacEachren, this is detrimental to the task of determining feature sizes.

Another challenge associated with 3D map representations is the drawing of text labels. While in a 2D map, each label is allocated to a visible area or point, in 2.5D or 3D occlusion has to be handled [Voz23]. Billen et al. [BCDM⁺14] identify visualization challenges that come with 3D city models. They note that avoiding interference between different visualization techniques in the same scene can be an issue. Furthermore, visualization techniques used for each type of data may not be compatible when combined into one

visualization. Even if the visualizations are compatible, the addition and superposition of them may result in visual clutter or cognitive overload proving detrimental to the comprehension of the 3D scene.

Semmo et al. [STJD15] turn to illustrative visualization techniques used in historic maps to overcome the challenges posed by 2.5D and 3D maps. They propose to use Non-Photorealistic Rendering (NPR) to build representations for map features such as terrain, water, and buildings in real-time. In particular, they present an iconification technique that renders optimized views of 3D landmarks on a 2.5D map. In their work on illustrative terrain rendering Buchin et al. [BSD⁺04] also employ NPR techniques for terrain rendering. They use hachures to encode slope steepness and lighting information. Hachures are lines following the slope of the terrain, perpendicular to contour lines, which are placed at a fixed altitude. Depending on the thickness, density, and perturbation of the hachures, terrain parameters such as slope steepness, expositions (via lighting), or slope curvature can be encoded into the terrain visualization. An example of this visualization can be seen in Figure 2.13.

The blending of data layers draped over a DEM is another challenge that has been investigated in terrain visualization. Use cases such as investigating the geomorphology of volcanic areas call for additional information being overlaid on the terrain as discussed by Favalli and Fornaciai [FF17]. In their use case, a hill-shaded terrain forms the basis of the visualization, which is then combined with additional data. They employ the Red Relief Image Map (RRIM) developed by Chiba et al. [CKS08]. RRIM uses the Hue-Saturation-Value (HSV) color model to blend a data layer with the underlying relief image. The red channel is used as it was empirically shown that it has the richest tone for the human visual system [CKS08]. An RRIM image allows for each of the HSV



Figure 2.12: Orthoimagery draped on a 2.5D terrain. Note how in the near-vertical areas on the right, the texture is stretched.

2. BACKGROUND

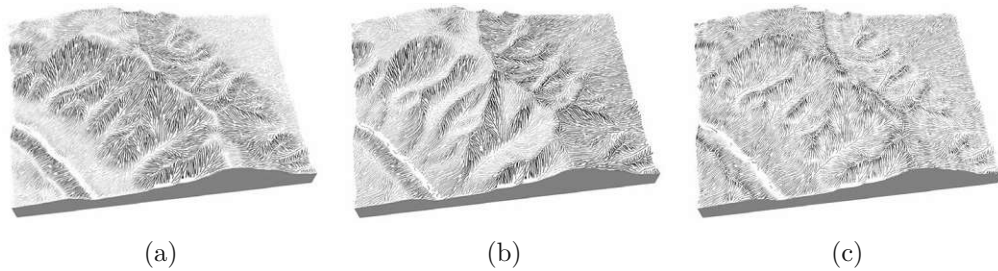


Figure 2.13: Terrain model with hachure texture encoding different terrain parameters: (a) slope, (b) exposition, (c) curvature. Images from [BSD⁺04].

parameters to be assigned to a data channel (see Figure 2.14). While the RRIM encoding is used within the geoinformation community, we could not find any uses outside the domain, e.g. for public information dissemination.

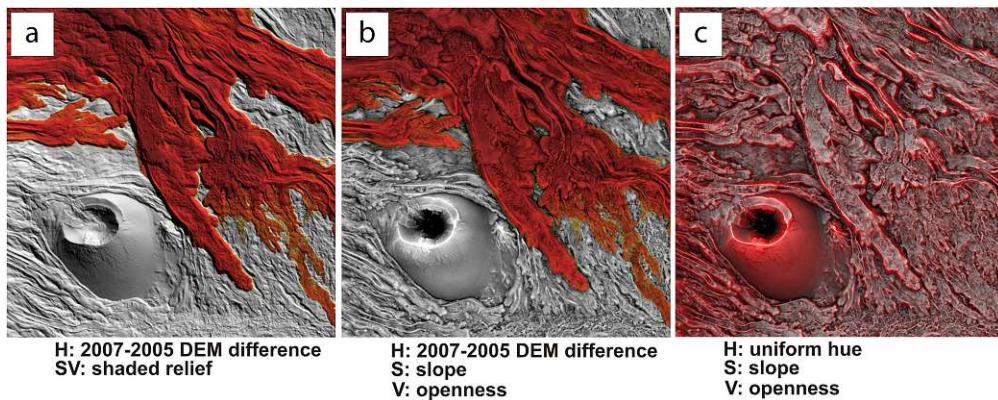


Figure 2.14: Three different visualizations showing data blending for a volcanic map. (a) The height difference between two different DEM capture dates is encoded in the red hue. (b) RRIM-style visualization of the height difference in combination with slope and openness, each encoded in a different HSV parameter. (c) RRIM with a uniform hue for the whole terrain while slope and openness are encoded in the saturation and value, respectively. Images adapted from [FF17].

In the context of visualization on a 3D terrain model Dübel et al. [DRTS17] present methods to encode the terrain features in combination with geospatial data and uncertainty. In their approach, they discuss combining different visualization techniques, such as color overlays and glyphs to encode the different channels. They argue, that due to the limited visual budget, prioritization has to be performed, visually emphasizing only those aspects which are in focus at a given time.

Finally, as color overlays are a widely used technique in map visualizations, rules and guidelines for color use in maps are of interest when developing a map visualization. ColorBrewer [HB03] provides a collection of curated mapping color schemes for different

visualization tasks. This collection includes encodings for sequential data in multi-hue and single-hue color maps as well as encodings for diverging and qualitative datasets.



Die approbierte gedruckte Originalversion dieser Diplomarbeit ist an der TU Wien Bibliothek verfügbar
The approved original version of this thesis is available in print at TU Wien Bibliothek.

Related Work

In this chapter, we present a review of related work in the field of avalanche risk visualization. First, we look into existing public platforms that use visualization to convey avalanche risk to recreationists. We find that there are two categories of avalanche risk visualizations: static and dynamic ones. Furthermore, we also present work investigating the impact of using 2.5D maps on the tasks of risk visualization and navigation.

3.1 Avalanche Risk Visualization

In the communication and dissemination of avalanche risk, visualization plays a central role. Avalanche reports as they are published by avalanche warning services already contain visualizations to characterize the type and severity of the avalanche danger. A detailed description of these visualizations can be found in Section 2.1.2.

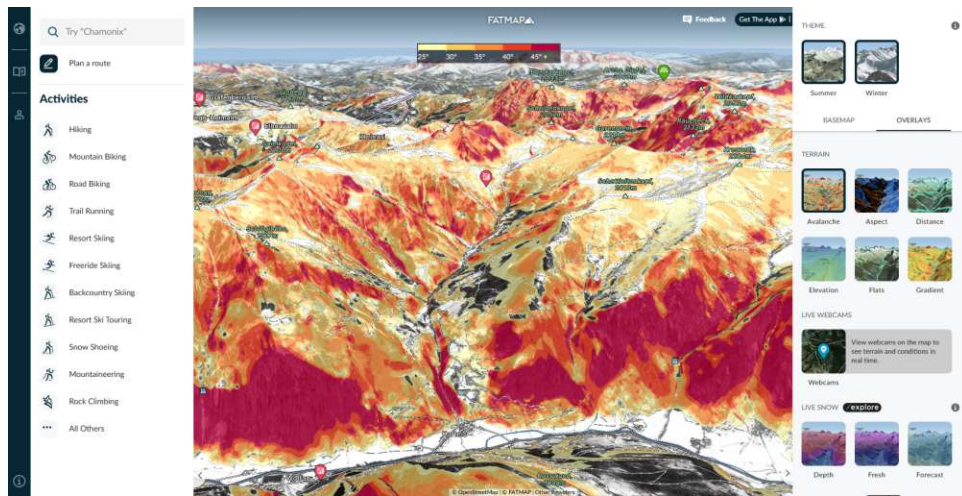
3.1.1 Static Avalanche Risk Visualization

Static avalanche risk visualizations are risk visualizations that are solely based on terrain features. Using terrain parameters to model static avalanche risk is an effective strategy as work by Kumar et al. [KSS18] shows. They present a prediction model which evaluates five terrain parameters (slope, exposition, elevation, curvature, and ground cover) to predict avalanche occurrences. A validation of prediction results using historical data for their study area shows that their model has an accuracy of 91.12% when predicting avalanche susceptibility.

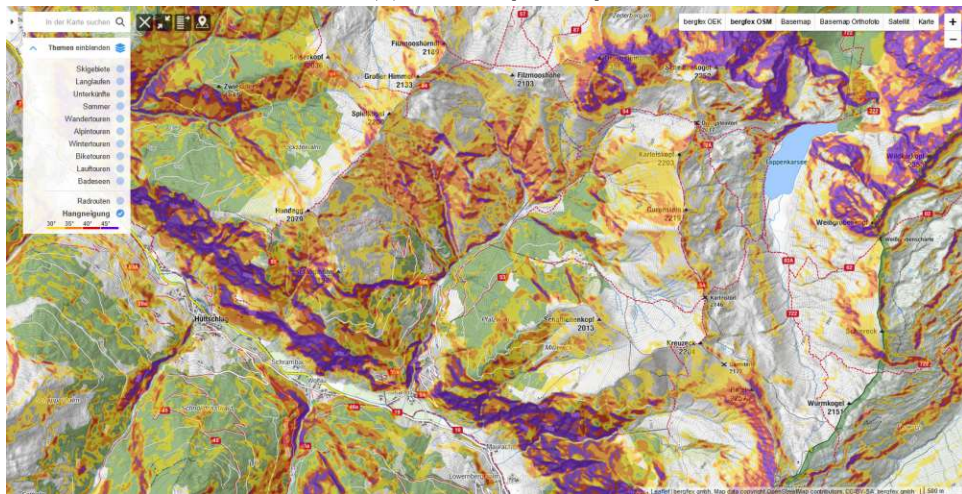
Static risk visualization is implemented in a broad range of outdoor map applications such as Bergfex [ber22] or Fatmap [FAT23]. Here, static overlays of slope steepness are utilized to highlight avalanche-prone terrain (see Figure 3.1). Fatmap provides its visualizations on a 2.5D map. Different terrain feature layers can be shown on the map as colored overlays. These static maps can be manually combined with external information

3. RELATED WORK

sources such as the current avalanche report. Recreationists then apply risk reduction methods to manually determine the avalanche risk while planning tours. Apart from the slope steepness, which is visualized using a binned color ramp ranging from 25° to $45^\circ+$ in 5° intervals (see Figure 3.1b), Fatmap also provides an exposition layer where the aspect angle of the terrain is visualized via a color scale with 45° intervals. Additionally, an elevation overlay provides color coding for different height regions in 500m intervals as well as contour lines in 50m intervals. More fine-grained height information can be sampled by hovering the mouse pointer over the map, which spawns a contour line at the brushed height, accompanied by a text label indicating the height.



(a) Fatmap [FAT23]



(b) Bergfex [ber22]

Figure 3.1: Two commercial applications visualizing static avalanche risk by overlaying slope steepness onto a base map.

The backcountry tour planning app White Risk [fSuLS23] was developed by the WSL Institute for Snow and Avalanche Research SLF. In addition to the standard slope angle overlay, this application also provides a Classified Avalanche Terrain (CAT) overlay, which is based on avalanche simulation data. In these simulations, the release potential in a given area as well as the runout zones for size-3 avalanches (10 000 m³ in volume) are computed. This map is, however, only available for Switzerland. The CAT map is obtained using a method presented by Harvey et al. [HSB⁺18]: a high-resolution DEM is used to calculate polygons of potential avalanche release areas. For each of these polygons, simulations of a size-3 avalanche are carried out. From these simulations, data on possible avalanche runout zones is collected. From the same simulation data, they also obtain the Avalanche Terrain Hazard (ATH). The ATH adds a notion of potential consequences of being caught in an avalanche to the terrain-based risk. Limitations of this classification as identified by the authors include focusing the simulation on human-triggered avalanches up to size 3 and not taking into account terrain features such as exposition and elevation. An overlay of the ATH for Switzerland is also available in the White Risk application (see Figure 3.2).

Jaedicke et al. [JSST14] developed a web-based avalanche warning system for Norway that combines geospatial data with other data sources such as weather, therefore falling into category (ii). This warning system is able to predict avalanches at a local level and to model single avalanche paths. In contrast to the other beforementioned applications, this warning system is an expert system designed to support avalanche forecasters in their work by fusing multiple data sources into a single application. The main challenge the authors identify is the multi-scale nature of avalanche modeling, covering both regional as well as more global scales. Furthermore, the availability, as well as the processing of real-time data, is identified as a challenge. Their solution is based on a rather sparse terrain model with a resolution of 15 × 15 meters.

3.1.2 Dynamic Avalanche Risk Visualization

The web platform Skitouren guru [Sch22] provides a dynamic avalanche risk visualization for recreational ski tour planning. Here, the main focus of the risk visualization lies in assessing the risk level associated with pre-defined tours. This risk level is provided at different scales. On the highest level, each tour track is assigned an overall avalanche risk value, which is categorized into three different color-coded levels: low (green), elevated (orange), and high (red). On a more detailed scale, a single tour is broken down into sections to which the same avalanche risk classification is applied. Figure 3.3 depicts an example of this risk classification. In addition to the dynamic avalanche risk, the visualization also draws glyph indicators in areas where an elevated static avalanche risk is present. These glyphs consist of concentric circles depending on the severity of the static avalanche risk: one circle indicates “avalanche terrain”, two circles “typical avalanche terrain”, and three circles “very typical avalanche terrain”.

To determine the terrain-based avalanche risk, which is the basis for the dynamic avalanche risk calculation, Skitouren guru uses the Avalanche Terrain Hazard Map (ATHM) [SK16]

3. RELATED WORK

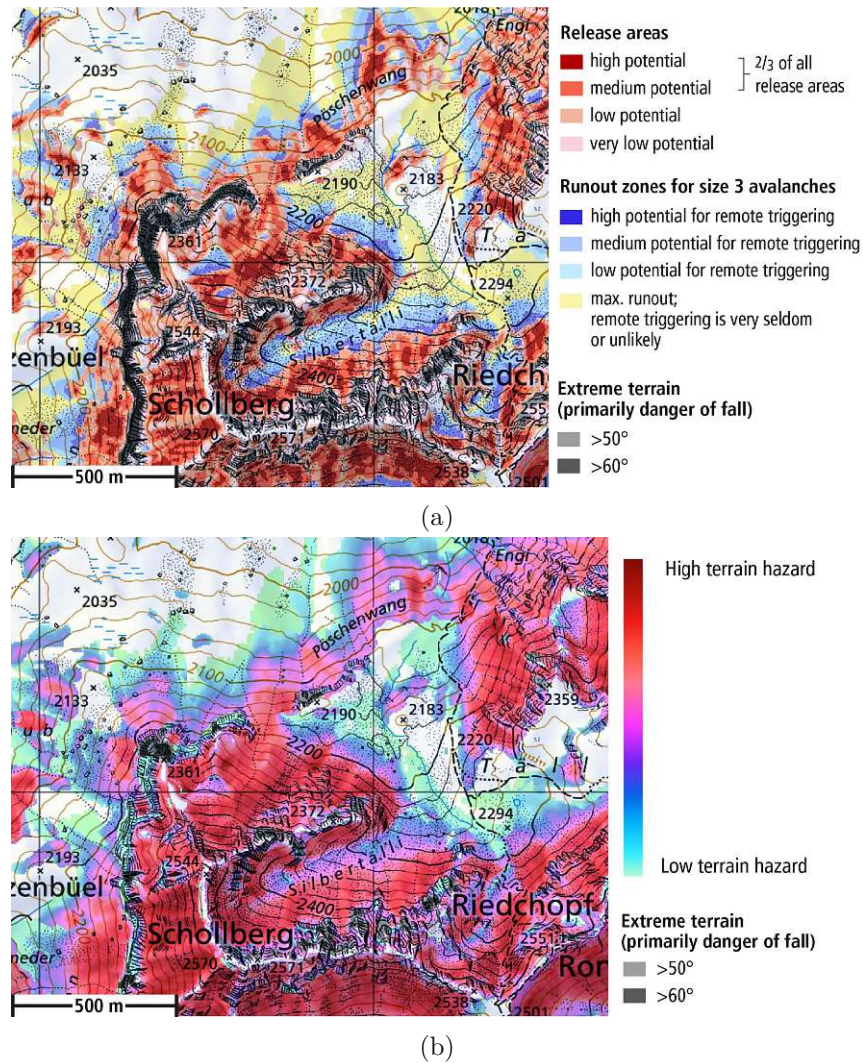


Figure 3.2: Classified avalanche terrain (a) and avalanche terrain hazard (b). Images from [HSB⁺18].

which classifies terrain based on the Avalanche Terrain Exposure Scale (ATES) developed by the Parks Canada Agency [SMT06]. Conceptually, the ATHM is similar to the ATH as used by White Risk. However, it uses additional terrain parameters, such as slope curvature, slope area, and forest cover. The slope area is determined by delimiting a polygon around the current position reaching out to the next ridge, the bottom line of a gully, hillside toe, or slope edge [SK16]. An example relevant slope area polygon can be seen in Figure 3.4.

For generating the ATHM for a region, a $10\text{ m} \times 10\text{ m}$ raster is used to calculate the ATES values in an offline pre-processing step. An example of the resulting map can be seen in Figure 3.5. In addition to a whole region, the evaluation can also be applied

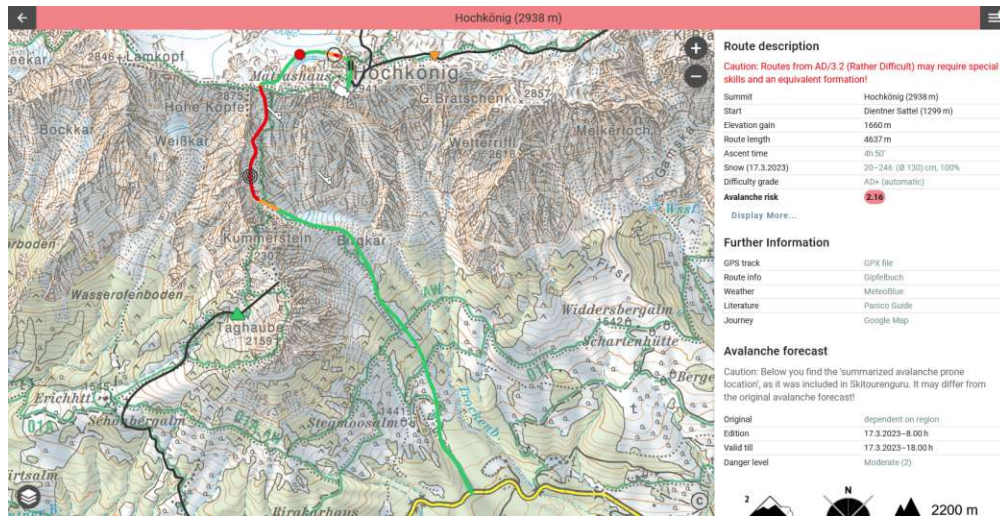


Figure 3.3: Dynamic avalanche risk for a single tour on SkitourenGuru [Sch22]. The different line segment colors correspond to the localized avalanche risk for each tour section. In the red section, a glyph with three concentric circles indicates a high static avalanche risk in that area.

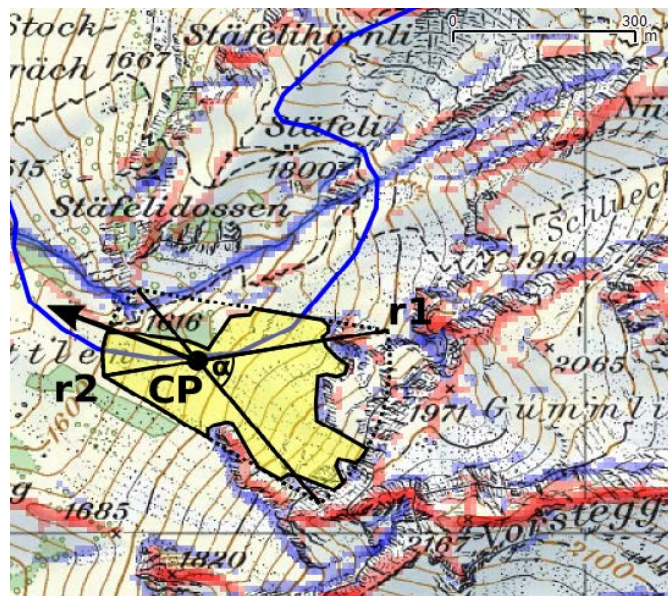


Figure 3.4: Relevant slope area delimitation from the ATHM. Image from [SK16].

3. RELATED WORK

along a pre-specified route such as a GPS Exchange Format (GPX) track. This per-tour evaluation, which incorporates the avalanche danger information as provided by the avalanche report, is also what is finally shown to the user in the Skitourenuru application. Showing the real-time risk only on existing tour tracks, however, limits the insight on the user side. In case a tour does not exist in the database, judging the avalanche risk for a given day once again requires the user to integrate multiple data sources. Additionally, not showing the risk in the context area of the tour may limit potential learnings the user can take away from the visualization. Gaining an understanding of where the risk in a certain section of a tour originates from is potentially harder when no real-time visualization of the risk in the surrounding area is shown.

In addition to the per-track visualization, Skitourenuru also offers an experimental view of static avalanche risk maps for Switzerland which are based on the *Quantitative Risk Reduction Method* by Sch mudlach et al. [SWK18]. In these maps, the danger rating from the avalanche report is included in the risk calculation for six different static danger ratings. However, to the best of our knowledge, no real-time implementation exists, which also takes the current avalanche situation into account and computes the risk map on-the-fly.

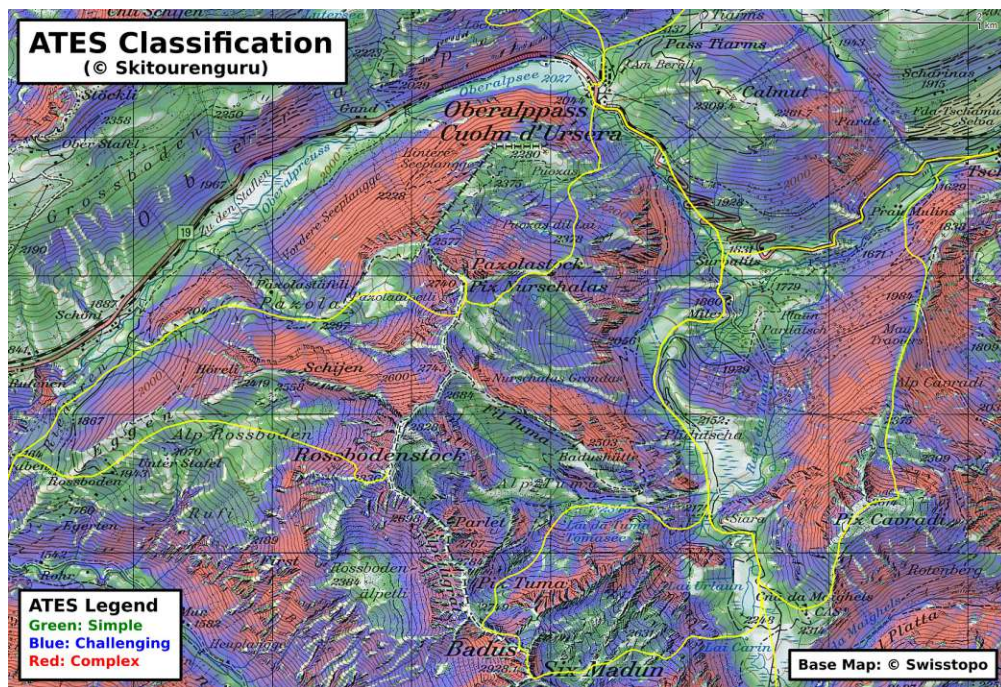


Figure 3.5: ATES map of the Oberalppass in Switzerland resulting from sampling on a $10\text{ m} \times 10\text{ m}$ raster. Image from [SK16].

3.1.3 Risk Awareness in Avalanche Risk Visualizations

An analysis of risk awareness in avalanche visualizations has been done by Šašinka et al. [ŠSK⁺19]. In one of their tests, they subjected two groups with different levels of map literacy to visualizations of avalanche risk. These risk ratings in the visualization were combined with uncertainty. Participants had to identify areas associated with a certain risk level and uncertainty. Two setups were compared: an intrinsic visualization where a bivariate color map was used to encode the avalanche risk in hue and the uncertainty in lightness. The second setup consisted of an extrinsic visual representation where the avalanche risk was encoded in the color variable while the uncertainty was encoded in dots with varying sizes. Subjecting the two groups with different map literacy levels to both visualization types, they found that for participants with high levels of map literacy, the performance at map-related tasks depends on their cognitive style in combination with the visualization style. In a follow-up study, they used eye-tracking sensors to monitor user gaze when solving tasks within the visualizations. Their findings show that for the intrinsic visualization, users more frequently switch between the legend and the map. Within the group of high map literacy subjects, the authors found that individuals with a globally-oriented cognition performed better when working with the extrinsic visualization while locally-oriented users performed better in the intrinsic visualization with the bivariate color map.

3.2 Risk Visualization and Navigation on 2.5D Maps

While the risk and uncertainty visualization as presented by Šašinka et al. [ŠSK⁺19] is based on 2D maps, we want to utilize 2.5D maps, which come with their own set of, as discussed in Section 2.4. However, in terms of navigation and wayfinding in steep terrain, using non-flat map representations is potentially beneficial.

In the context of urban navigation, Zheng and Hsu [ZH21] investigate the impact of 2.5D maps on the wayfinding performance of users. In their study, they found that using environmental features in 2.5D maps can improve the recollection of map users. Therefore, they conclude that “2.5D maps are suitable for users with lower spatial ability” [ZH21]. Secondly, they show that full reconstruction of the environment is not necessary for orientation as representing key landmarks at intersections is sufficient for wayfinding. Finally, they also conclude that map representations with higher view angles (e.g. 60° or 90°) are superior to ones with lower angles of 30° in the context of urban wayfinding.

Preppernau and Jenny [PJ15] present results from a study where 3D volcanic hazard maps are compared against conventional 2D ones. For their study, two conditions were tested: a 2D contour map against a 3D perspective map and 2D markers against isochrones for evacuation travel times. With 80 participants in their study, they found that participants preferred the 3D map representations for interpreting the terrain and evaluating escape routes. In the terrain interpretation task, participants were presented with pairs of points for which they had to determine which one was at a higher elevation and which one had the steeper slope. Users of the 3D map scored higher in these tasks. For the task

3. RELATED WORK

of locating themselves on the map, the investigators found no evidence that a 3D map improves users' ability to do so. In the final comparison task between 3D and 2D maps, the users were asked to choose evacuation routes. In this context, Preppernau and Jenny found that for on-foot routes participants choose routes with a greater margin of safety when using 3D maps. For car routes, however, they found no significant effect.

For avalanche risk visualizations Buckley et al. [BHK⁺04] argue that 3D maps can facilitate the intuitive interpretation of landscape forms, which are an important factor for understanding avalanche risk. Especially slope and aspect information are easily derived from 3D representations, which - according to Buckley et al. - moves the focus of avalanche risk visualization toward depicting other influencing factors, such as snow conditions or meteorological data. Therefore, we focus on depicting the integrated avalanche risk in our terrain visualization.

Overview

In this chapter, we provide an overview of our system. We start by gathering requirements and then look at existing frameworks for web-based real-time terrain rendering before discussing the software architecture and its components.

4.1 Requirements

Our objective is to build a dynamic avalanche risk visualization based on a high-resolution DEM and the avalanche report, without introducing new risk evaluation heuristics. To achieve this goal, our prototype application has to fulfill the following requirements:

Utilize established reduction methods for risk assessment (R1): Existing risk reduction methods, such as the SnowCard and Stop-or-Go are well accepted by backcountry skiers and are recommended by alpine clubs. The effectiveness of these methods is empirically supported (see Section 2.2.4) and they follow clear heuristics that can be implemented algorithmically. For off-site tour planning both the SnowCard and Stop-or-Go require data from the avalanche report in combination with information on the terrain.

Convey the risk through an effective visual encoding scheme (R2): Visual encodings of static and dynamic avalanche risk are widely used in risk communication including in the avalanche report itself (see Section 2.1.2). Visualizing risk on a 2.5D map comes with challenges, such as visual clutter, which we have to overcome in our implementation.

Guide user attention toward critical areas (R3): As part of the visual risk encoding, critical areas with potentially high avalanche risk should be highlighted in a way such that user focus is directed toward them. This is important because our

implementation does not cover the on-site checks that are part of reduction methods (e.g. “Check 2” of Stop-or-Go). By guiding attention toward critical areas, we can, however, facilitate the on-site evaluation by indicating where to look.

Support on-site orientation and identification of critical areas (R4): As an extension to **R3**, it is important that users are able to recognize previously identified critical areas on-site. For this, the visualization should allow them to orientate themselves on-site by providing detailed representations of the real-world terrain. The map should therefore contain a faithful depiction of landscape forms and also contain landmarks as they have been shown to facilitate orientation in 2.5D maps (see Section 3.2).

Provide an overview of the avalanche situation (R5): While our primary focus lies on evaluating the avalanche risk on smaller scales, the input data from the avalanche report is provided for larger regions covering up to hundreds of square kilometers. We want to transparently show this mismatch in scales so that users are able to understand potential inconsistencies in the risk visualization that could arise from discrepancies between different regions of the avalanche report.

Incorporate a detail view for an in-depth examination of critical areas (R6): Next to the overview, we also need a detail view to evaluate the avalanche risk at smaller scales, for example in the direct vicinity of a tour. This detailed examination is directly connected to **R3** as the critical areas usually are visible at smaller scales. The requirement for both overview and detail views poses a challenge for the design and implementation of the visual risk encoding.

Facilitate real-time interaction with the risk visualization (R7): Interactions such as changing the location and zoom level of the map are necessary to inspect critical areas and match the map view for orientation purposes. Furthermore, users should also be able to change between overview and detail views in real-time. Especially during map navigation, the frame rate of the application should be sufficiently high (i.e. at least 30 frames per second) to avoid lag.

Expand the risk visualization beyond pre-defined tours, incorporating the surrounding terrain (R8): While other applications such as Skitourenguru [Sch22] show the dynamic avalanche risk only for pre-defined tracks, our implementation should also visually encode the risk on the surrounding terrain. This can give users an understanding of where the avalanche risk originates from and can potentially help them to learn where to look during on-site evaluations. Not all tours come with exact pre-defined tracks and, therefore, evaluating the risk along tracks is not sufficient. Even if there is a tour track available, skiers may not follow it precisely. Expanding the risk evaluation from essentially one-dimensional tracks to a large-scale 2.5D terrain poses a big challenge for the implementation as the whole map area has to be re-evaluated every time the avalanche report is updated. As a result of the expanded risk visualization, the emphasis

on real-time interaction (**R7**) becomes even more important to allow users to explore the surroundings of a tour.

Visualize the avalanche risk for previous, current, and upcoming avalanche reports (R9): Our visualization should provide the ability to display avalanche reports other than the current one. Having the ability to view a tour or area under different avalanche conditions, enables users to gain an understanding of typical critical areas. Access to archived risk visualizations could also be used for tour descriptions: there users could view the avalanche risk situation on the exact day the tour description was written, providing historical context and a more accurate understanding of the conditions at that time.

Perform real-time evaluation of terrain properties (R10): The evaluation of the DEM to extract features such as slope and exposition should be performed in real-time on the client side. To render the terrain, the elevation data has to be sent to the client. The same data source can be used to perform the terrain-based risk evaluation on the client side, reducing the network bandwidth requirements of our application.

4.2 Frameworks for Real-Time Terrain Rendering on the Web

There are multiple frameworks, which allow for terrain rendering on the web. Google, with both Google Maps [Goo23b] and Google Earth [Goo23a], offers worldwide 2.5D coverage and even 3D maps for some parts of the world. While these services offer terrain rendering in real-time, they are not open to customization, such as loading custom DEM or raster image sources. Therefore, they cannot serve as a basis for our avalanche risk visualization. Customizable terrain rendering frameworks for the web include commercial solutions such as Mapbox [Map23a] and Cesium JS [Ces23] and non-commercial, open-source source frameworks such as MapLibreGL JS [Map23c].

These terrain rendering frameworks are written in JavaScript and use the WebGL 1.0 graphics API for rendering. WebGL 1.0 provides support for a wide range of graphics hardware but misses more modern OpenGL features such as Uniform Buffer Objects. Mapbox and MapLibre have commonalities as MapLibre is an open-source fork of Mapbox. These commonalities include the elevation data encoding format as described in Section 2.3.2.

MapLibre allows for rendering multiple data sources as layers, which are then overlaid onto the terrain model. The layers are defined in a style document, which is then rendered top to bottom, blending all layers into a single texture, which is subsequently used as a texture map for the displaced 2.5D terrain mesh. Additionally, MapLibre provides a hill shading pipeline - which using the terrain elevation data in combination with a light source - computes shaded relief maps on a per-tile level (see Section 2.4 for a detailed description of hill shading).

All of the presented map frameworks also support vector layers for features such as labels and streets to be overlaid onto the map. Furthermore, they offer interaction such as zooming, panning, tilting, and rotating the map to view the content. These interaction modes are also present for mobile and touch-based devices, enabling a wide range of viewing options.

4.3 Software Components

The software stack for our visualization consists of three main components. The first component is static data preprocessing, which is performed offline to transform our input datasets to our internal data formats. This includes the terrain data as well as information on administrative regions, on which the avalanche reports are based. After these sources are processed the resulting data is stored on the tile server. The second main component is responsible for dynamic preprocessing. Here, time-varying data sources, such as the daily avalanche reports, are parsed and processed on a server to transform them into a format compatible with the renderer. Finally, the terrain renderer consolidates the static and dynamic data inputs into an interactive 3D visualization within the browser. The client-side terrain renderer is part of the user interface that allows interaction with the displayed data. An overview of the software components and their responsibilities can be seen in Figure 4.1.

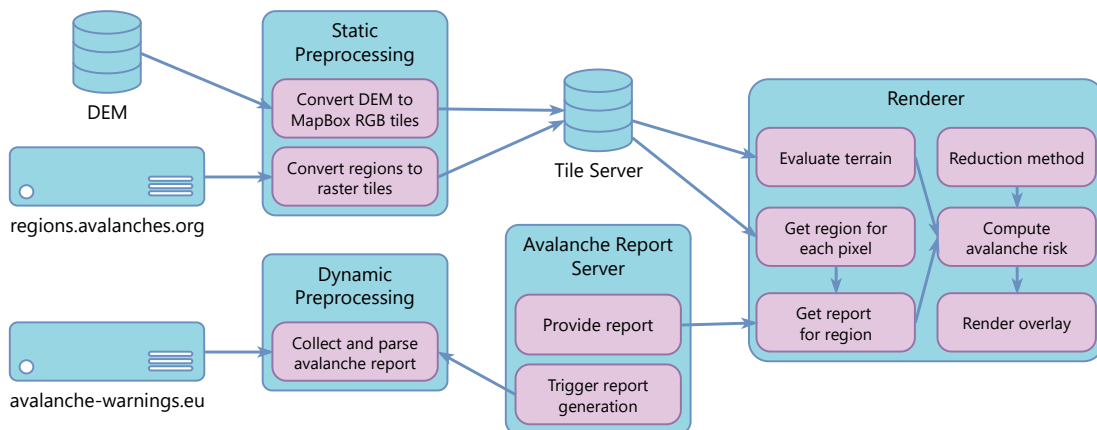


Figure 4.1: Schematic overview of the software components required for our avalanche risk visualization.

The next two chapters of this thesis are organized based on the structure of the software components: First, the visualization and interaction design of the renderer is presented in Chapter 5. Then, the implementation of our prototype application is discussed in Chapter 6, covering static and dynamic preprocessing as well as the implementation of the renderer and user interface.

Visualization and Interaction Design

In this chapter, we discuss the design process of our visualization. This includes both the design of the risk overlays for the terrain visualization as well as the design of the user interface. The design of our visual risk encoding is focused on answering **RQ2**, which is: *How can we visually encode the avalanche risk on a 3D terrain visualization to guide attention toward the high-risk areas?* This question can be split into two subtasks: visual encoding of the risk on a 3D terrain (**R2**) and guiding attention toward high-risk areas (**R3**).

5.1 Avalanche Risk Overlays

The renderer for our risk visualization has to fulfill two main requirements: rendering the high-resolution terrain at interactive framerates to enable interaction in real-time (**R7**) and visualizing the avalanche risk depending on the terrain, the current avalanche report, and the selected reduction method (**R1**). With the terrain rendering itself covered by a map rendering framework, the focus of the design lies in the rendering of the avalanche risk visualization.

A big challenge that comes with draping overlays onto the terrain is that the underlying information, especially the orthoimagery, becomes partially or fully obscured. This, in turn, limits the recognizability of terrain features and thereby affects the users' ability to orientate themselves in the terrain (as required in **R4**). While strategies such as RRIM exist to perform blending between terrain data and additional overlays, these do not blend well with the color information of the orthoimagery. Adjusting the transparency of the overlays to allow blending with the underlying color information alleviates the problem somewhat. However, higher transparency values also increase the color variation

in the overlays, which decreases their readability. An alternative approach could be to use glyphs to visually encode the avalanche risk on the map. However, the critical areas we want to identify and highlight are not necessarily restricted to single points. For visualizing the risk on a tour track a glyph can be used to highlight a crux. In our visualization, the risk is evaluated for the surrounding terrain as well (**R8**), therefore requiring an area of the terrain to be highlighted.

Taking these challenges into consideration, our final design uses blending for the overlays. We set the alpha value of the overlays to 0.5. This way, key features of the underlying orthoimagery are still recognizable while the impact on the uniformity of the color in the overlay is minimal. In addition, we draw labels and vector overlays on top of the risk visualization overlays to provide further guidance for orientation. As our design also allows for quickly switching between different overlays, users may use the map task-dependently: for an overview of the general avalanche situation, the avalanche danger rating with additional text labels is sufficient. When pre-planning for a single tour is performed, the user switches to a view of the tour in combination with the SnowCard or Stop-or-Go overlays. Potential high-risk areas, highlighted in these views, can then be analyzed in detail by reviewing the plain terrain model with orthoimagery. With this interaction design, the different scales of the visual risk encoding (as required in **R5** and **R6**) are incorporated into the planning workflow. Qualitative data gathered in our pilot user study shows that this workflow matches the strategy that backcountry skiers employ in their tour planning process (see Section 7.6.1).

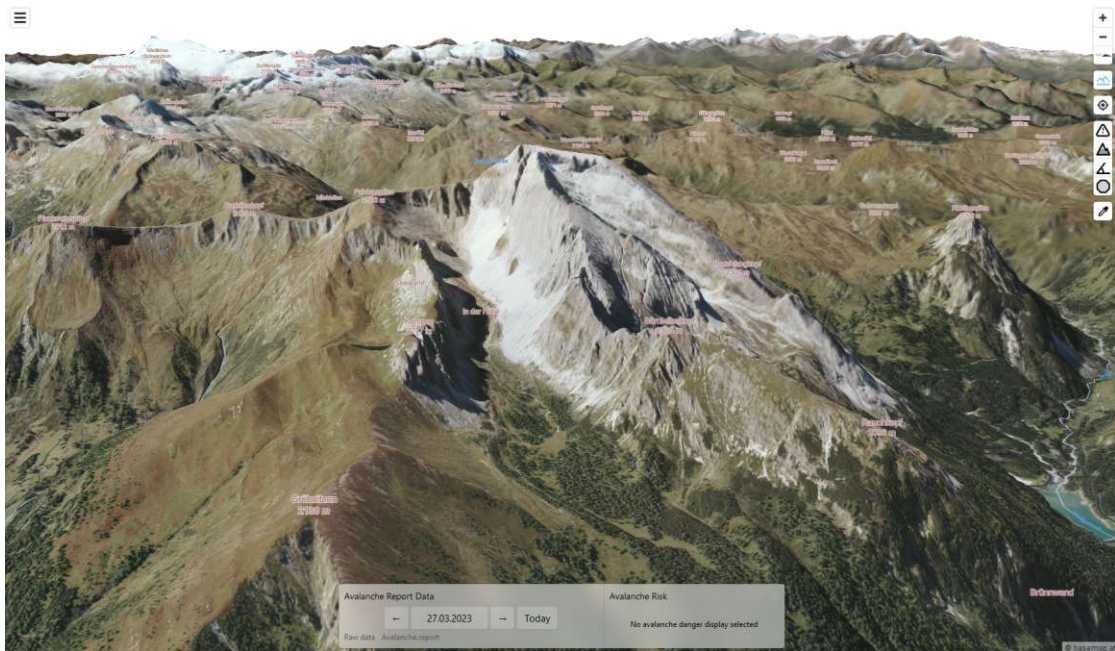


Figure 5.1: 2.5D terrain visualization without overlays.

To encode the terrain-specific aspects of the chosen risk reduction method, an analysis

of the terrain has to be performed. For this, the concept of hill shading as described in Section 2.4 can be adapted to obtain the slope angle as well as the aspect angle for every position on a given terrain model. This way we can calculate and visualize the avalanche risk within the terrain renderer. Working in an existing terrain renderer comes with the benefit of having a multi-scale representation already built in. The terrain tiles, which are the input data for the calculation already have a filtering step for different scales included. Furthermore, by having access to both the DTM and the DSM, we can render the terrain using the DSM with the surface features included for better orientation (**R4**) and recollection of landmark features (see Figure 5.1) while the terrain analysis is based on the DTM. In the following subsections, we present the design of the overlays which we use for avalanche risk visualization.

5.1.1 Slope Steepness Overlay

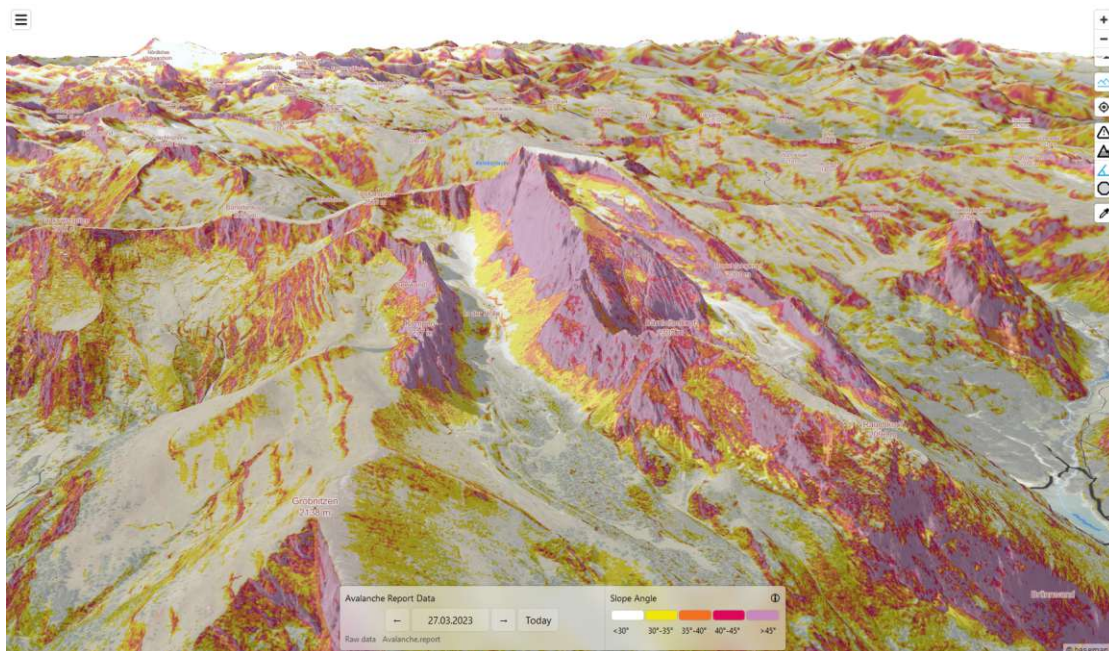


Figure 5.2: 2.5D terrain visualization with slope steepness overlay.

The first overlay for the visualization is a static avalanche risk visualization, which shows the slope angle encoded in a color ramp, akin to implementations in applications such as Bergefex or Skitounguru (see Section 3.1 for details). In contrast to the aforementioned applications, which use pre-computed raster maps for their slope overlay, in our design the slope angle is computed in real-time on the Graphics Processing Unit (GPU), fulfilling requirement **R10**.

Using the method for hill shading by Horn [Hor81] (see Section 2.4), we calculate the slope angle and set the shading color according to a pre-determined color ramp. An example of the slope angle overlay can be seen in Figure 5.2. The slope angle is binned

into five intervals ($[0^\circ, 30^\circ]$, $[30^\circ, 35^\circ]$, $[35^\circ, 40^\circ]$, $[40^\circ, 45^\circ]$, $[45^\circ, 90^\circ]$), each of which is assigned a color value.

For the visual encoding of slope steepness, there exists an established color scheme that can be found across other applications such as Skitouren guru, White Risk, Bergfex, and Fatmap (see Section 3.1). The color encoding uses a multi-hue sequential color scheme as seen in Figure 5.3. As this color scheme is widely used, we choose it to represent the slope steepness in our visualization.



Figure 5.3: Color scheme used for encoding the slope angle.

5.1.2 Avalanche Danger Rating Overlay

Finding a suitable visual encoding for the risk level is a difficult task as the visualization style has to bridge the gap between an intuitive, accessible encoding and existing visualizations that are familiar to users. As discussed in Section 2.1, the standardized avalanche report already comes with a visual encoding for avalanche danger, which is widely known to the users. The red-green color map is omnipresent in online reports, maps, and even visualizations of risk reduction methods, such as the SnowCard or Stop-or-Go. Skitouren guru (Section 3.1) has adopted a modified version of this color scale for its risk encoding on individual tours. While the red-green color scale is problematic for people with deuteranopia, it can be argued that changing the risk encoding to an unfamiliar color scale decreases the intuitiveness of the visual encoding when it comes to visualizing legacy avalanche danger levels as provided by the reports. For this reason, we keep the red-green color scheme for the avalanche danger rating in our visualization, being fully aware that it limits the accessibility of our visualization when it comes to users with a color vision deficiency. The final color scheme used for the avalanche danger rating is shown in Figure 5.4.

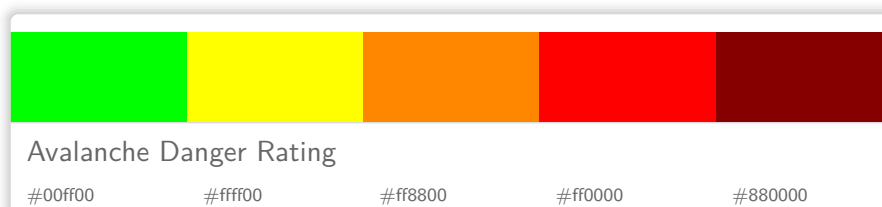


Figure 5.4: Color scheme used for encoding the avalanche danger rating.

The avalanche danger rating overlay visualizes the time-dependent avalanche report information on the terrain and therefore is a dynamic avalanche risk visualization. For this visualization, the terrain data, the parsed avalanche report, and the region areas are the inputs. To determine the avalanche danger rating for a point on the map, a lookup in the parsed avalanche report is performed. For this lookup the elevation value is extracted from the terrain data and the region index is computed from the region data. Table 5.1 shows an example snippet of the internal avalanche report representation.

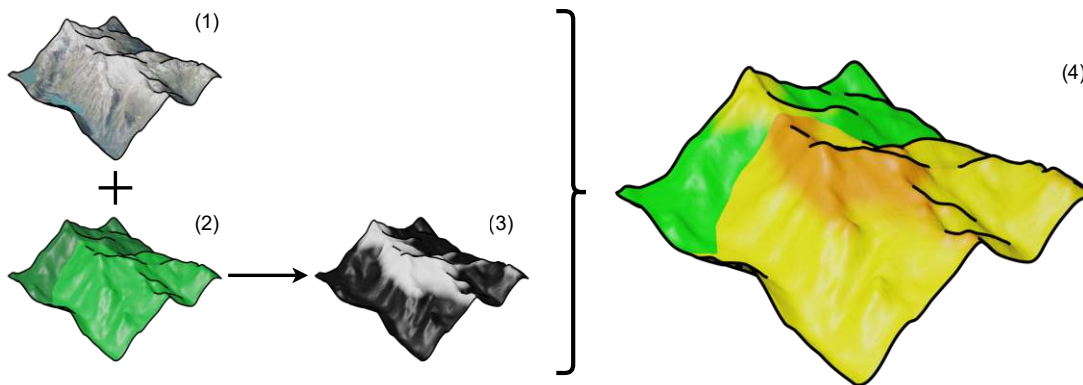


Figure 5.5: Inputs and processing steps for the avalanche danger rating overlay. The terrain model (1) and the region IDs (2) are texture inputs. For each fragment, the height is evaluated, and the height border is set according to the region and avalanche report (3). Finally, each height section and region is colored according to the danger rating (4).

Index	Danger Border	Rating High	Rating Low	Unfavorable
0	1800	2	1	221
1	2000	3	1	0
2	2000	3	2	255
3	2200	3	2	255

Table 5.1: Example lookup table for the internal avalanche danger rating representation on the GPU side. Note that the “Unfavorable”, which encodes unfavorable expositions is not used for the avalanche danger rating overlay. For more information on the processing of expositions see Section 6.2.

For each position on the terrain, the region index is read from the region texture, and the avalanche danger information is looked up in the danger rating table. In addition, the height information is extracted from the terrain data. With the height information and the danger rating, we then color the overlay according to the selected danger rating. An overview of the input data and the processing steps is shown in Figure 5.5. In the

region close to the danger border, the danger rating is linearly interpolated to avoid a hard border in the visualization. This interpolation is performed by shifting the border height 200 m towards the lower rating and filling the gap with an interpolation between the two rating values. The interpolation is visible in Figure 5.5 (4), where orange (danger level 3) blends with yellow (danger level 2).

As the border elevation in the avalanche report may also be given as the treeline or timberline, we have to consider this in the design of this overlay. For our prototype implementation, we set this height to a fixed value of 1600 m. This is based on a survey of timberline elevations in the Alps by Köstler and Mayer [KM70], who set the lower bound for the timberline to 1600 m. As this value may vary from region to region, a potential future improvement could be to set the timberline border per region or to use an additional map that contains the timberline data at a higher resolution.

5.1.3 Reduction Method Overlays

While we have decided on the SnowCard and Stop-or-Go reduction methods for the overlays in the prototype application, the general design decisions for visualizing reduction methods could also be applied to implement other methods. For this reason, in this section, we discuss the abstract design decisions before detailing the individual reduction methods in the following two sections.

Risk reduction methods compute the terrain-based risk factor using the avalanche danger rating, the slope steepness, and the favorable or unfavorable expositions. The outcome of this computation can then be visualized using a color scheme. In our design, the inputs for the evaluation are realized as a three-dimensional lookup table. Each cell in the table represents the risk value for a given combination of slope steepness, danger rating, and exposition, as illustrated by Table 5.2.

	Danger Ratings		Danger Ratings
Slope Steepness	Risk Values	Slope Steepness	Risk Values

(a) Favorable expositions (b) Unfavorable expositions

Table 5.2: Lookup table structure for reduction method overlays.

To arrive at a risk value for a position on the terrain, the slope steepness is obtained from the terrain model using the method described in Section 5.1.1. The value of the avalanche danger rating is obtained using the method described in Section 5.1.2. Note, that this value may be an interpolated value between two integers. In the implementation

of the specific reduction method, this must be handled by either rounding to an integer or interpolating the risk value accordingly. For the third and final dimension, we perform a check on whether the terrain position lies in a favorable or an unfavorable exposition. The exposition is calculated using the method by Burrough and McDonnell [BM98] (see Section 2.4). To evaluate whether an exposition is unfavorable, we use Algorithm 5.1.

Algorithm 5.1: Evaluate Exposition

Input: Aspect angle α (in degrees), integer I encoding unfavorable expositions
Output: Returns *true* when α is unfavorable.

```

1  $range \leftarrow \frac{360}{8}$ ;
2  $index \leftarrow \lfloor \frac{(\alpha + 22.5) \bmod 360}{range} \rfloor$ ;
3 if  $2^{7-index} \wedge I$  then
4   | return true;
5 end
6 return false;
```

The algorithm for evaluating the exposition takes the aspect angle α of the point on the terrain and the integer I containing the 8-bit encoded unfavorable expositions (see Section 6.2) as inputs. The aspect angle is converted into an index ranging from 0 to 7, each representing one exposition (north to northwest). For the calculation, the angle is shifted by 22.5 degrees such that north corresponds to the interval $[0^\circ, 45^\circ]$. To determine whether the current exposition overlaps with the unfavorable expositions encoded in I , I is compared with $2^{7-index}$ using the logical AND operator. If the comparison returns *true*, the point has an unfavorable exposition.

With all three dimensions known, we perform a lookup in the table and arrive at the risk value for the terrain position. To visualize this value, we encode it in a color value based on the color scheme for the given reduction method. Using this generalized design for applying reduction methods algorithmically, we could, conceptually also implement hybrid methods. For example, a modified lookup table for Stop-or-Go could visually encode the risk level in “Stop” areas using multiple colors similar to the SnowCard. This flexibility also allows us to add new methods or update existing ones, without having to change the design of our system.

5.1.4 SnowCard Overlay

For the visual risk encoding of the SnowCard overlay, we base our design on a custom color scheme. The SnowCard uses the same red-green color map as the avalanche report. Using the same encoding for different data, however, might be confusing to the users. Especially for our design, where an important aspect of the interaction is to quickly switch between overlays, the data type should immediately be recognizable from the visual encoding. One potential encoding for the SnowCard risk would be to combine it with an additional data channel, such as the static slope or ATEs map. As highlighted by

Šašinka et al. [ŠSK⁺19] the effectiveness of bivariate color maps depends on the cognitive style of users and may therefore impact the readability of our visualization.

As the risk evaluation resulting from the SnowCard heuristic is a one-dimensional strictly rising numerical value, a sequential color map provides an intuitive representation. Therefore, we use a sequential multi-hue color map instead of the diverging red-green color map in the SnowCard. The final color scheme for the SnowCard risk encoding can be seen in Figure 5.6. It is a modified version of the 5-class YlOrRd color map by ColorBrewer [HB03] where we exchanged the first field for white, instead of the original yellow hue. This is done to lower potential conflicts between the color-encoding of the low-risk level and the underlying orthoimagery. An alternative would be to make the lowest risk level 100% transparent. This, however, would conflict with our encoding for areas with missing data, as these are rendered without any overlay by default.

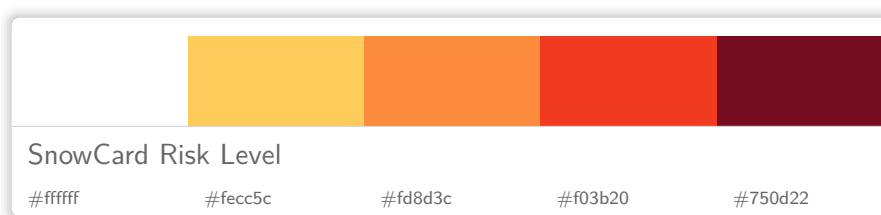


Figure 5.6: Color scheme used for encoding the risk level based on the SnowCard.

For the SnowCard risk encoding, an additional consideration we have to make is the fact that the SnowCard is only defined for slope angles between 27° and 42°. Values outside of this interval are not covered by the model. In our design the risk for slope angles below 27° is rendered in the same style as for those with 27°, effectively clamping the slope angle to a lower bound of 27°. This can be justified by the fact that at worst it leads to an overrepresentation of the risk level for these areas. For areas with a slope angle above 42°, however, we cannot make the same assumption as it cannot be assumed that avalanche risk stays constant beyond this value. Instead, we take 45° as a boundary to introduce a sixth color class in this visualization. 45° matches the cutoff found in the slope map, making it consistent with the classification for very steep terrain. The values between 42° and 45° are clamped to the highest rating of the SnowCard, analogous to the lower boundary. The areas that are steeper than 45° are encoded with a dark gray color to indicate that the underlying terrain is likely rocky and no definitive risk value is associated within the framework of the SnowCard. In addition, at slope angles beyond 45° the danger of falling increases, which is thereby also indicated by the change in color. This design choice is in line with visual encodings used for the CAT and ATH maps (see Section 3.1). In their case, extreme terrain is also encoded with gray values, although the cutoff is set to 50° instead of 45° as in our design.

For this overlay, the SnowCard reduction method is evaluated based on the general reduction method evaluation described in Section 5.1.3. Figure 5.7 displays an overview of the inputs and processing steps necessary to obtain the SnowCard risk overlay.

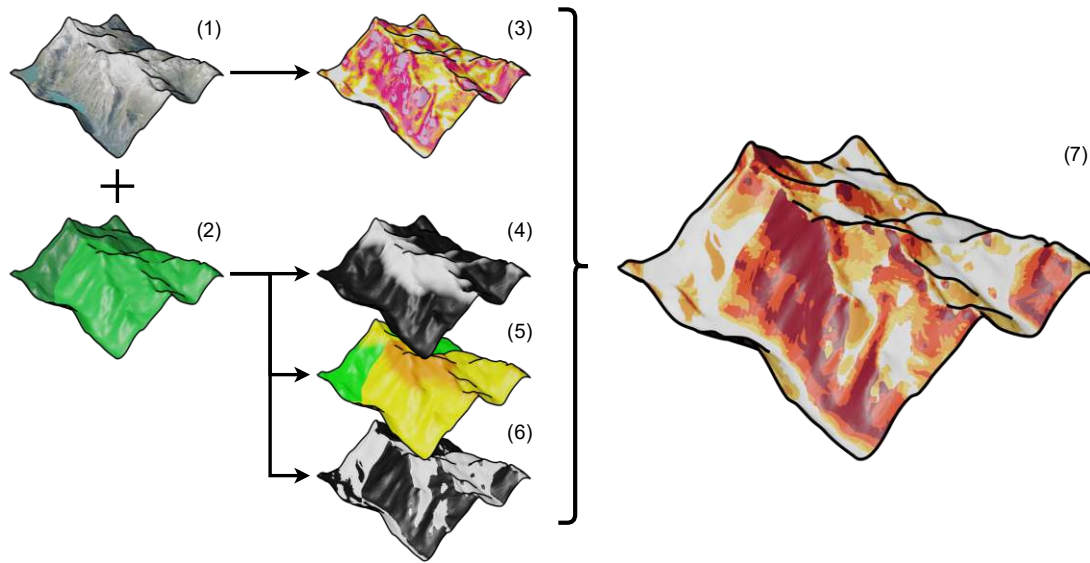


Figure 5.7: Overview of the SnowCard overlay. The terrain model (1) and the region IDs (2) are texture inputs. From the terrain model, the slope map (3) is calculated. For each fragment, the height border is set according to the region (4) and the rating is calculated according to the avalanche report (5). The exposition is classified as favorable (white) or unfavorable (black) (6) for each region. By combining slope, danger rating, and exposition, the risk level is calculated and displayed on the terrain model (7).

As the danger rating is provided as integer values, we perform a discretization of the SnowCard, only keeping the values at the top-right corners of the original grid cells (see Figure 2.4). Using the three-dimensional lookup table, we obtain the SnowCard risk rating by sampling our discretized version. Table 5.3 shows our discrete version of the SnowCard for both favorable and unfavorable expositions. Due to the linear interpolation along the border of two avalanche danger rating values, the rating for a given position is not necessarily an integer value in our internal danger rating representation. Therefore, within the SnowCard lookup table, we also perform a linear interpolation. The final result of the SnowCard layer overlaid on the terrain model can be seen in Figure 5.8.

By evaluating the risk in real-time for the current zoom level, the risk visualization fulfills the multi-scale requirements (**R5** and **R6**). However, when obtaining the slope angle at lower zoom levels, the slope will automatically be smoothed, skewing the risk level calculation. Small-scale steep parts disappear altogether, which lowers the overall danger rating. To overcome this problem an aggregation instead of interpolation would be necessary for lower zoom levels. Alternatively, a pre-computed slope map could be used. These methods, however, would skew the risk visualization in the opposite direction, amplifying the rating based on small-scale risks. As both options may lead to confusion

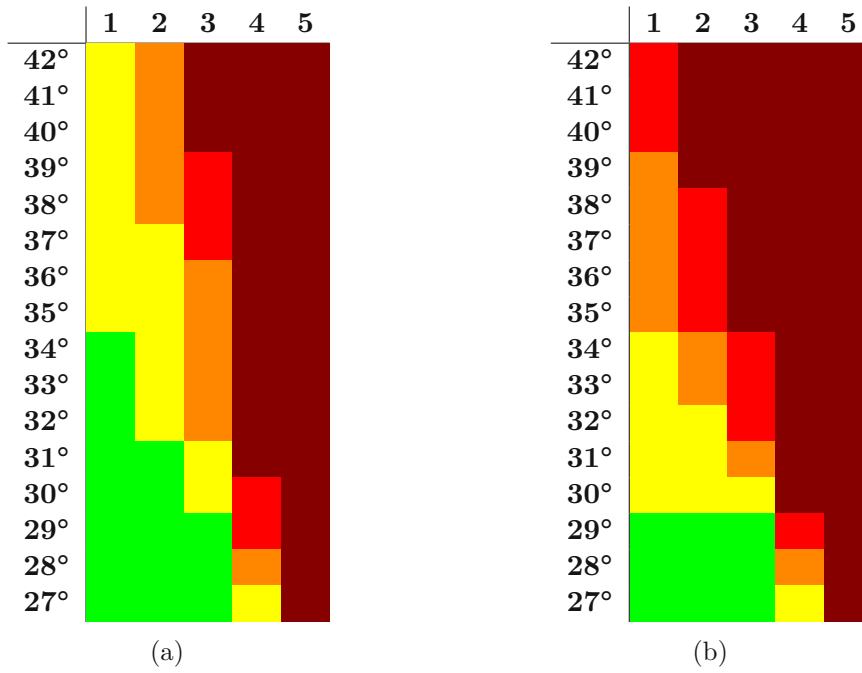


Table 5.3: Discretized lookup table for the SnowCard risk overlay, showing risk(a) favorable expositions and (b) unfavorable conditions.

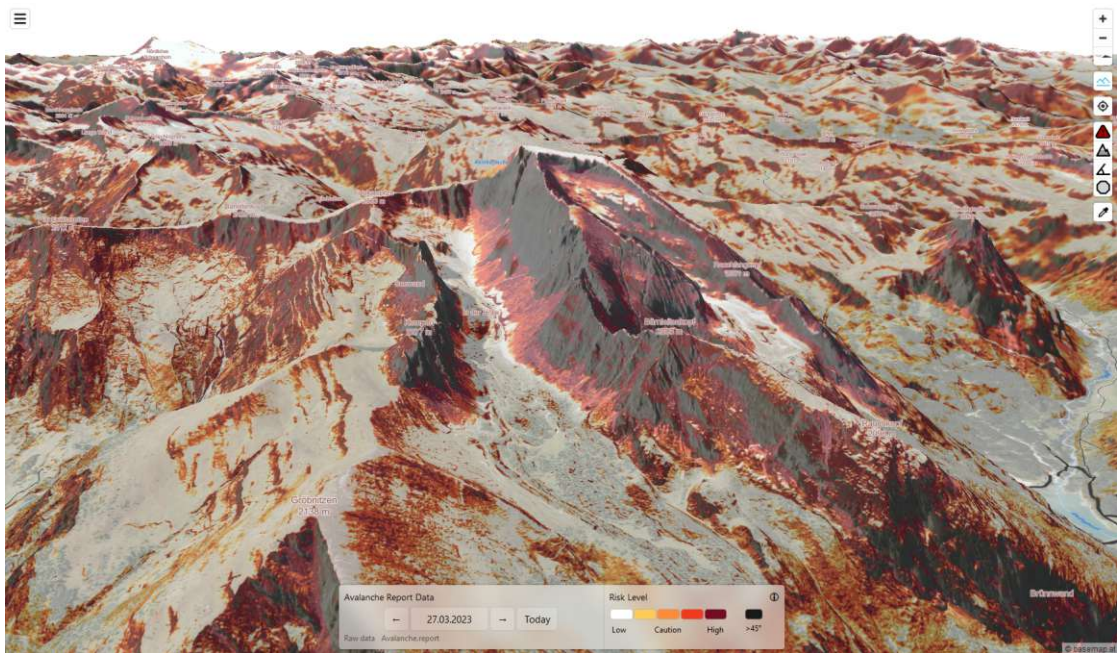


Figure 5.8: 2.5D terrain visualization with SnowCard risk overlay.

for the user we instead provide different visualization types for different scales: for a large-scale overview we provide the avalanche danger rating and for small-scale detail views, we provide the terrain-based risk overlays. The final choice of visualization style is, however, up to the user with both options available at all zoom levels.

5.1.5 Stop-or-Go Overlay

The second dynamic avalanche risk visualization overlay implements the terrain evaluation of the Stop-or-Go method (see Section 2.2). Similarly to the SnowCard, this visualization is a dynamic risk visualization as it combines terrain data with time-dependent data from the avalanche report. Implementing the generalized reduction method overlay from Section 5.1.3, each point on the terrain is classified as either “Stop” or “Go”, depending on the avalanche danger rating and the slope steepness (see Figure 5.9). Slope steepness is binned in four classes for the intervals $[0^\circ, 30^\circ]$, $[30^\circ, 35^\circ]$, $[35^\circ, 40^\circ]$, and $>40^\circ$. Note that the Stop-or-Go method does not define an overall maximum steepness. Therefore, we do not add an extra encoding for extremely steep areas, with a slope angle of more than 45° . As the version of Stop-or-Go we choose to implement does not explicitly contain expositions in the terrain evaluation, we also do not consider the exposition in the Stop-or-Go computation, even though we have the data available. The resulting lookup table (Table 5.4) is therefore only two-dimensional.

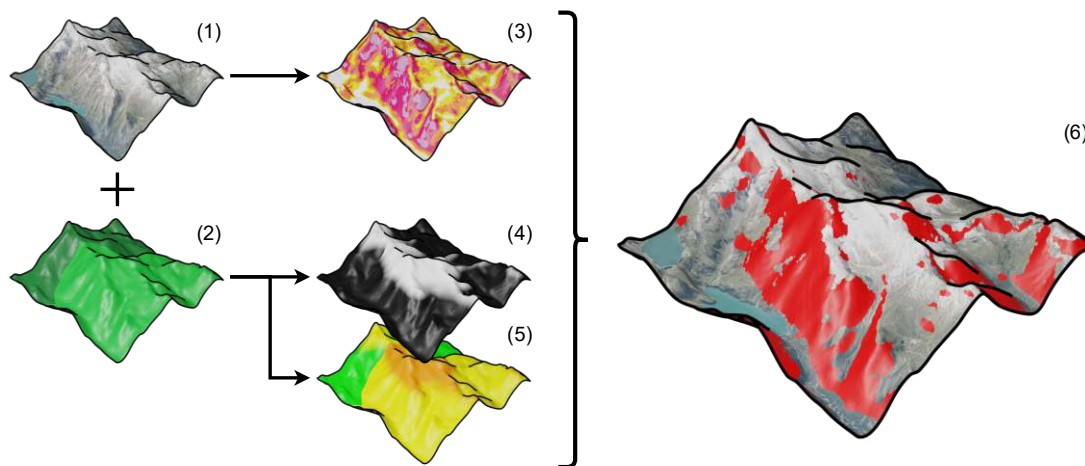


Figure 5.9: Overview of the Stop-or-Go avalanche risk overlay. The terrain model (1) and the region IDs (2) are texture inputs. From the terrain model, the slope map (3) is calculated. For each fragment, the height border is set according to the region (4) and the rating is calculated according to the avalanche report (5). The final visualization (6) shows areas marked “Stop” in red, overlaid on the terrain model.

This risk overlay differs from the other overlays as it displays a binary value. To that extent, we also adjust the visualization to only highlight areas where the “Stop” condition

	1	2	3	4	5
0°-30°	1	1	1	1	0
30°-35°	1	1	1	0	0
35°-40°	1	1	0	0	0
>40°	1	0	0	0	0

Table 5.4: Stop-or-Go lookup table. 1 = “Go”, 0 = “Stop”.

is met. These areas are highlighted with a red overlay using the same semi-transparent blending scheme as the other overlays. This way, areas classified as “Go” do not have the problem of visual interference between the orthoimagery and the overlay, as we set the alpha value to 0. While the downside of this design choice is that we lose the distinction between missing data and “Go” values, the recognizability of key terrain features is much improved. This increased recognizability is advantageous for orientation, as additional factors such as tree cover influence the final risk assessment of a given tour. Since there is no sensible interpolation between “Stop” and “Go”, the marked areas have a hard border. Figure 5.10 displays an example of how this overlay integrates with the terrain model.

Apart from the tree cover, the Stop-or-Go reduction method contains other additional factors. These factors include catchment areas or previous tracks. In the risk visualization, however, these factors are not considered as information about these factors is not present in the input data. For tour planning purposes, the user therefore still has to manually integrate these missing factors into the decision-making process.

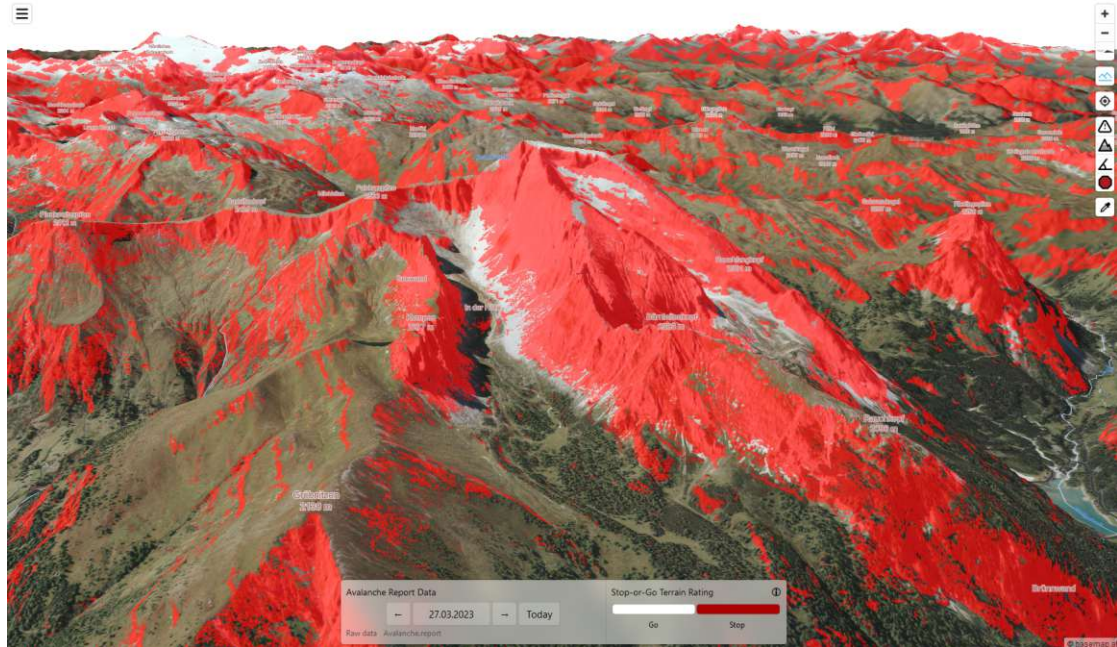


Figure 5.10: 2.5D terrain visualization with Stop-or-Go overlay.

5.2 User Interface

The design of the user interface is centered around guiding user attention toward areas of high risk in the tour planning process (**R3**) as well as providing a detailed terrain representation for on-site recognition of terrain features (**R4**). As a result of these design considerations, the main element of the user interface is a map view, which covers the whole viewport. Apart from the map view, the user interface contains an area for controlling the avalanche report display on the bottom, a collapsible panel to manage tour planning on the left, and a control panel for the map, which allows for switching between the different overlays. A schematic overview of the interface is shown in Figure 5.11.

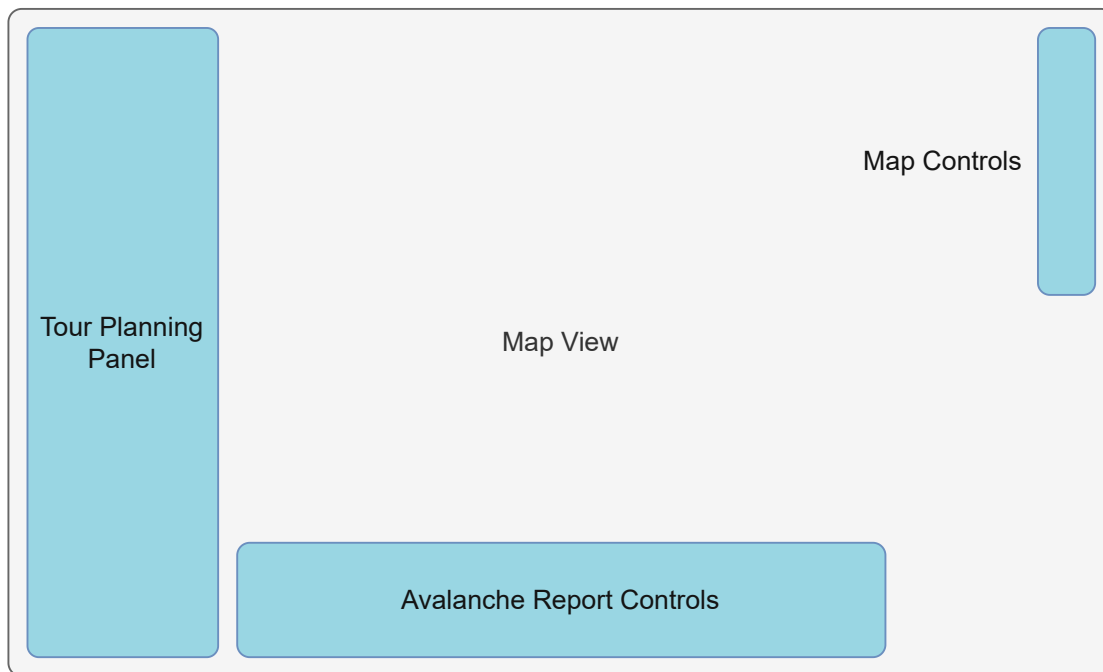


Figure 5.11: Schematic overview of the desktop user interface of our map application.

The main map view is set to display the orthoimagery as the base map layer, with the option to overlay the previously mentioned layers on top of it. This functionality is present in similar applications and therefore does not require users to re-learn map interaction. In addition to the orthoimagery, the base map layer also includes text labels for map features such as roads, settlements, and mountain peaks. As we are working with a 3D map application, we have to manage occlusion and cluttering among the labels as discussed in Section 2.4. In particular, this means performing depth tests for labels and fading them out in case they are occluded by terrain geometry.

To fulfill the interactivity design requirement (**R7**), the user interface offers options to navigate the map via panning, zooming, and changing the view angle using mouse controls and touch gestures on mobile devices. As an additional navigation option, the

tour planning panel contains a search box that allows for direct access to geocoded locations. Furthermore, a geolocation option is present to allow the user to display their current location on the map.

Interaction for the time-dependent avalanche report data, as required by requirement **R9** is handled through a separate control panel, which is located at the bottom of the viewport. This panel is split into two sections, the one on the left is dedicated to manipulating the avalanche report data input. Here, a date picker allows for choosing for which day the avalanche data should be displayed. The right side of the panel is related to the currently selected avalanche risk visualization mode. It shows a text label with the overlay name, the legend for the color encoding scheme, and an info button that toggles a short description of the visualization which links to more in-depth information sources. As our visualization only displays the machine-readable part of the avalanche report data, we provide a link to the full avalanche report, which includes the detailed written report, in the avalanche report control panel.

The design of the tour planning aspect centers around the ability to display tour tracks on the map, which can then be viewed in context with different risk visualization overlays. Adding tour tracks is possible via the tour planning panel, where tracks can be uploaded by the user. In contrast to other tools, however, the tour tracks are not required for the risk visualization as we expand the risk visualization beyond pre-defined tour tracks (**R8**).

Apart from the map-related interactivity, our design requirements call for the ability to display the risk at different scales (**R5** and **R6**). In the user interface, this is realized through a group of buttons, which correspond to the different risk overlays. The overlays can be selected one at a time, with none selected as the default option.

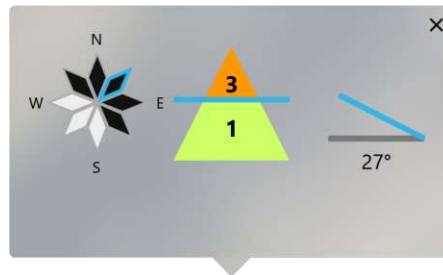


Figure 5.12: Popup with glyphs representing the current exposition (left), elevation with regards to the avalanche danger rating (center), and slope angle (right).

To allow the users to gain additional insights and to make the computations performed in our algorithmic reduction method implementations more transparent to them, we introduce an interactive *picker mode* to our visualization. This tool, when activated, allows the users to sample any location on the map to obtain information on exposition, avalanche danger rating, and slope angle. The picker mode is independent of the active overlay, which allows for accessing slope and danger rating information without changing

to the respective overlay. The information for a picked coordinate is visualized in a popup via three dynamic glyphs (see Figure 5.12). The exposition is represented using a stylized wind rose with the same visual encoding as present in the avalanche report. A blue highlight indicates the exposition at the picked coordinated while all unfavorable expositions for the current region are marked in black. For the danger rating information, a glyph displays the danger ratings present at different elevations with a blue line indicating the current elevation relative to the danger ratings in the respective area. The slope angle is visualized with a blue line, which mimics the slope of the picked terrain. In addition, the numerical slope value is displayed.

To provide an understanding of what the context of a given tour is, we draw the tour track overlaid on top of all other layers such that it is always recognizable on the map. Here, we choose a blue hue, which is far removed from the color schemes used for the overlays, providing the necessary contrast to avoid interference with the risk overlay. Figure 5.13 shows how the track interacts with different risk visualization overlays.

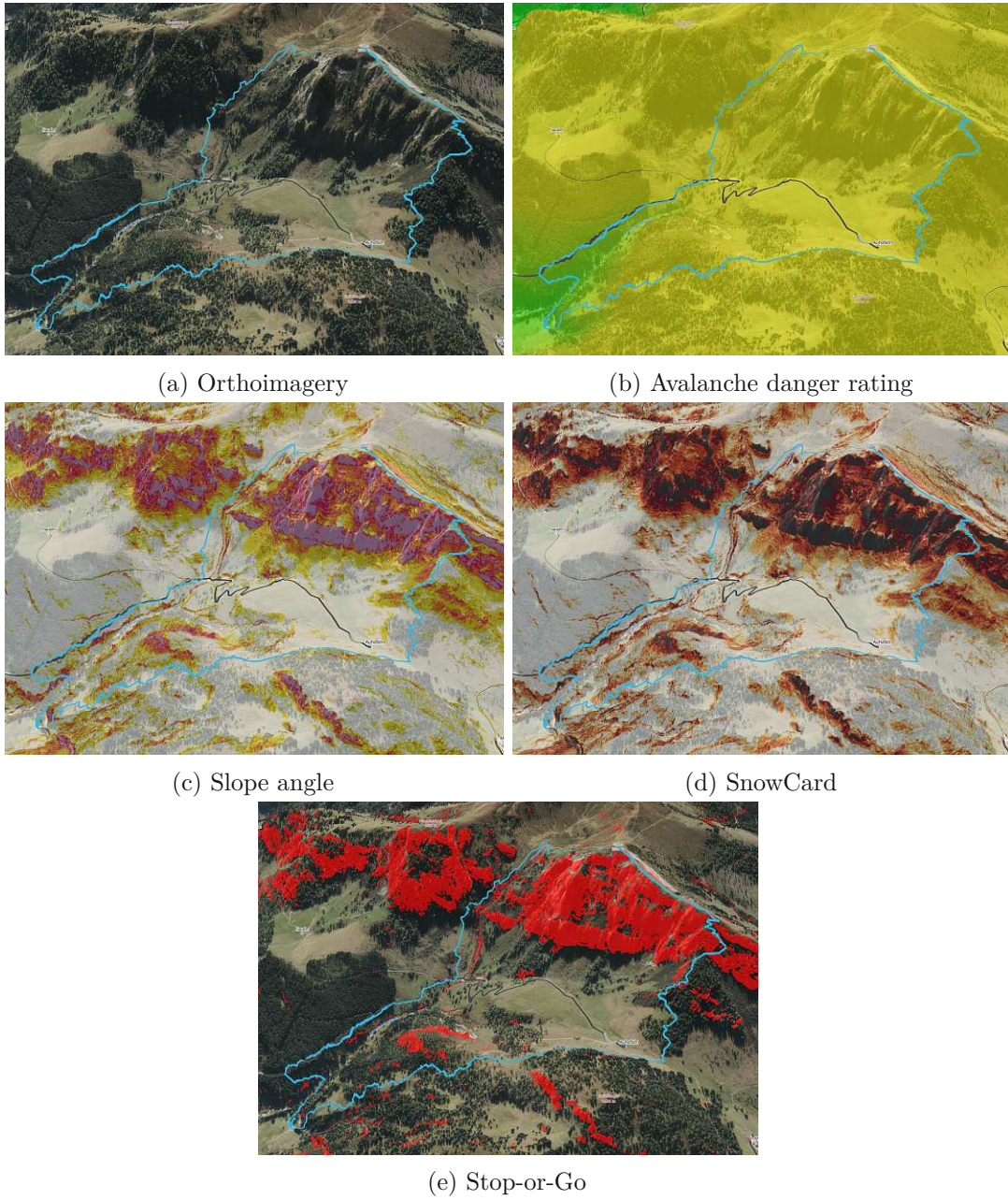


Figure 5.13: Tour track in combination with different overlays.

Implementation

Having settled on a design for our visualization, in this chapter, we present the implementation of our prototype application. This implementation includes a pipeline for performing pre-processing to transform the raw data into a format compatible with our visualization pipeline. The pre-processing steps cover both static and dynamic data. Furthermore, we present how we extend the MapLibre [Map23c] map rendering framework to render our visualization using a custom shader pipeline. We present details of the implementation of the user interface and interaction and conclude with a look at the real-time performance of our implementation.

6.1 Static Data Preprocessing

As illustrated in the system overview (Figure 4.1), the static preprocessing stage converts static data from external sources into an internal representation, which is then stored on our tile server. For our DEM, this preprocessing consists of building a tile pyramid, that is compatible with the web renderer. The raw elevation data we utilize is provided by the Austrian government via its open data initiative [Geo23]. The DEM is available as a DTM and a DSM, which both need to be transformed into raster tiles compatible with the map renderer.

As our prototype application is based on the MapLibre framework [Map23c], we have to preprocess our DEM data to be compatible with the encoding scheme in MapLibre. Therefore, we utilize the Mapbox RGB encoding scheme as described in Section 2.3.2. We use tiles with a resolution of 256×256 pixels, which we generate up to zoom level 18. The height encoding is performed using Algorithm 6.1, applied to each pixel in a tile.

This elevation encoding provides a base-256 number for each data point. The tile generation is performed using a parallelized implementation on a machine with an AMD Ryzen 9 3900X 12-Core processor and 128 GB RAM, which is able to process an average

Algorithm 6.1: Encode Elevation in RGB

Input: Height h (in meters)
Output: \vec{x} with $\vec{x} = (r, g, b)$

- 1 $h = h + 10000$;
- 2 $h = h/0.1$;
- 3 $b \leftarrow \lfloor \frac{h}{256} - \lfloor \frac{h}{256} \rfloor * 256 \rfloor$;
- 4 $g \leftarrow \lfloor \lfloor \frac{h}{256} \rfloor / 256 - \lfloor \lfloor \frac{h}{256} \rfloor / 256 \rfloor * 256 \rfloor$;
- 5 $r \leftarrow \lfloor \lfloor \lfloor \frac{h}{256} \rfloor / 256 \rfloor / 256 - \lfloor \lfloor \lfloor \frac{h}{256} \rfloor / 256 \rfloor / 256 \rfloor * 256 \rfloor$;
- 6 $\vec{x} = (r, g, b)$;
- 7 **return** \vec{x} ;

of 50 tiles per second. Generating tiles for levels 0-18 (approximately 28.8 million tiles) for the bounding rectangle of Austria, therefore, takes approximately 160 hours.

As we eventually need to access the region information in the fragment shader to process the avalanche risk for each pixel, the region data need to be rasterized. Therefore an additional preprocessing step is performed for the regions for which the avalanche report is published. Instead of rasterizing in a preprocessing step, the region information could also be passed to MapLibre as a vector layer. While this layer could be directly drawn on the map in MapLibre, this approach would require an additional render pass to first rasterize the polygon features and then pipe them to the GPU. Another possible option would be to directly pass the polygons of the region shapes to the GPU and perform an inside test for each fragment when the risk is evaluated. As all the other data is rasterized, the approach would introduce unnecessary complexity to the system. So instead, we perform the rasterization offline and access the region information via a texture lookup. This approach decreases the computational complexity but increases the bandwidth as an additional raster tile set has to be loaded.

The regions are provided by the EAWS [Ser23b] as GeoJSON files. Since the regions are a static information source, the rasterization step can happen as a static preprocessing step.

The preprocessing for the region ID raster tiles is done using QGIS [QGI23]. In the first step of the region data rasterization, the regions are sorted in ascending order for each state and their IDs are converted into 24-bit RGB values. For example, the region with the ID AT-05-17 is encoded as 000101 010001 0000 00100010, where the first 6 bits are the state ID (05 in this case), the next 6 bits are the region ID (17), 4 bits are reserved for an optional 4-bit sub-region ID, and the final 8 bits represent the total offset in the list of regions. The resulting 24-bit number is converted to an RGB value and added to the regions GeoJSON file as a fill color. The results of the color-to-ID encoding are visualized in Figure 6.1. The GeoJSON file is then imported into QGIS and a raster tile pyramid is created for zoom levels 0-18.

All generated raster tiles are hosted on a tile server, which is indexed using the *Slippy*

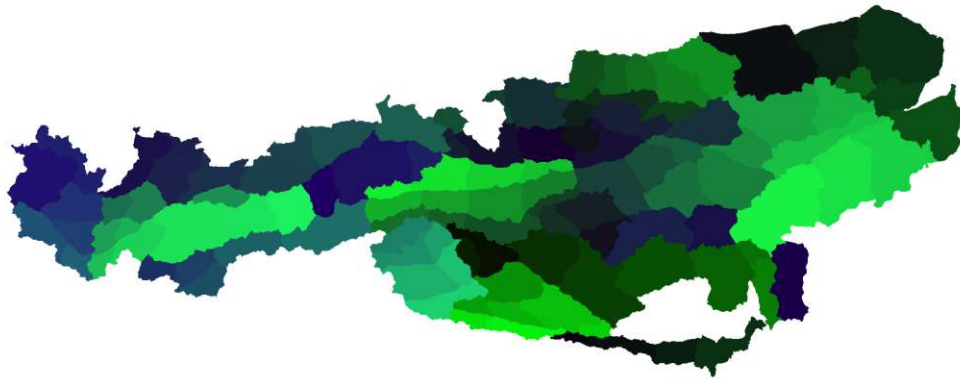


Figure 6.1: Regions of Austria covered by the Avalanche Warning services. Regions IDs are encoded in the color values for each region.

Map tiling scheme. Each raster tile type is added to MapLibre as a so-called “raster source” and can then be directly drawn on the map.

6.2 Dynamic Data Preprocessing

The dynamic data preprocessing step takes place every time avalanche report data is requested by the renderer (see Figure 4.1). For a given date and time, avalanche reports in the CAAML format are fetched from the central avalanche warnings server of Austria. This is handled by a custom Node.js server. The server listens for a GET request at the URL `/get-current-report`, which has an optional `date` URL parameter, expecting a date in the format `YYYY-MM-DD`. If no parameter value is provided, the server will try to get the report for the current day in reference to the server time.

For requesting and parsing avalanche reports, the server application comes with an `avalancheReportAPI` module. To avoid unnecessary requests to the server of the avalanche warning services and to not parse the same data multiple times, the server caches the processed reports. When a request for an avalanche report is received, the server checks whether a cached version is available. If so, the locally cached avalanche report is returned immediately. As the Austrian Avalanche Warning Services publish at most two reports for a single day, it is sufficient to only request the live report if the requested date is no older than 24 hours. For requests concerning the current or future days we set a cache interval of 10 minutes, within which repeat requests are allowed. Apart from receiving a potentially updated version of the report, this also allows us to compensate for publishing time variance. Not all states publish their reports at the same time. In our internal data representation, however, the avalanche report data from all states are consolidated into a single file. As a result, as soon as there is data from a single

state available, we will have a valid file, albeit with missing data for the remaining states.

In case no cached version of the avalanche report is present on the server, or the cache validity has expired, we fetch the avalanche report data from the live server. The CAAML report files on the avalanche warnings server are stored as XML files with unique IDs. Via an API endpoint on the server, we get a JSON file containing a mapping from a date to the corresponding IDs. For each EAWS region defined in our regions map (see Section 6.1), an empty report object in our internal data representation is generated. Finally, we parse the CAAML files and fill in the obtained avalanche danger ratings into the empty report objects.

For the parsed reports, we use an internal data representation, which allows us to store avalanche danger rating information in one object per region. Listing 6.1 shows an example of two avalanche danger rating objects for two regions of Carinthia.

```

1 [
2   {
3     "regionCode": "AT-02-01-00",
4     "dangerBorder": 1800,
5     "dangerRatingHi": 3,
6     "dangerRatingLo": 1,
7     "startTime": "2023-01-16T23:00:00.000Z",
8     "endTime": "2023-01-17T23:00:00.000Z",
9     "unfavorable": 255
10  },
11  [...],
12  {
13    "regionCode": "AT-02-04-00",
14    "dangerBorder": null,
15    "dangerRatingHi": 3,
16    "dangerRatingLo": 1,
17    "startTime": "2023-01-16T23:00:00.000Z",
18    "endTime": "2023-01-17T23:00:00.000Z",
19    "unfavorable": 243
20  },
21  [...],
22 ]

```

Listing 6.1: Internal representation of avalanche report data for two example regions.

Each internal avalanche report data object contains a unique `regionCode` ID, which includes country code, state ID, region ID, and sub-region ID. For the regions in Listing 6.1, the sub-region is 00, as there are no sub-regions defined for these regions. The `dangerBorder` property defines the elevation at which the rating changes from the rating for lower elevations (`dangerRatingLo`) to the one for higher elevations (`dangerRatingHi`). For this internal representation, we make the assumption that there is a maximum of two different danger ratings present for a single region. This is compliant with how the unified avalanche report is currently published in Austria. In case there is only a single, height-independent danger rating within a region, the border height is set to 0. A null value in the `dangerBorder` field indicates that there is no

numerical value provided by the avalanche report. This is the case when “Treeline” is reported as the height border in the avalanche report. In this case, the renderer has to find a suitable `dangerBorder` value to be displayed. For our prototype application, this handling is discussed in Section 5.1.2.

Next to the danger rating the report, object also contains information on the timespan for which the report is valid (`startTime` and `endTime`) and information on unfavorable expositions via the `unfavorable` field. Unfavorable expositions are defined via avalanche problems in the avalanche report. They can be present in eight orientations (north, northeast, east, southeast, south, southwest, west, northwest), and multiple avalanche problems can be present in a single region. As the standardized CAAML reports do not distinguish between elevation levels when it comes to avalanche problems, our representation treats them as a global, height-independent influence. With eight sectors, each with the options “favorable” or “unfavorable” we have $2^8 = 256$ possible options for the exposition field. Therefore, the `unfavorable` field takes an 8-bit integer, with each bit representing an orientation. With this setup merging of multiple avalanche problems can be achieved by using the logical OR operator. If problem *A* is present in sectors NW-N-NE (binary 11000001) and problem *B* is present in sectors SE-S-SW (binary 00011100) the operation

$$A \vee B \tag{6.1}$$

or, in binary

$$11000001 \mid 00011100 \tag{6.2}$$

provides the final exposition value as 11011101 or 221.

For regions with sub-regions, the avalanche report may contain a merged representation of the danger rating for the parent region. Since our region data, however, is statically preprocessed, we have to account for this in the report parsing step, duplicating the report object of the parent region for each of the sub-regions. If the opposite is the case and there are multiple reports within a single region, the parser will merge the two report data objects in a conservative manner: it keeps the higher value for each of the danger rating fields, the danger border is moved towards the lower danger rating value (usually decreasing the elevation), and the two values from the unfavorable field are merged again using the logical OR operator. Multiple reports within a region can occur when a region gets subdivided into sub-regions and this change is not yet reflected in the statically processed region data.

After the processing is done, the report object in the internal data format is returned as a response to the initial GET request to the server. In addition, the data is also saved in the server cache.

6.3 Extending the MapLibre Framework with a Custom Shader Pipeline

The core of our prototype implementation consists of a modified version of the MapLibreGL JS web-based map rendering framework. In Figure 4.1, this core is represented as the renderer component group on the right-hand side. The components of this group define the structure of this section.

MapLibre comes with support for rendering 2.5D terrains and the ability to drape raster and vector layers onto the terrain model. We use these features as the basis for implementing our custom shader pipeline for visualizing avalanche risk.

6.3.1 Terrain Evaluation

In MapLibre, a hill shading layer is available, which implements the hill shading method by Horn [Hor81] (see Section 2.4). This layer performs the hill shading calculations for each tile and renders the hill shading using two draw calls: first, in the prepare stage elevation values are queried for an 8-neighborhood around the current fragment, and the slope is calculated via the derivative. The resulting data is saved into a frame buffer. In the second stage, the data from the frame buffer is used to calculate the shading. This color value is then blended with the terrain texture to overlay the hill shading value on the map color data. We use the same terrain evaluation pipeline to compute the slope and aspect angles for the subsequent avalanche risk visualization.

In order to avoid discontinuities in the slope calculation, each tile has to be padded with one pixel per side. The padded border pixels contain the elevation values from the eight neighboring tiles (see Figure 6.2). This padding step is performed at runtime when the tile cache is built.

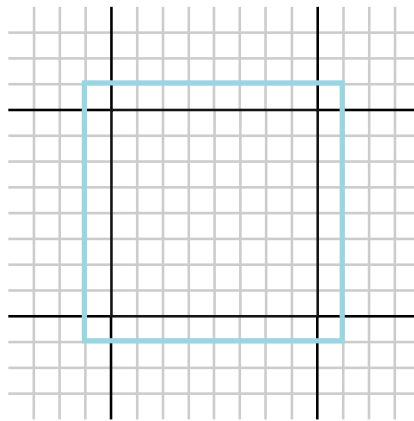


Figure 6.2: Tile padding performed to allow access to elevation data from neighboring tiles in the fragment shader. The padded tile (blue) contains pixels from adjacent tiles.

6.3.2 Passing Region Information to the GPU

As MapLibre limits layers to a single source, the region raster tiles have to be added as an additional layer with their respective raster source. The tile cache from this layer can then be referenced in the avalanche layer specification, to bind the region raster image for each tile to its avalanche prepare shader.

6.3.3 Obtaining the Avalanche Report

As WebGL 1.0, which is the version that MapLibre uses, does not support Uniform Buffer Objects, we use data textures to transfer the avalanche report data to the fragment shader. When initializing the avalanche layer, the report data is parsed and converted into a texture. Each row of the texture contains the avalanche report information for a single region. The rows are indexed in the order of the total offset defined in our internal avalanche report format. The data is encoded into single pixel values similar to the DEM data encoding (see also Section 5.1.2 and Table 5.1 for the avalanche report data encoding). Float values are converted into a 4-digit base-256 number. Values for the `dangerBorder`, which contain `null` are replaced with a configurable height value that represents the timberline.

The avalanche report data texture is generated once when the layer is initialized and is then cached. In case the avalanche report data changes, the texture is regenerated. As WebGL 1.0 only supports textures with a resolution of 2^n pixels, we have to pad the texture array with zeros before binding it to the GPU.

6.3.4 Computing the Avalanche Risk

For our GPU-based avalanche risk visualization, we use the same architecture as the hill shading, where we have two render passes. The first render pass is the prepare stage which is used for evaluating the terrain in conjunction with a lookup of the avalanche rating. By implementing the generalized algorithm for reduction methods (see Section 5.1.3), we obtain a color overlay. The second render pass is then used to blend that overlay with the underlying color texture.

To determine whether a fragment lies in an unfavorable exposition, we convert the aspect angle from the terrain evaluation into the same 8-bit format used in our internal avalanche report representation. In the shader, we then use an explicit binary encoding for the exposition, where the eight binary digits are split into two 4-dimensional vectors. Here, the current exposition of a fragment is represented by two `vec4` variables (e.g. `vec4(1, 0, 0, 0)` and `vec4(0, 0, 0, 0)` for a north-facing fragment). The vectors are both encoded in a single RGBA pixel, where each channel represents one exposition class. As WebGL 1.0 does not support bitwise operators in the shader code, we can cast the RGBA data to `vec4` inputs in the shader and use the dot-product as an emulation for the logical AND operator to perform the exposition check as described in Section 5.1.3. Taking the dot-product of the exposition vectors for the current fragment

and the respective unfavorable exposition values and then summing up the results, we get 1 if the current exposition is unfavorable and 0 otherwise.

6.3.5 Rendering Overlays

The avalanche risk overlay is wrapped in a custom avalanche layer, which takes the DTM raster source, the regions raster source, and the avalanche report JSON as inputs. Additionally, the color mapping and the type of avalanche risk overlay can be specified in the layer definition. This layer is added to the MapLibre core by extending the style specification. An overview of how the avalanche layer is integrated into MapLibre is shown in Figure 6.3. The user selects an avalanche risk overlay in the user interface, which passes the information to the *AvalancheStyleLayer*. Here the style information is parsed to be set as uniforms via the *AvalancheProgram* class. Additionally, the data textures containing the avalanche report information and risk encoding are generated. When the MapLibre *Painter* issues a draw call to the *DrawAvalanche* function, the data textures are bound to the GPU, and the two draw calls are executed for the preparation and blending stages. The final result is saved in a texture buffer, which is then used as a color map for the terrain.

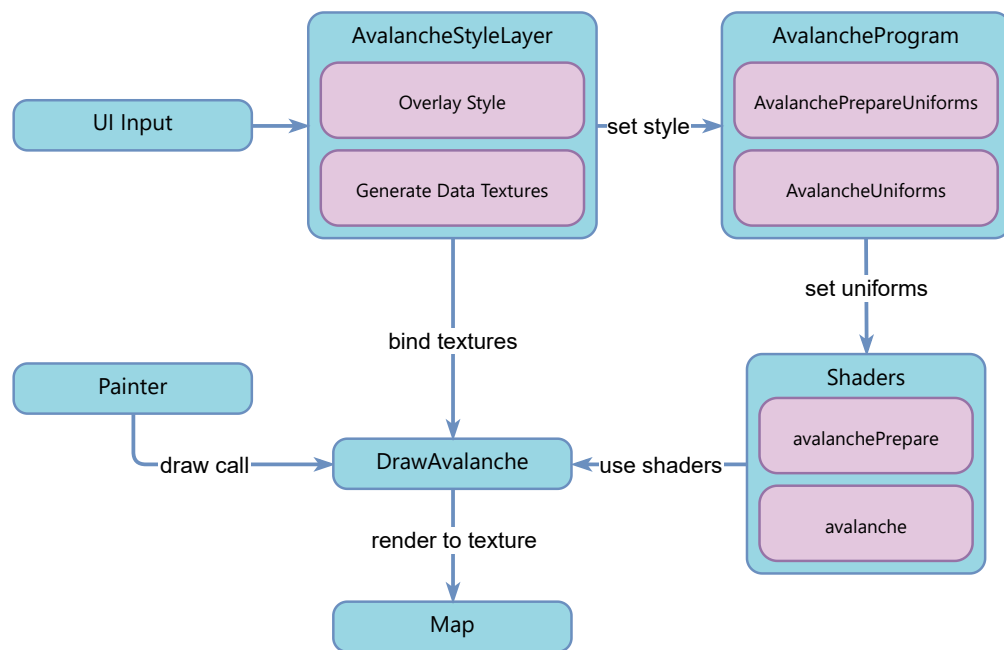


Figure 6.3: Schematic overview of the avalanche layer and its integration into the MapLibre framework.

The overlays that depend on the danger rating from the avalanche report are only drawn for areas that have a valid avalanche report for the selected timeframe. For other areas, the default map style without overlays is drawn (see Figure 6.4).

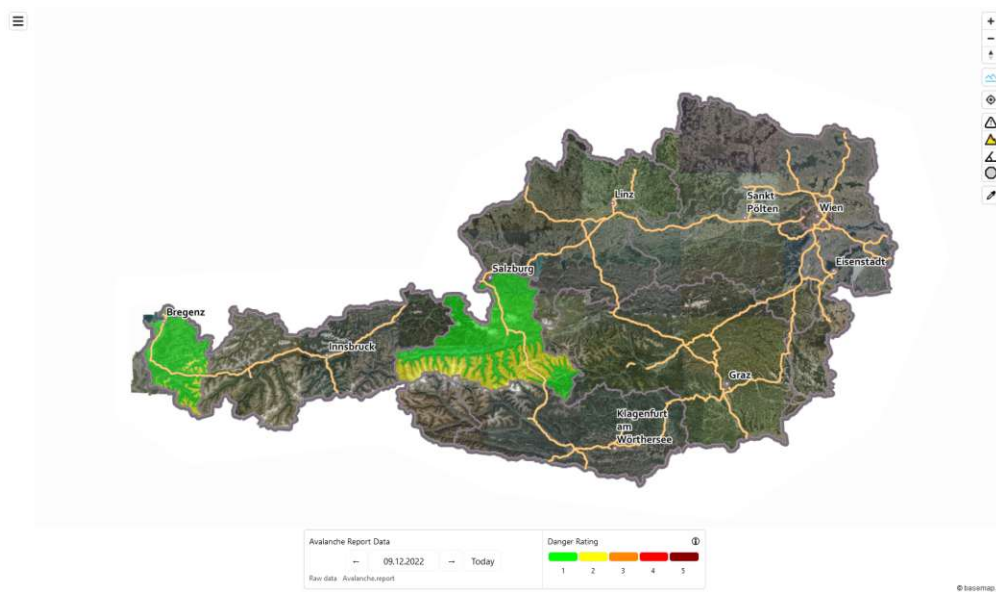


Figure 6.4: For December 9th 2022 only the states of Salzburg and Vorarlberg published avalanche reports. Therefore, the visualization displays dynamic risk information only for these areas.

6.4 User Interface and Interaction

For the implementation of the user interface, the design as described in Section 5.2 is integrated into MapLibre. The default installation of MapLibre contains a map view and basic controls for manipulating the view. The avalanche report visualization on the map implements the `IControl` interface provided by MapLibre. Custom controls can be added to an existing MapLibre installation and therefore do not require modifications to the core. This allows us to adapt the styling of the custom avalanche layer without the need of recompiling the renderer. A custom `avalancheControl` object is added to the main map view on initialization. This control is responsible for populating the layer switcher with the different display options and updating the map and legend according to the currently selected visualization style. The color scheme for the visual risk encoding is also defined via the configuration of this control. In case additional visualization styles are to be added to the map, appending a new entry to the control configuration in combination with the accompanying shader code is sufficient. Each avalanche risk visualization mode is represented by an icon with an alt-text displayed on hover.

The implementation of the tour planning user interface also utilizes the control interface. In the collapsible side panel on the left, a search bar and a list of tour tracks are displayed. Users can add their own tour tracks by uploading a GeoJSON file using drag and drop. Multiple tracks can be added to compare the avalanche situation between several potential tours during the planning process. In the tour track list, there are two buttons attached to each entry, one for setting the map focus on one tour and the other for removing the

tour from the view. An example view of the side panel can be seen in Figure 6.5. In the prototype implementation, the tour name is extracted from file metadata.

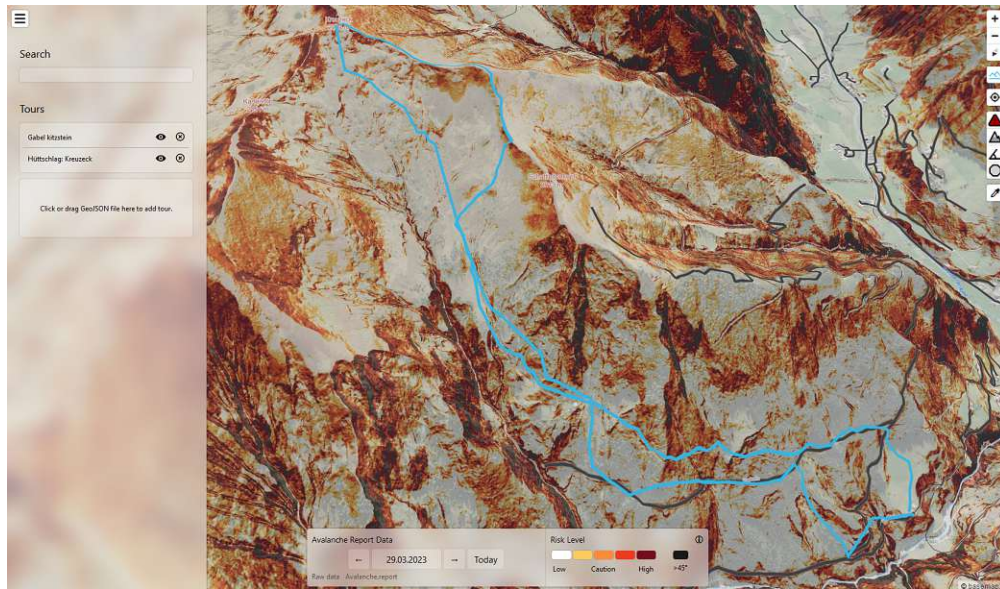


Figure 6.5: Side panel for adding tour tracks. The list of currently displayed tracks shows two entries, each with a *focus* and *delete* button. More tracks can be added by dropping them in the drop zone below the list.

The implementation of the picker mode, which samples slope, exposition, and avalanche danger rating uses the “feature querying” functionality in MapLibre. Here, information on the underlying map features is passed back to the application when we sample the map using the mouse cursor. In order to compute the three properties to be displayed, we need to access the elevation data as well as the avalanche report per region. For this, we have the option to either implement a data write-back from the GPU to the client application or to re-implement the evaluation on the CPU side. For the prototype application, we implement the second option where the sampling is done on the CPU side. As feature querying in MapLibre is only implemented for vector layers, we add the region data GeoJSON as a vector layer when the picker mode is active. On a mouse click event, we extract the region ID of the clicked position and load the avalanche danger rating from the same avalanche report data structure which we use for the risk visualization overlays. For sampling the slope and aspect, we query the raster DEM data from the underlying DTM tile via a custom sampler implementation on the CPU. The sampling is done on a $3\text{m} \times 3\text{m}$ grid. From the values on this grid, the terrain slope and aspect angle are calculated analogously to the implementation in the shader. The resulting data are rendered as glyphs into a popup marker instantiated via the MapLibre API.

6.5 Performance

Our requirements call for real-time interaction with the risk visualization (**R7**) and real-time evaluation of terrain properties (**R10**). The requirement for real-time performance is also reflected in **RQ1**, which is phrased as: *How can we evaluate reduction methods in real-time to determine localized avalanche risk on a terrain model?* The successful algorithmic implementation of reduction methods in our prototype application shows that we can use existing reduction methods in combination with a terrain model.

To fully answer **RQ1**, we conducted a brief performance analysis of our prototype application to highlight its real-time capabilities. For this analysis, performance tests were conducted in Google Chrome running on Windows 11 using an Nvidia GTX 1080 GPU. Here, the map application consistently ran at over 30 frames per second, averaging 43.3 frames per second during a simulated tour planning session.



Die approbierte gedruckte Originalversion dieser Diplomarbeit ist an der TU Wien Bibliothek verfügbar
The approved original version of this thesis is available in print at TU Wien Bibliothek.

Pilot User Study

To answer **RQ2** we perform an exploratory pilot user study in which we compare two conditions in a simulated tour planning process. The first condition uses our SnowCard overlay as an example of an integrated 3D visualization. We choose this overlay as it is the most comprehensive reduction method in our implementation. The second condition represents a more traditional risk assessment method using a 2D slope map and the EADS avalanche report independently.

7.1 Hypotheses

State-of-the-art methods for backcountry tour planning prior to arrival on site call for consultation of the avalanche report as well as for information gathered from maps on terrain steepness and exposition (see Section 2.2). In contrast, our risk visualization integrates data from the avalanche report with the terrain model into a single visual representation. In our design, we want to provide users with an overview of the avalanche situation for a certain area (**R5**). In this regard, our first hypothesis is that *choosing between two tours, both visualized in our integrated 3D visualization, the user selects the safer route based on the information available through the visualization* (**H1**).

Since we show the computed avalanche risk on a textured 2.5D surface of the terrain, we suspect that users gain a better understanding of the terrain features compared to a 2D map. This assumption is directly linked to requirement **R6** where we want to have a detail view for in-depth examination of critical areas. We hypothesize that *users will more accurately point out high-risk areas along and around the track on our integrated 2.5D risk map* (**H2**). This hypothesis is backed up by previous work which suggests that a 3D representation aids in interpreting terrain features and route finding [BHK⁺04] [PJ15].

As the two sources of information are computationally combined into our risk visualization, our third hypothesis is that *users will be more certain when assessing the risk in the*

integrated 3D visualization in comparison to the traditional workflow (H3). Here, we choose the certainty measure as it provides us with a direct measure, which we expect to correlate with easier decision-making, facilitated by the integrated 2.5D risk visualization.

7.2 Tasks

Users are presented with different pre-selected scenarios for which they have to perform an off-site avalanche risk evaluation. The selected tours are real but not named and not labeled on the map as the risk assessment should be purely based on the visualization and not on potential prior knowledge the user has of the area. For each scenario, the whole tour is shown from an overview perspective as tracks overlaid on the base map. The avalanche report for which the users have to perform the risk evaluation is chosen from a past date. Users are explicitly told that the chosen report does not represent the current avalanche situation. The selection of past avalanche reports for the risk evaluation of each tour is based on the following criteria:

1. One or more sections of the tour should have an avalanche risk that lies in the “caution” zone of the SnowCard, between high and low risk.
2. The tour should cover both favorable and unfavorable expositions.
3. There should be slopes with considerable avalanche risk (i.e. danger level 3) located above the route.

An in-depth description of how the tours are displayed can be found in Section 7.4. For each risk assessment, the users have to perform one of the following tasks:

T1: To test **H1** we present them with a map on which two tour tracks (“route 1” and “route 2”) are shown. The task for the user is to choose and verbally justify which route they would do based on the avalanche risk.

T2: To test **H2**, users have to point out the route’s most critical areas on the map. For this, we ask the users to add markers on the map by clicking on each high-risk area they have identified. If they come to the conclusion that no high-risk areas are present on the map, we ask them to not add any markers.

7.3 Design

We use a within-subject design with the following conditions:

- **2D slope steepness map and written avalanche report (2D slope map + report):** A non-tiltable, north-up 2D raster map that shows a base map layer in combination with a slope steepness overlay. For the slope steepness overlay, we use the visual encoding described in Section 5.1.1. In addition, a text document that contains the avalanche report for a specific day and region is provided to the user.

- **2.5D map with our integrated avalanche risk visualization (2.5D risk map):** Our implementation of the integrated avalanche risk visualization, which uses the SnowCard reduction method, is displayed on a tiltable and rotatable 2.5D base map. While some aspects of the written avalanche report are already embedded into the visualization, we still provide access to the written report. This allows the users to consult the textual descriptions for further details. In contrast to our prototype application, some features are disabled in this condition. Users do not have access to the picking tool, to overlays other than the SnowCard layer and the map does not contain any labels.

A visual comparison of the two conditions can be seen in Figure 7.1.

Each user performs both tasks once with each condition which makes a total of 2 tasks \times 2 conditions = 4 trials.

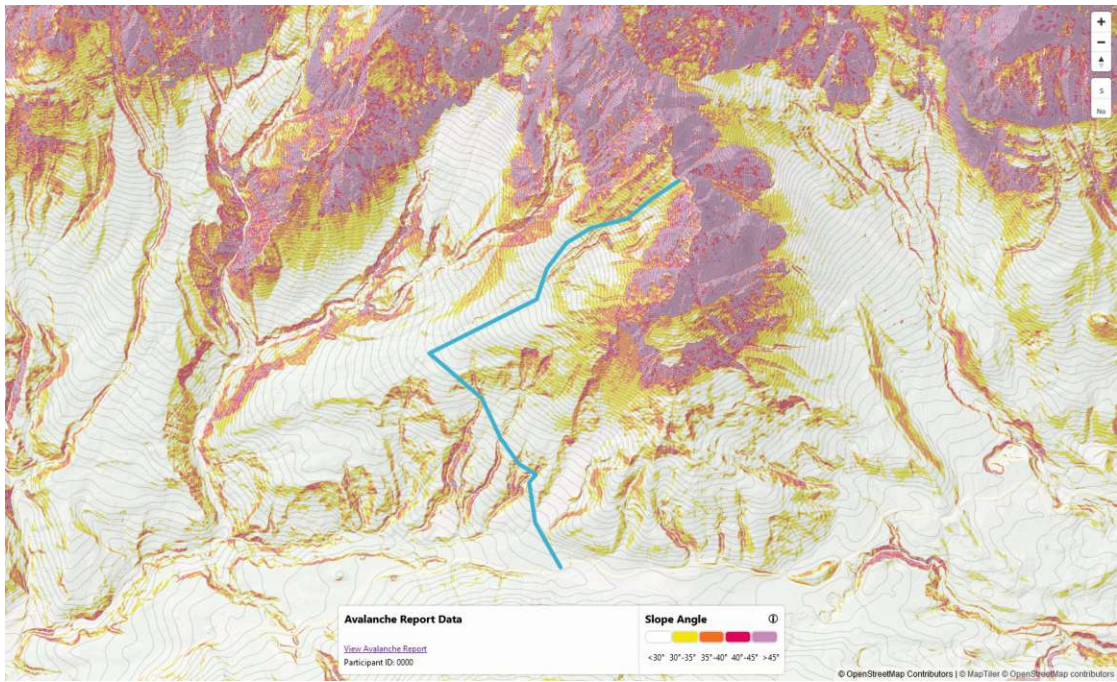
After each trial the user completes, there is a short questionnaire consisting of a five-point Likert scale in which we ask the user how certain they are that they have correctly identified the high-risk areas or overall avalanche risk of the tours provided. The scale ranges from “very uncertain” to “very certain”. These self-reported certainty values are used to test **H3**. Additionally, they will be asked to give any further feedback on the task they just performed. Users will be encouraged to “think aloud” and inform the study operator about the reasons for their decisions.

7.4 Procedure and Apparatus

The study was conducted via Zoom. Each user was invited to a meeting for which we performed a recording of video, audio, and screen capture. To conduct the study, we used a modified version of our prototype implementation, which was adjusted to fit the individual tasks. Apart from the recording, the coordinates at which the users placed markers on the map were also recorded to allow for measuring the accuracy and consistency of high-risk area identification (**H2**). To minimize learning effects, we used a pre-defined order of appearance for the tasks. This pre-defined scheme is given in Table 7.1. The trials were grouped by tasks: users first performed the two overview tasks (T1), followed by the two detailed risk assessment tasks on single routes (T2) or vice versa. For each task group, we varied the order of conditions as well as the order of tours to be evaluated. Overview tasks (**H1**) consisted of either the tour pair 1/2 or 3/4 respectively. For the detailed risk assessment tasks (**H2**), we again had two different tour tracks (“Track A” and “Track B”), for which we varied the order of appearance.

Before the start of the study, users had to read and sign two consent forms, one of which contained a written description of the study and one to consent to anonymized data collection and the GDPR. In this questionnaire, we also asked for their consent to record the study via Zoom. After we had the users’ written consent, we provided them with a demographic questionnaire asking for their age, sex, and self-assessed experience with ski

7. PILOT USER STUDY



(a) 2D slope map + report.



(b) 2.5D risk map.

Figure 7.1: Both study conditions with “Track A” overlaid on the map.

	Task 1	Task 1	Task 2	Task 2
User 1	2D + Pair 1/2	2.5D + Pair 3/4	2D + Track A	2.5D + Track B
User 2	2.5D + Pair 1/2	2D + Pair 3/4	2.5D + Track A	2D + Track B
User 3	2D + Pair 3/4	2.5D + Pair 1/2	2D + Track B	2.5D + Track A
User 4	2.5D + Pair 3/4	2D + Pair 1/2	2.5D + Track B	2D + Track A
User 5	2D + Pair 1/2	2.5D + Pair 3/4	2D + Track A	2.5D + Track B
User 6	2.5D + Pair 1/2	2D + Pair 3/4	2.5D + Track A	2D + Track B

Table 7.1: Order of risk assessment scenarios presented to the study participants.

touring. Additionally, we performed a short interview on how they currently perform off-site avalanche risk evaluation before a ski tour.

At the start of the study, we first provided the users with a short guided overview of the map application, in which we explained the interaction, as well as how to switch overlays on and off. After the introduction, the four conditions were shown in the order determined by our balancing, preceded by a short oral and written task description, and succeeded by the questionnaire described in Section 7.3.

After the study has been completed, a semi-structured interview is conducted. Here, we ask participants to give a ranking on which risk assessment method they preferred. Furthermore, we ask the users to give additional feedback on the overall experience of using both risk assessment methods. All study materials, including interview questionnaires and task descriptions, are reprinted in Appendix A.

7.5 Recruiting

As we only performed a pilot study, we chose six participants as our target sample size. Due to the low number of participants, we did not perform significance tests and instead investigated the effects of our measurements. Using the material from the interviews, videos, and transcripts we looked for explanations of our findings in a qualitative manner.

Since our study required domain knowledge in backcountry skiing, we only recruited participants who had prior experience in ski touring. We, therefore, recruited participants within the backcountry skiing community through personal connections. We only recruited adults aged 18 and above. Also, prior to the final interview, participants needed to be unaware that the condition **2.5D risk map** has been developed in the course of this thesis. To prevent possible re-traumatization of avalanche victims, we exclude participants who were previously involved in an avalanche incident.

7.6 Results

In total, six users aged between 24 and 55 participated in the study. Five participants were male and one female. None of the participants indicated that they were ever involved

in an avalanche incident. Four of the participants indicated that they were *somewhat experienced* with planning backcountry ski tours, while the remaining two indicated that they were *very experienced*. One of the *very experienced* participants was a professional ski touring guide. All participants completed the study and no participant was excluded according to our exclusion criteria.

7.6.1 Interview I: Tour Planning

The qualitative feedback gathered from the two semi-structured interviews was categorized with open coding (see Appendix B for the coded answers). For the first interview, categories of common tour planning strategies were compiled from the participants' answers. For the first question, where the participants were asked to describe their tour planning process, we formed four common themes: (i) *using maps for tour selection*, (ii) *checking the weather conditions*, (iii) *checking the avalanche danger rating*, and (iv) *applying risk reduction methods*. Of these four methods all six participants reported that they use maps for tour planning and check the avalanche report. Five out of six mentioned they apply risk reduction methods and check the weather conditions. As a follow-up users were asked to comment on which tools they use for their planning process. Here, we again used the same four categories and counted the number of mentions for tools from each category. Figure 7.2 shows the total number of tool mentions per category. The most frequently mentioned tools were the avalanche report and using maps for tour planning. Users also mentioned that they check the weather report sometimes for a couple of days in the past to get an idea of the snow conditions. Furthermore, they mentioned that they employ risk reduction methods such as Stop-or-Go for evaluating the overall suitability of a tour as well as potential high-risk areas along a selected tour.

Participants noted that their planning process usually starts with an overview of the region they consider going to. Here, potential tours are selected which are then examined in greater detail to determine potential high-risk areas. Based on the outcome of this examination as well as factors such as snow conditions and tour properties, a final decision on a tour is made.

During the first interview, participants were also asked which reduction methods they know. Here, all participants named the Stop-or-Go method, with two participants additionally mentioning both the SnowCard and the 3 × 3 method. Finally, the users were also asked what avalanche-risk-related checks they perform on-site. We again devised two coding categories into which we categorized the answers. In this case, the common themes were: (i) *checking the on-site weather* and (ii) *evaluating pre-identified high-risk areas*. Three users mentioned that they perform on-site weather checks and five that they evaluate pre-identified high-risk areas. For the evaluation of high-risk areas, users noted that, depending on the outcome of the evaluation, they will look for alternate routes on-site.

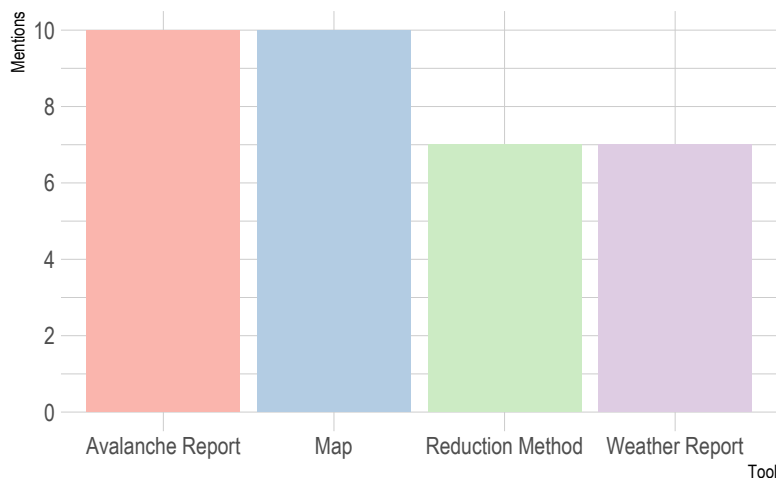


Figure 7.2: Frequency of tool category mentions in tour planning interview.

7.6.2 Tour Selection (H1)

For tour safety, we use the rating from Skitouren guru as a ground truth. To obtain this rating, we used Skitouren guru to calculate the risk factor for each tour with an avalanche danger rating matching the conditions presented to the users during the study. Based on this evaluation, for “Pair 1/2” the tour “p2” is deemed safer at a rating of 1.11, while for “Pair 3/4” the tour “p3” is the safer choice with a risk factor of 1.84. An overview of the tour ratings can be seen in Table 7.2.

Tour	Preference 2D slope map + report	Preference 2.5D risk map	Skitouren guru Rating
p1	1	0	1.26
p2	2	1	1.11
p3	2	0	1.84
p4	1	1	2.19

Table 7.2: User preference for Task 1 per condition and tour with Skitouren guru avalanche risk rating as ground truth (lower is better). The safer tour of each pair is highlighted in bold.

For the condition **2D slope map + report**, two out of three users chose the safer tour, with all users reaching a definitive choice. For the condition **2.5D risk map**, however, four out of six decision processes did not result in a conclusive decision. Here, users indicated that they have no preference in choosing between the two tours based on the avalanche risk. For the two conclusive decisions that were reached with the **2.5D risk**

map, the one for “Pair 1/2” was for “p2” whereas the one for “Pair 3/4” was for “p4”.

The self-reported certainty ratings (see Figure 7.3) for the tour selection task also show that users were more certain when choosing a tour based on the **2D slope map + report**. For each of the tour pairs, two of the decisions were reported as *certain* and one as *very certain*. For the evaluation based on the **2.5D risk map**, only one decision for each pair was reported as *certain*, while for “Pair 1/2” the remaining two decisions were reported as *undecided*. For “Pair 3/4” the remaining two decisions were reported as *undecided* and *uncertain*, respectively. **H1** is therefore not supported: *choosing between two tours visualized in our integrated risk visualization, users do not select the safer route, but instead have difficulties in reaching a conclusive decision.*

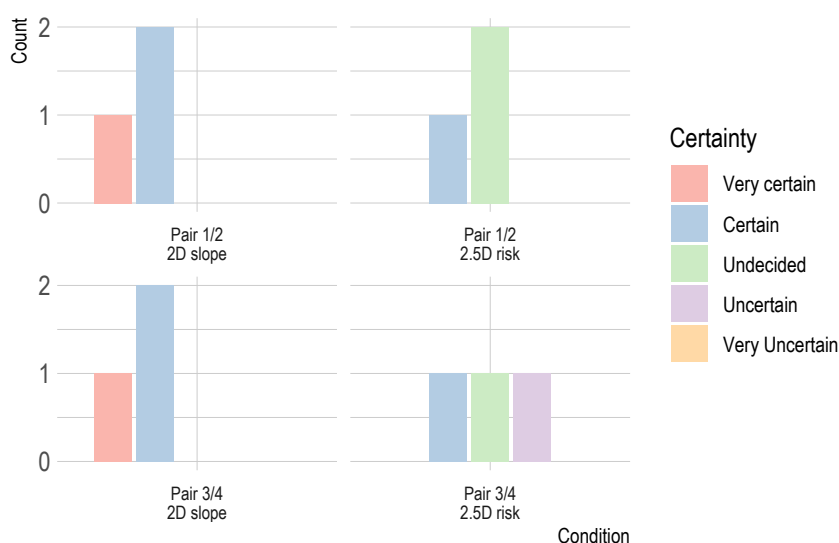


Figure 7.3: User reported certainty for correct tour selection in Task 1, grouped by condition and tour pair.

7.6.3 Accuracy in Detecting High-Risk Areas (H2)

To determine the accuracy by which users detected high-risk areas, we compare the marker placement to an evaluation using risk reduction methods as well as cruxes identified by Skitourenguru on the tour tracks used. Overall, users placed more markers when evaluating the tour under the condition **2.5D risk map** as can be seen in Table 7.3.

Furthermore, we observe the between-subject consistency of the marker placement for both conditions. A visualization of the results can be seen in Figure 7.4 for “Track A” and in Figure 7.5 for “Track B”. Looking at the marker placements, we see that users placed markers in outlier locations when evaluating the tour under the condition

Tour	2D slope map + report	2.5D risk map
Track A	10	12
Track B	15	18

Table 7.3: Number of markers placed grouped by tour and condition for Task 2.

2D slope map + report. This is especially visible in the lower regions of “Track A” (Figure 7.4a), where markers were placed in areas for which both, Stop-or-Go and the SnowCard reduction methods, indicate low avalanche risk. Results for “Track B” are similar, as visible in Figure 7.5a. Here one marker was placed at the starting point of the tour where risk reduction methods show no elevated risk. Furthermore, multiple markers were placed along the wide ridgeline.

Judging visually from Figure 7.4 and Figure 7.5, when users evaluated a tour under the condition **2.5D risk map**, the identification of potential high-risk areas is more spatially consistent while at the same time, more potential high-risk areas were pointed out. These results indicate support for **H2**: *Users identify high-risk areas more consistently and more accurately when using the integrated 3D visualization.*

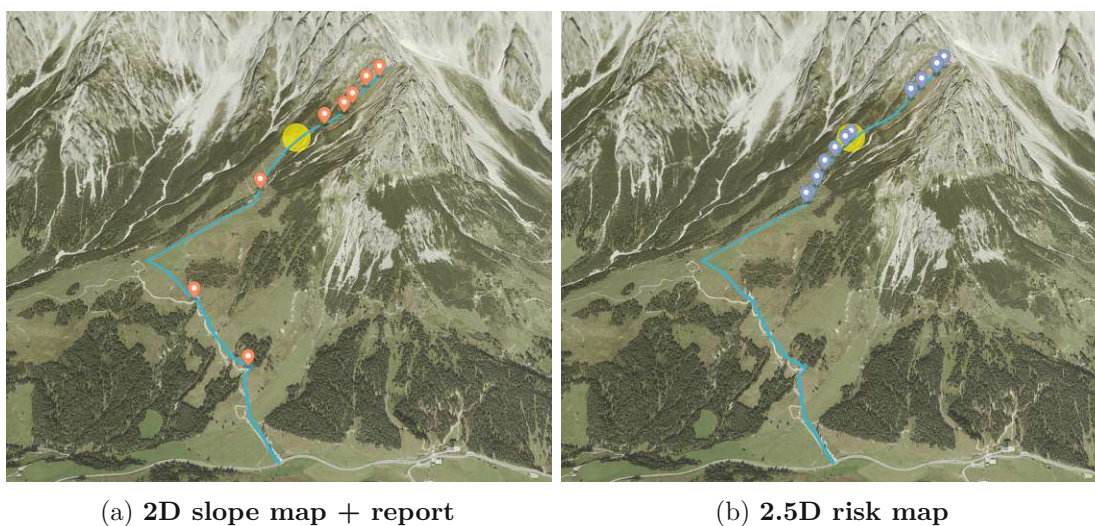


Figure 7.4: Marker placements for “Track A”. The yellow circle highlights a crux identified by Skitourenguru.

7.6.4 User Certainty During Risk Assessment (H3)

Over a total of 24 completed tasks, users reported higher certainty values for the **2D slope map + report** (see Figure 7.6). Under this condition, four tasks were solved with users reporting being *very certain* and the remaining eight tasks with them being *certain*. For the tasks solved using the **2.5D risk map**, only one solution was self-reported as *very certain*, while six were reported as *certain*. Using this map representation users

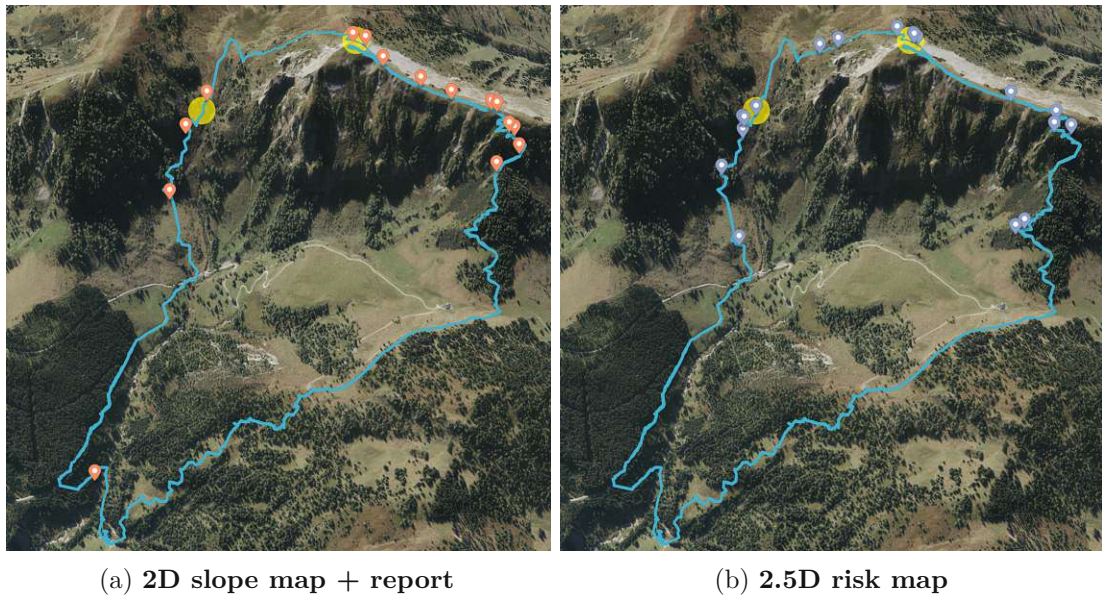


Figure 7.5: Marker placements for “Track B”. The yellow circles highlight cruxes identified by Skitourenguru.

labeled four of their answers as *undecided* and one answer was reported as *uncertain*. The hypothesis **H3** is, therefore, not supported: *users are more certain when they are assessing the risk in the traditional workflow in comparison to the integrated risk visualization*.

7.6.5 Interview II: Qualitative Feedback

In the second interview, which was performed after the users completed the four simulated tour planning tasks, we asked for their feedback on the two avalanche risk visualizations they used during the study. The interview again consisted of open questions where participants were asked to comment on how the overall study was going for them, which one of the two conditions they preferred and why, and finally what additional feedback they have regarding the visualization. The answers to all four questions were again categorized using open coding (see Appendix B for the coded answers). Here, statements were categorized into three categories: (i) *how the users trust is affected by the visualization*, (ii) *user comments on the risk encoding*, and (iii) *statements on the information content within each visualization*. In a second coding iteration, the extracted statements were grouped into positive and negative statements and counted up. The results of this count are visualized in Figure 7.7.

Users uttered more statements on the **2.5D risk map** (25), which is also the condition they considered unfamiliar, compared to the **2D slope map + report** (11). Notably, the category associated with the most negative statements is **trust** in the **2.5D risk map**. Here, users mentioned that the visualization is unfamiliar to them and that they

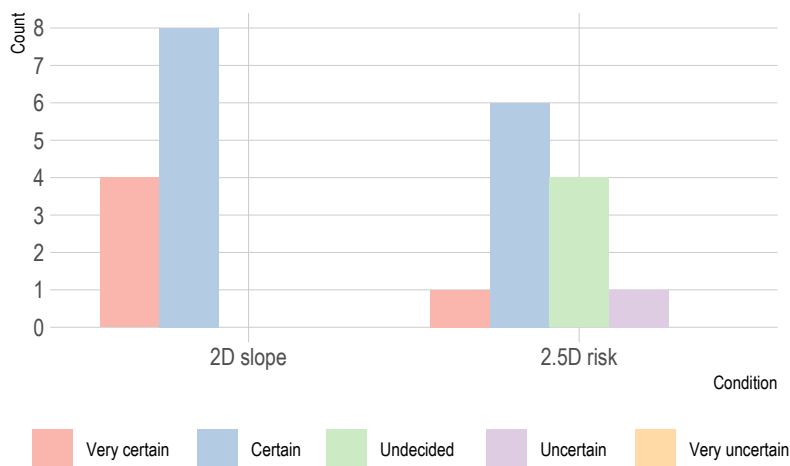
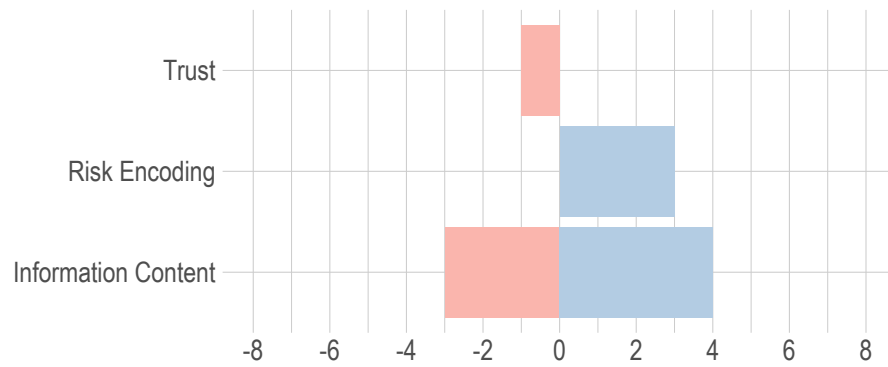


Figure 7.6: User reported certainty for overall correct task completion, grouped by condition.

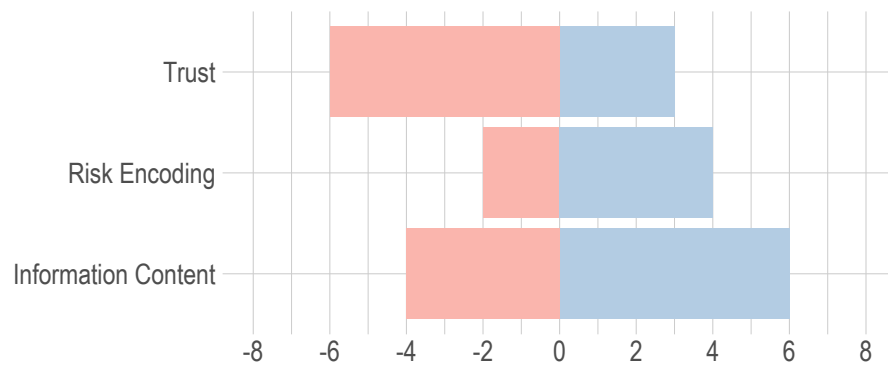
feel like they have to trust the computer without understanding where the risk encoding comes from. It was mentioned by four users that information is missing when just the risk is displayed and one user stated they had to undo the risk calculations in order to arrive at the familiar slope steepness metrics (“However, you then always have to reverse the calculation in order to be able to estimate the slope.”). Another concern with the **2.5D risk map** was the fact that by “blindly” trusting the risk visualization, users may stop critically evaluating the danger themselves as one user mentioned: “If I only go by these risk assessments, at some point, I switch off my thinking.”. On the positive side, participants mentioned that they believe the risk encoding in the **2.5D risk map** offers more safety and that they should trust the machine more. One negative statement regarding the **2D slope map + report** mentioned that, though it looks simpler, information is missing from this visualization in comparison to the other condition.

Regarding the risk encoding, no negative statements about the encoding in the **2D slope map + report** were made. Here, one user mentioned that the slope overlay is practical, while another stated that it contains an encoding they understand and that it gives them a feeling of being in control. Regarding the **2.5D risk map**, four out of six statements on the risk encoding were also positive. Here, one user mentioned that they liked having all the information available at once and that they would use this layer to evaluate potential high-risk areas. It was also mentioned that having the visualization point out high-risk areas may raise on-site awareness: “There the program already tells me I have to pay attention then I just look especially good.”. On the negative side, one user was missing

the direct encoding of the slope steepness in this visual encoding. Furthermore, one user was concerned with the simplified visual encoding of the risk, drawing comparisons to Skitourenguru, where the decision may finally be based on observing a singular color value.



(a) **2D slope map + report.**



(b) **2.5D risk map.**

Figure 7.7: Results of the coding for qualitative user feedback by condition.

The most frequent number of user feedback was given in the category of information content. For the **2D slope map + report**, three of the positive user statements noted the presence of contour lines. On the negative side for the **2D slope map + report**, users noted that the map style contained less information on vegetation than the

orthoimagery in the **2.5D risk map**. Users also mentioned that both representations were missing information, such as textual tour descriptions, that they usually use in their tour planning process. For the **2.5D risk map**, one user noted that the imagery was unfamiliar to them and another mentioned that the map orientation was harder to grasp in comparison to the north-up 2D map. On the positive side of the information content category in the **2.5D risk map**, it was mentioned by two users that 3D and the ability to tilt the map help with judging slope steepness. Seeing the border of forest areas was also noted by one user as a benefit of the 3D visualization.

Out of the six participants, three stated that they preferred the **2.5D risk map** as map representation style. Two participants indicated that they preferred the **2D slope map + report**, while one participant had no preference between the conditions.

7.7 Discussion

From the results of our pilot user study, we draw the following conclusions/lessons learned (note that the sample size of the pilot study was very small and the findings are mostly based on qualitative measures):

Tour planning tools should include a multitude of information sources allowing for manual and automatic risk evaluation. Our study showed that users consult multiple information sources during their tour planning process. Almost all users stated that current and past weather reports are an integral part of their tour planning process. While including weather data that goes beyond what is embedded in the avalanche report is outside the scope of this thesis, it is important to note that a fully integrated tour planning tool should include weather data. Additionally, users want further tour information beyond just tour tracks, such as written tour reports and an overview of available tours in a given region. In our implementation, we provide the integrated risk visualization in conjunction with a static slope steepness overlay and the per-region avalanche danger ratings.

An integrated risk visualization tool with an evaluation process that is intransparent leads to low trust. In our study, the users were provided with a very limited explanation of how the integrated risk evaluation was performed (see application overview in Appendix A). Users stated that they did not trust the visualization and preferred to have full control over the risk evaluation by performing it themselves using a slope map. A possible reason for the distrust could be that the chosen risk reduction method was not well-known among the study participants, as the SnowCard is primarily promoted by the German Alpine Association (DAV), and the study was conducted with Austrian participants. Another reason for the distrust could be that users are used to the 2D map with a slope overlay and have adapted their avalanche risk evaluation accordingly. Furthermore, users also stated that they believed they should trust the integrated visualization more but the lack of understanding of why a certain area was highlighted

as high-risk kept them from doing so. In the study setup, the picker mode was not available and participants had no knowledge of its existence. In the post-interview, users mentioned that one of the features they wanted in order to gain a better understanding was a picker to see the raw data the risk visualization is based on. Therefore, a future re-evaluation with this feature enabled may show improvements in trust.

High-resolution terrain data with orthoimagery may improve off-site recognition of potentially hazardous areas. We observed a positive effect on potential high-risk area identification when users were using the integrated 3D visualization. It is, however, unclear which factors of the 3D view contribute most to this effect. According to qualitative user feedback, both the orthoimagery as well as the ability to rotate and tilt the 3D map were seen as beneficial. Here, a follow-up investigation is necessary to accurately determine the impact of individual factors. There also is a mismatch between the performance in highlighting potential high-risk areas and selecting the overall safer tour. In the latter task, users performed worse and were less certain when using the integrated risk visualization. Based on these findings, our goals were fulfilled for the visualization on a detail level, but we may need a different approach to the overview visualization.

Risk evaluation is a multi-step, multi-scale process. In the semi-structured interviews where participants described their tour planning process, a pattern of decisions taking place at different scales was apparent. Initial tour selection was described as a process of getting an overview of available tours in a region followed by gathering broad information on the avalanche situation and the weather situation in general. From this initial selection, one or more tours are then evaluated in more detail to find potential high-risk areas. In our implementation, we try to support this approach by providing different interchangeable overlays in combination with the picker tool. By looking at the general avalanche situation via the avalanche report overlay, users can find a suitable area. In this area, singular tours can be evaluated using static and dynamic avalanche risk overlays. To gain a detailed insight into how the risk at a location is formed, the picker tool can be used. A limitation of the current implementation is, that there are no tours added to the map by default and the user has to upload them manually. In this regard, other applications, such as Skitouren guru [Sch22], better follow the “overview first, zoom and filter, details-on-demand” Visual Information Seeking Mantra by Shneiderman [Shn96], while also providing a selection of pre-defined tours for the user to select from.

Conclusion

In this chapter, we provide a summary of the contributions of this thesis. We also discuss the limitations of the work presented and give an outlook on possible improvements and future work.

8.1 Conclusion

In this thesis, we introduced an integrated approach to avalanche risk visualization, which uses a combination of a high-resolution DEM and real-time avalanche report data to visually encode the dynamic avalanche risk in the alpine terrain. We reviewed existing risk reduction methods in order to arrive at a risk evaluation strategy, which is based on established methods. By processing the data sources using algorithmic implementations of the SnowCard and Stop-or-Go reduction methods, we have shown that it is possible to use a combination of existing methods and data sources to visualize areas with high avalanche risk on a 2.5D terrain model in real-time (**RQ1**). Our implementation performs the risk evaluation on the GPU using WebGL, which is compatible with desktop and mobile browsers.

In contrast to conventional avalanche risk evaluation methods where separate visualizations for static risks such as slope steepness and the dynamic avalanche risk via the avalanche report are manually integrated by the user, our approach provides the user with an integrated visual encoding. The implications of this integration were evaluated in a pilot user study. In the study, participants had to solve avalanche risk evaluation tasks in a conventional setting and in a setting consisting of our integrated risk visualization. The results showed that experienced recreationists may have adapted their tour planning and risk evaluation strategy to the existing methods and therefore have difficulties trusting an integrated approach. Quantitative results of the study showed that using the high-resolution terrain model in combination with our integrated risk visualization, users'

performance in identifying potential high-risk detail areas was more consistent than with the conventional method (**RQ2**), but overview judgment was impaired.

8.2 Limitations

Although the technical basis is now here, an open question remains regarding the usefulness of integrated risk visualization for risk communication. Encouraging recreationists to perform proper tour planning and preparation is integral to reducing the number of avalanche casualties. As McCammon and Hägeli [MH04] point out in their work, a substantial number of lethal accidents happen on tours where no proper planning was performed. Lowering the cognitive barrier by assessing reduction methods computationally might make tour planning more accessible to a wider range of users.

By encoding the resulting risk levels in a color map and draping this color overlay on the terrain, we can guide user attention toward potential high-risk areas. One of the limitations of this overlay approach is that information about the underlying terrain features is lost or degraded. Here, future work needs to be performed to optimize the risk area highlighting in a way such that information loss is minimized. Through user feedback in our pilot user study, we learned that it is important to communicate how the integrated risk evaluation arrives at its risk levels and that the type and scale of the visual risk encoding has to adapt to the users' tour planning workflows.

Finally, the scope of the avalanche risk visualization prototype is currently limited to the alpine regions of Austria. While this was a deliberate decision, expanding beyond a single country would greatly improve the accessibility and impact of our work.

8.3 Future Work

While we have shown both the technical feasibility and potential to improve the tour planning workflow with our integrated visualization, there are some limitations that will have to be addressed in future work.

8.3.1 Additional Application Features

While we aimed to include a comprehensive collection of overlays and information sources in our map prototype, the following feature improvements can be made:

Add Support for other Countries: The visualization is currently limited to Austria, thus expanding to other regions is a high-priority task in terms of future improvements. To enable this expansion, we would need additional high-resolution DEM datasets, covering the respective areas. Furthermore, it would be necessary to adapt the avalanche report parsing pipeline to account for variations present in different reports. To this extent, an evaluation of the consistency of avalanche reports in the European Alps, performed by Techel et al. [TMC⁺18] could be a potential starting point.

Weather Report Data: The results of our pilot study show that data from the weather report play an important role in the tour planning process. A fully integrated tour planning and risk evaluation tool should therefore include weather data. One possible way to include this data is to add weather stations to the map with the ability to view previously recorded data as well as future trends. Alternatively, additional overlays with visual encodings of data points, such as snow depth, could be added to the map. These visual weather data encodings could go so far as to perform nowcasting on the terrain visualization itself showing cloud cover and snow with the 3D map representation.

Improved Imagery: In the current implementation, the orthoimagery we use as a base map consists of aerial images captured during summer. As one of the aims of our integrated visualization is to provide a faithful representation of the on-site condition, winter imagery showing snow cover would likely improve the recognizability of features between our representation and on-site observations. Furthermore, the current 2.5D approach leads to the stretching of overlays in near vertical areas. Here, extra data would be needed to reduce the information loss. User feedback also highlighted the lack of contour lines in the 2.5D map. Here, a suitable representation for 2.5D terrain would have to be developed. A possible starting point could be the elevation map present in Fatmap [FAT23].

Tour Database: In the prototype application, users have the option to upload custom tour tracks to be displayed on the map. Participants of the pilot study noted that they usually browse for tours on sites like Skitouren.guru [Sch22] or Bergfex [ber22]. This browsing for tours is also part of their risk evaluation process as the choice of which tour to take is influenced by the avalanche risk and vice versa. Having a collection of tours built into the application could therefore help the tour planning and selection process.

Personalized and Adaptive Maps: Results gathered from the tour planning interviews in our pilot study suggest that recreationists use maps for different use cases beyond avalanche risk evaluation. This includes finding a suitable downhill run, evaluating different options for the ascent, or finding alternative, less frequented slopes for a given tour. Therefore, the ability to adjust the map style to the user's needs should be part of a future iteration of an integrated tour planning tool. A personalized map display would adapt to the current use case and for example, provide a simplified landmark-based map for navigation as well as a map version that highlights risk or alternative tour options.

8.3.2 Visual Risk Encoding

Our visual risk encoding is currently based on semi-transparent overlays draped on the terrain model. This visualization strategy comes with the drawback of interfering with the underlying base map. The following potential improvements could be investigated to overcome this limitation:

Hachuring as Risk Encoding: Hachuring, as presented in Section 2.4, allows for overlaying data using lines instead of color-coding areas. Hachure lines could encode potential avalanche paths, while additional information, such as the risk level or potential avalanche sizes, could be encoded in the line parameters, such as length, thickness, density, or color. This additional information is, however, not covered by existing reduction methods, and alternative data sources such as the ATHM would likely have to be incorporated into the visualization pipeline.

Terrain Classification: Next to the machine-readable risk information, avalanche reports also contain textual information, which often specifies terrain features where elevated avalanche risk is present. A future improvement to our integrated risk visualization could be to parse these texts and extract the terrain information that could then be matched with a terrain classification performed on the DEM. A delimitation of catchment areas similar to the relevant slope area delimitation approach by Schmudlach and Köhler [SK16] could also be added to the implementation of the SnowCard and Stop-or-Go methods, as this step still has to be performed by the user in the current implementation.

Improved Blending: Apart from the blending of risk overlays, the vector data blending has some limitations when combined with our high-resolution elevation model. In areas with high-frequency elevation changes, such as forests, tour track overlays are heavily distorted. Here, a potential solution would be to render the vector overlays on the DTM and then render the additional data from the DSM on top of that with a blending strategy.

8.3.3 Validation and User Studies

Our pilot user study included a limited number of participants and a small subset of possible conditions to evaluate. Further, more in-depth user studies are necessary to obtain statistically significant conclusions on the effectiveness of our integrated avalanche risk visualization. The following studies are potential starting points for this evaluation:

Larger Study based on Pilot Study: A follow-up study testing the conditions from our pilot study on a larger number of users would allow us to make statistically significant statements regarding our hypotheses. For such a study it would also be important to recruit a representative sample of users ranging from novices with no experience in ski tour planning to experts such as professional mountain guides.

Field Studies: An important aspect next to identifying high-risk areas in the off-site tour planning phase is to be able to recognize the same areas on-site. While it is our hypothesis that a 3D map can facilitate this process, a user study in the form of a field study would be needed to validate this. Such a study would conceivably accompany users

throughout the planning and execution of backcountry ski tours using both conventional planning methods as well as our integrated risk visualization.

Separate Testing of Factors: In the design of our pilot study, we deliberately tested two distinct conditions that vary in multiple factors to keep the number of conditions low. We combined the 2.5D map, the risk overlay, and the orthoimagery into a single condition. This leads to confounding factors that prevent us from assessing why we saw certain results. In a follow-up study, the individual factors should be separated in a clean multi-factorial design. Furthermore, the factors of the reduction methods should be assessed individually, and finally, separate testing of additional interactive methods like the picking tool should be performed.

Our integrated visualization prototype is available for the Austrian alpine regions and can be used as a supplementary tool in the planning process for backcountry ski tours. In its current state, it is, however, a prototype implementation and therefore requires additional future improvements and validation to be fully incorporated into the tour planning workflow. In summary, the prototype application and our preliminary evaluation provide a solid foundation for further validation and thereby move us one step closer toward improving safety in backcountry skiing.



Die approbierte gedruckte Originalversion dieser Diplomarbeit ist an der TU Wien Bibliothek verfügbar
The approved original version of this thesis is available in print at TU Wien Bibliothek.

List of Figures

2.1	Glyphs with a typical color scheme for encoding avalanche danger levels. Note that level 5 uses a checkerboard pattern instead of dark red. Images from [Ser23a].	6
2.2	Overview of the avalanche report for the state Salzburg for December 25 th 2022 [Wal22].	8
2.3	Detail view of a single region from the avalanche report for the state of Salzburg for December 25 th 2022 [Wal22].	9
2.4	Both versions of the SnowCard for different expositions (a) and (b). Legend for the risk encoding (c). Risk values range from “low risk” to “caution” to “high risk”. Images taken from Deutscher Alpenverein [Deu23].	13
2.5	Portable Stop-or-Go card published by Österreichischer Alpenverein [Ö23].	14
2.6	(a) A raster image with a resolution of 16×16 pixels with the height encoded in the pixel intensity. (b) The resulting terrain mesh. Images from [CR11].	16
2.7	Triangle mesh creation from a 5×5 height map (a). (b) Vertices are placed at the center of each pixel. (c) Triangles are obtained by connecting the vertices. Images from [CR11].	17
2.8	Orthoimagery of the Austrian Alps. Image from [Geo23].	17
2.9	Section of Mapbox [Map23a] RGB-encoded elevation data showing the Austrian Alps. Dark blue areas have an elevation beyond 3107.1 meters, at which point the red channel is incremented by one.	20
2.10	Indices of elevations in 8-neighborhood around the elevation value z_{00} . Image adapted from [Hor81].	21
2.11	2.5D representation of alpine terrain (a) without and (b) with hill shading enabled.	22
2.12	Orthoimagery draped on a 2.5D terrain. Note how in the near-vertical areas on the right, the texture is stretched.	23
2.13	Terrain model with hachure texture encoding different terrain parameters: (a) slope, (b) exposition, (c) curvature. Images from [BSD ⁺ 04].	24
		87

2.14	Three different visualizations showing data blending for a volcanic map. (a) The height difference between two different DEM capture dates is encoded in the red hue. (b) RRIM-style visualization of the height difference in combination with slope and openness, each encoded in a different HSV parameter. (c) RRIM with a uniform hue for the whole terrain while slope and openness are encoded in the saturation and value, respectively. Images adapted from [FF17].	24
3.1	Two commercial applications visualizing static avalanche risk by overlaying slope steepness onto a base map.	28
3.2	Classified avalanche terrain (a) and avalanche terrain hazard (b). Images from [HSB ⁺ 18].	30
3.3	Dynamic avalanche risk for a single tour on Skitouren guru [Sch22]. The different line segment colors correspond to the localized avalanche risk for each tour section. In the red section, a glyph with three concentric circles indicates a high static avalanche risk in that area.	31
3.4	Relevant slope area delimitation from the ATHM. Image from [SK16]. . .	31
3.5	ATES map of the Oberalppass in Switzerland resulting from sampling on a 10 m × 10 m raster. Image from [SK16].	32
4.1	Schematic overview of the software components required for our avalanche risk visualization.	38
5.1	2.5D terrain visualization without overlays.	40
5.2	2.5D terrain visualization with slope steepness overlay.	41
5.3	Color scheme used for encoding the slope angle.	42
5.4	Color scheme used for encoding the avalanche danger rating.	42
5.5	Inputs and processing steps for the avalanche danger rating overlay. The terrain model (1) and the region IDs (2) are texture inputs. For each fragment, the height is evaluated, and the height border is set according to the region and avalanche report (3). Finally, each height section and region is colored according to the danger rating (4).	43
5.6	Color scheme used for encoding the risk level based on the SnowCard. . .	46
5.7	Overview of the SnowCard overlay. The terrain model (1) and the region IDs (2) are texture inputs. From the terrain model, the slope map (3) is calculated. For each fragment, the height border is set according to the region (4) and the rating is calculated according to the avalanche report (5). The exposition is classified as favorable (white) or unfavorable (black) (6) for each region. By combining slope, danger rating, and exposition, the risk level is calculated and displayed on the terrain model (7).	47
5.8	2.5D terrain visualization with SnowCard risk overlay.	48
88		

5.9	Overview of the Stop-or-Go avalanche risk overlay. The terrain model (1) and the region IDs (2) are texture inputs. From the terrain model, the slope map (3) is calculated. For each fragment, the height border is set according to the region (4) and the rating is calculated according to the avalanche report (5). The final visualization (6) shows areas marked “Stop” in red, overlaid on the terrain model.	49
5.10	2.5D terrain visualization with Stop-or-Go overlay.	50
5.11	Schematic overview of the desktop user interface of our map application.	51
5.12	Popup with glyphs representing the current exposition (left), elevation with regards to the avalanche danger rating (center), and slope angle (right).	52
5.13	Tour track in combination with different overlays.	54
6.1	Regions of Austria covered by the Avalanche Warning services. Regions IDs are encoded in the color values for each region.	57
6.2	Tile padding performed to allow access to elevation data from neighboring tiles in the fragment shader. The padded tile (blue) contains pixels from adjacent tiles.	60
6.3	Schematic overview of the avalanche layer and its integration into the MapLibre framework.	62
6.4	For December 9 th 2022 only the states of Salzburg and Vorarlberg published avalanche reports. Therefore, the visualization displays dynamic risk information only for these areas.	63
6.5	Side panel for adding tour tracks. The list of currently displayed tracks shows two entries, each with a <i>focus</i> and <i>delete</i> button. More tracks can be added by dropping them in the drop zone below the list.	64
7.1	Both study conditions with “Track A” overlaid on the map.	70
7.2	Frequency of tool category mentions in tour planning interview.	73
7.3	User reported certainty for correct tour selection in Task 1, grouped by condition and tour pair.	74
7.4	Marker placements for “Track A”. The yellow circle highlights a crux identified by Skitourenguru.	75
7.5	Marker placements for “Track B”. The yellow circles highlight cruxes identified by Skitourenguru.	76
7.6	User reported certainty for overall correct task completion, grouped by condition.	77
7.7	Results of the coding for qualitative user feedback by condition.	78



Die approbierte gedruckte Originalversion dieser Diplomarbeit ist an der TU Wien Bibliothek verfügbar
The approved original version of this thesis is available in print at TU Wien Bibliothek.

List of Tables

2.1	Acceptable combinations of danger rating and slope steepness for the ERM [Mun01].	12
2.2	Number of tiles and pixel size on equator per zoom level [Ste17].	19
5.1	Example lookup table for the internal avalanche danger rating representation on the GPU side. Note that the “Unfavorable”, which encodes unfavorable expositions is not used for the avalanche danger rating overlay. For more information on the processing of expositions see Section 6.2.	43
5.2	Lookup table structure for reduction method overlays.	44
5.3	Discretized lookup table for the SnowCard risk overlay, showing risk(a) favorable expositions and (b) unfavorable conditions.	48
5.4	Stop-or-Go lookup table. 1 = “Go”, 0 = “Stop”.	50
7.1	Order of risk assessment scenarios presented to the study participants. . .	71
7.2	User preference for Task 1 per condition and tour with Skitouren guru avalanche risk rating as ground truth (lower is better). The safer tour of each pair is highlighted in bold.	73
7.3	Number of markers placed grouped by tour and condition for Task 2. . . .	75



Die approbierte gedruckte Originalversion dieser Diplomarbeit ist an der TU Wien Bibliothek verfügbar
The approved original version of this thesis is available in print at TU Wien Bibliothek.

List of Algorithms

5.1	Evaluate Exposition	45
6.1	Encode Elevation in RGB	56



Die approbierte gedruckte Originalversion dieser Diplomarbeit ist an der TU Wien Bibliothek verfügbar
The approved original version of this thesis is available in print at TU Wien Bibliothek.

List of Listings

2.1	Shortened example CAAML file which contains the avalanche report for the state of Salzburg for December 25 th 2022 [Wal22].	10
6.1	Internal representation of avalanche report data for two example regions.	58



Die approbierte gedruckte Originalversion dieser Diplomarbeit ist an der TU Wien Bibliothek verfügbar
The approved original version of this thesis is available in print at TU Wien Bibliothek.

Bibliography

- [Age14] National Geospatial-Intelligence Agency. Department of Defense World Geodetic System 1984. Technical Report NIMA TR8350.2, National Geospatial-Intelligence Agency, Springfield, VA, 2014.
- [BCDM⁺14] Roland Billen, Anne-Françoise Cutting-Decelle, Ognen Marina, José-Paulo De Almeida, Matteo Caglioni, Gilles Falquet, Thomas Leduc, Claudine Métral, Guillaume Moreau, Julien Perret, et al. 3d city models and urban information: Current issues and perspectives-european cost action tu0801. 2014.
- [BDD⁺16] H. Butler, M. Daly, A. Doyle, S. Gillies, S. Hagen, and T. Schaub. The geojson format. RFC 7946, RFC Editor, August 2016.
- [ber22] bergfex GmbH. Bergfex. <https://www.bergfex.at/>, 2022. Accessed: 2023-01-23.
- [BHK⁺04] Aileen Buckley, Lorenz Hurni, Karel Kriz, Tom Patterson, and Jeff Olsenholler. Cartography and visualization in mountain geomorphology. *Geographic information science and mountain geomorphology*, pages 1–27, 2004.
- [BM98] Peter A Burrough and Rachael McDonnell. *Principles of geographical information systems*. Oxford university press, 1998.
- [BSD⁺04] Kevin Buchin, Mario Costa Sousa, Jürgen Döllner, Faramarz Samavati, and Maike Walther. Illustrating terrains using direction of slope and lighting. In *4th ICA Mountain Cartography Workshop*, pages 259–269, 2004.
- [Ces23] Cesium GS, Inc. CesiumJS. <https://cesium.com/>, 2023. Accessed: 2023-01-15.
- [CKS08] Tatsuro Chiba, Shin-ichi Kaneta, and Yusuke Suzuki. Red relief image map: new visualization method for three dimensional data. *The international archives of the photogrammetry, remote sensing and spatial information sciences*, 37(B2):1071–1076, 2008.

- [CR11] Patrick Cozzi and Kevin Ring. *3D Engine Design for Virtual Globes*. CRC Press, 1st edition, June 2011. <http://www.virtualglobebook.com>.
- [Deu23] Deutscher Alpenverein. Deutscher Alpenverein. <https://www.alpenverein.de/>, 2023. Accessed: 2023-02-05.
- [DRTS17] Steve Dübel, Martin Röhlig, Christian Tominski, and Heidrun Schumann. Visualizing 3d terrain, geo-spatial data, and uncertainty. In *Informatics*, volume 4, page 6. MDPI, 2017.
- [EM01] Martin Engler and Jan Mersch. *SnowCard: Lawinen-Risiko-Check; Risikomanagement für Skitourengeher, Snowboarder, Variantenfahrer, Schneeschwanderer*. Bergverlag Rother, 2001.
- [Eng01] Martin Engler. SnowCard & Faktorencheck: Lawinenkunde vom Anfänger bis zum Profi. *Berg & Steigen*, 01(4):37–41, 2001.
- [EPS20] EPSG. *EPSG:3857 WGS 84 / Pseudo-Mercator*. European Petroleum Survey Group Geodesy, 2020.
- [FAT23] FATMAP. Fatmap. <https://fatmap.com/>, 2023. Accessed: 2023-03-15.
- [FF17] Massimiliano Favalli and Alessandro Fornaciai. Visualization and comparison of dem-derived parameters. application to volcanic areas. *Geomorphology*, 290:69–84, 2017.
- [fSuLS23] WSL-Institut für Schnee-und Lawinenforschung SLF. White Risk. <https://whiterisk.ch/>, 2023. Accessed: 2023-03-15.
- [Geo23] Geoland. basemap.at. <https://basemap.at/>, 2023. Accessed: 2023-02-17.
- [Goo23a] Google LLC. Google Earth. <https://earth.google.com/web/>, 2023. Accessed: 2023-02-20.
- [Goo23b] Google LLC. Google Maps. <https://www.google.com/maps>, 2023. Accessed: 2023-02-20.
- [HB03] Mark Harrower and Cynthia A Brewer. Colorbrewer.org: an online tool for selecting colour schemes for maps. *The Cartographic Journal*, 40(1):27–37, 2003.
- [HHNG20] Pascal Hägeli, Johannes Hörtnagel, Patrick Nairz, and Matthias Gerber. CAAML V5.0 Profile - Bulletin EAWS. <http://caaml.org/Schemas/V5.0/Profiles/BulletinEAWS/index.html>, 2020. Accessed: 2023-01-15.
- [Hir15] Christian Hirt. Digital terrain models. In Erik Grafarend, editor, *Encyclopedia of Geodesy*. Springer, Berlin, New York, 2015.

- [Hor81] Berthold K.P. Horn. Hill shading and the reflectance map. *Proceedings of the IEEE*, 69(1):14–47, 1981.
- [HSB⁺18] Stephan Harvey, Günter Schrudlach, Yves Bühler, Lukas Dürr, Andreas Stoffel, and Marc Christen. Avalanche terrain maps for backcountry skiing in switzerland. In *Proceedings ISSW*, pages 1625–1631, 2018.
- [Hö17] Peter Höller. Avalanche accidents and fatalities in austria since 1946/47 with special regard to tourist avalanches in the period 1981/82 to 2015/16. *Cold Regions Science and Technology*, 144:89–95, 2017. International Snow Science Workshop 2016 Breckenridge.
- [ISO20] ISO. Codes for the representation of names of countries and their subdivisions — Part 2: Country subdivision code. Standard, International Organization for Standardization, Geneva, CH, August 2020.
- [JSST14] Christian Jaedicke, Egil Syre, and Kjetil Sverdrup-Thygeson. Gis-aided avalanche warning in norway. *Computers & Geosciences*, 66:31–39, 2014.
- [KM70] Josef Nikolaus Köstler and Hannes Mayer. Waldgrenzen im Berchtesgadener Land. *Jahrbuch des Vereins zum Schutze der Alpenpflanzen und -Tiere*, 35:121–153, 1970.
- [KSS18] Satish Kumar, Pankaj Kumar Srivastava, and Snehmani. Geospatial modelling and mapping of snow avalanche susceptibility. *Journal of the Indian Society of Remote Sensing*, 46(1):109–119, Jan 2018.
- [Lar99] Michael Larcher. Stop or Go: Entscheidungsstrategie für Tourengelher. *Berg & Steigen*, 99(4):18–23, 1999.
- [Mac04] Alan M MacEachren. *How maps work: representation, visualization, and design*. Guilford Press, 2004.
- [Map23a] Mapbox, Inc. Mapbox. <https://mapbox.com/>, 2023. Accessed: 2023-02-20.
- [Map23b] Mapbox, Inc. Mapbox Elevation Data Documentation. <https://docs.mapbox.com/data/tilesets/guides/access-elevation-data/>, 2023. Accessed: 2023-02-20.
- [Map23c] MapLibre Contributors. MapLibre GL JS. <https://maplibre.org/maplibre-gl-js-docs/api/>, 2023. Accessed: 2023-01-15.
- [MB21] Jan Mersch and Wolfgang Behr. There is no Glory in Prevention! Klarstellungen zur Lawinenkunde. In *Tagungsband des 4. internationalen Lawinensymposiums, Graz*, pages 12–19, 2021.

- [MH04] Ian McCammon and Pascal Hägeli. Comparing avalanche decision frameworks using accident data from the united states. In *International Snow Science Workshop, Jackson, WY*, 2004.
- [MHW⁺12] Helena Mitasova, Russell S. Harmon, Katherine J. Weaver, Nathan J. Lyons, and Margery F. Overton. Scientific visualization of landscapes and landforms. *Geomorphology*, 137(1):122–137, 2012. Geospatial Technologies and Geomorphological Mapping Proceedings of the 41st Annual Binghamton Geomorphology Symposium.
- [MLW22] Gerhard Mössmer, Michael Larcher, and Verlagsanstalt Würtl, Walter. *Sicher am Berg: Skitouren Risikomanagement Stop or Go © und Notfall Lawine*. Österreichischer Alpenverein, Innsbruck, Austria, 2022 edition, 2022.
- [Mun97] Werner Munter. *3 x 3 Lawinen: entscheiden in kritischen Situationen*. Agentur Pohlmann & Schellhammer, Garmisch Patenkirchen, Germany, 1997.
- [Mun01] Werner Munter. Reduktionsmethode Vom Minutenentscheid zum synthetischen Blick. *Berg & Steigen*, 01(4):35–36, 2001.
- [Ö23] Österreichischer Alpenverein. Österreichischer Alpenverein. <https://www.alpenverein.at/>, 2023. Accessed: 2023-02-05.
- [PEH20] Laurent Polidori and Mhamad El Hage. Digital elevation model quality assessment methods: A critical review. *Remote sensing*, 12(21):3522, 2020.
- [Pfe02] Norbert Pfeifer. *3D terrain models on the basis of a triangulation*, volume 65. Inst. für Photogrammetrie u. Fernerkundung d. Techn. Univ. Wien, 2002.
- [PJ15] Charles A Preppernau and Bernhard Jenny. Three-dimensional versus conventional volcanic hazard maps. *Natural Hazards*, 78(2):1329–1347, 2015.
- [QGI23] QGIS Development Team. *QGIS Geographic Information System*. QGIS Association, 2023.
- [Sch22] Günther Schudlach. Skitouren guru. <https://www.skitouren guru.ch/>, 2022. Accessed: 2023-01-19.
- [Ser23a] European Avalanche Warning Services. EAWS Glossary. <https://www.avalanches.org/glossary/>, 2023. Accessed: 2023-01-15.
- [Ser23b] European Avalanche Warning Services. EAWS Regions - Geodata of avalanche warning regions. <https://regions.avalanches.org/>, 2023. Accessed: 2023-01-15.

- [Shn96] Ben Shneiderman. The eyes have it: A task by data type taxonomy for information visualizations. In *Proceedings 1996 IEEE symposium on visual languages*, pages 336–343. IEEE, 1996.
- [SK16] Günter Schmudlach and Jochen Köhler. Method for an automatized avalanche terrain classification. In *International Snow Science Workshop 2016 Proceedings*, Breckenridge, CO, USA, 2016.
- [SL01] Jürg Schweizer and Martina Lütschg. Characteristics of human-triggered avalanches. *Cold Regions Science and Technology*, 33(2):147–162, 2001. ISSW 2000:International Snow Science Workshop.
- [SMT06] Grant Statham, Bruce McMahon, and Ian Tomm. The avalanche terrain exposure scale. In *Proceedings of the International Snow Science Workshop, Telluride, CO, USA*, pages 491–497. Citeseer, 2006.
- [SNS⁺20] Arnold Studeregger, Bernhard Niedermoser, Florian Stifter, Willi Ertl, and Fritz Salzer. Der neue Lawinenlagebericht für Salzburg, Kärnten, Oberösterreich, Steiermark und Niederösterreich. *Berg & Steigen*, 20(4):84–90, 2020.
- [ŠSK⁺19] Čeněk Šašinka, Zdeněk Stachoň, Petr Kubíček, Sascha Tamm, Aleš Matas, and Markéta Kukaňová. The impact of global/local bias on task-solving in map-related tasks employing extrinsic and intrinsic visualization of risk uncertainty maps. *The Cartographic Journal*, 56(2):175–191, 2019.
- [Ste17] Emmanuel Stefanakis. Web mercator and raster tile maps: two cornerstones of online map service providers. *Geomatica*, 71(2):100–109, 2017.
- [STJD15] Amir Semmo, Matthias Trapp, Markus Jobst, and Jürgen Döllner. Cartography-oriented design of 3d geospatial information visualization – overview and techniques. *The Cartographic Journal*, 52(2):95–106, 2015.
- [SWK18] Günter Schmudlach, Kurt Winkler, and Jochen Köhler. Quantitative risk reduction method (qrm), a data-driven avalanche risk estimator. In *Proceedings ISSW*, pages 1272–1278, 2018.
- [TMC⁺18] F. Techel, C. Mitterer, E. Ceaglio, C. Coléou, S. Morin, F. Rastelli, and R. S. Purves. Spatial consistency and bias in avalanche forecasts – a case study in the european alps. *Natural Hazards and Earth System Sciences*, 18(10):2697–2716, 2018.
- [Voz23] Vit Vozenilek. The atlas cookbook: Ten ingredients how to edit an atlas. 2023.
- [Wal22] Matthias Walcher. Lawinenwarndienst Salzburg. <https://lawine.salzburg.at/en/avalanche-report/news>, 2022. Accessed: 2023-01-15.

- [Zec20] Silvana Zechmeister. Interactive visualization of vector data on heightfields. Master's thesis, Research Unit of Computer Graphics, Institute of Visual Computing and Human-Centered Technology, Faculty of Informatics, TU Wien, Favoritenstrasse 9-11/E193-02, A-1040 Vienna, Austria, October 2020.
- [ZH21] Meng-Cong Zheng and Yi-Wen Hsu. How 2.5 d maps design improve the wayfinding performance and spatial ability of map users. In *Informatics*, volume 8, page 88. MDPI, 2021.

Appendix A: Study Materials

Interview Questionnaires

Application Overview

Task Descriptions

Semi-structured Interview I

User ID	
Describe what you usually do when you plan a tour?	
Which tools do you use?	
Do you know reduction methods like Stop-or-Go or Snowcard?	
What do you do beforehand, what do you do on-site?	

Semi-structured Interview II

User ID	
How was it going?	
Which of the two conditions did you prefer?	
Why?	
What additional feedback do you have?	

User Study Avalanche Risk Visualization

Application Overview

In this study you are presented with a map application which displays data related to the planning of backcountry ski tours.

At the start of a task the map view is centred around the for which you will perform the off-site planning process. The map application consists of **three main parts**:

1. The **map** which contains terrain information, overlays and the tour track
2. The **legend** at the bottom which shows a color key for the selected overlay and a link to the corresponding avalanche report
3. The **controls** at the top right which allow for basic navigation as well as switching overlays on and off

The following **map controls** are available in the **2D map**:

- Left Click + drag to move the map
- Mouse wheel to zoom in and out
- Left Click to set a marker
- On the top right you can switch between two display modes:
 - "S" for the slope map overlay
 - "No" for no overlay

The following **map controls** are available in the **3D map**:

- Left Click + drag to move the map
- Mouse wheel to zoom in and out
- Right Click (or Ctrl+Left Click) + drag to tilt/rotate the map
- Left Click to set a marker
- On the top right you can switch between two display modes:
 - "T" for the avalanche risk overlay
 - "No" for no overlay
- On the top right there is a compass symbol, which when clicked resets the tilt and rotation of the map

User Study Avalanche Risk Visualization

Comparison Task

You get two different tours which are visualized on the map. Additionally, you get the two avalanche reports for the according regions. Open all four elements in separate tabs.

Your task is the following:

Using the visualization features of the map in combination with the avalanche report, chose one tour which you would consider doing based on the avalanche risk. Verbally justify your decision. Please also comment and explain your actions while evaluating the tours.

Vergleichsaufgabe

Sie erhalten zwei verschiedene Touren, die auf der Karte visualisiert werden. Zusätzlich erhalten Sie die beiden Lawinenberichte für die jeweiligen Regionen. Öffnen Sie alle vier Elemente in separaten Tabs.

Ihre Aufgabe ist die folgende:

Wählen Sie anhand der Visualisierungsmöglichkeiten der Karte in Kombination mit dem Lawinenlagebericht eine Tour aus, die Sie aufgrund der Lawinengefahr in Betracht ziehen würden. Begründen Sie Ihre Entscheidung mündlich. Bitte kommentieren und erklären Sie auch Ihr Vorgehen bei der Beurteilung der Touren.

User Study Avalanche Risk Visualization

Critical Area Identification Task

You get the track of a tour which is visualized on the map. Additionally, you get the avalanche report for the according region. Open both of these elements in separate tabs.

Your task is the following:

Using the visualization features of the map in combination with the avalanche report, identify the most critical areas on the route which will need further attention on site. Mark the critical areas by placing a marker on the location. To place a marker, left-click on the map. You can move a marker around by clicking and dragging it. If you want to remove a marker, click on it and then click the button "Remove Marker".

Please comment and explain your decisions process by thinking aloud.

Aufgabe zur Identifizierung kritischer Bereiche

Sie erhalten den Track einer Tour, die auf der Karte visualisiert wird. Zusätzlich erhalten Sie den Lawinenlagebericht für die entsprechende Region. Öffnen Sie diese beiden Elemente in separaten Tabs.

Ihre Aufgabe ist die folgende:

Ermitteln Sie anhand der Visualisierungsmöglichkeiten der Karte in Kombination mit dem Lawinenlagebericht die kritischsten Stellen auf der Tour, die vor Ort weiter beachtet werden müssen. Markieren Sie die kritischen Bereiche, indem Sie einen Marker an der betreffenden Stelle anbringen. Um einen Marker zu setzen, klicken Sie mit der linken Maustaste auf die Karte. Sie können einen Marker durch Klicken und Ziehen verschieben. Wenn Sie einen Marker entfernen möchten, klicken Sie ihn an und dann auf den Button "Remove Marker".

Bitte kommentieren Sie und erläutern Sie Ihren Entscheidungsprozess durch lautes Denken.

Appendix B: Coded Interviews

Interview I: Tour Planning

Interview II: Qualitative Feedback

Avalanche Report	<ol style="list-style-type: none"> 1. ...ansonsten schaue ich in den LLB. 2. ...ich hole mir den LLB über lawine.at... 3. Natürlich berücksichtige ich auch die Lawinenwarnstufen. 4. ...für den LLB die Landesseite der Warndienste vom Land Salzburg oder was auch immer. 5. ...LLB im Gebiet über SnowSafe App. 6. ...schau mir den LLB an von den Tagen [an]. 7. Den LLB hole ich vom jeweiligen Bundesland. 8. Ich schau wie schaut der LLB aus. 9. ... warte ich auf den LLB der jetzt immer schon am Vorabend kommt, um 18 Uhr gibt es den. 10. Den LLB hole ich vom jeweiligen Bundesland Tirol, Südtirol haben jetzt schon einen gemeinsamen.
Map	<ol style="list-style-type: none"> 1. Ich benutze in der Region Alpenverein Aktiv weil die eine schöne Hangneigungskarte haben. 2. Dann schau ich mir auf Bergfex oder auf diversen solchen Seiten an welche Touren es da gibt. Dann suche ich mir was aus, was von den Höhenmetern und von der Dauer her passend ist und wo auch eine schöne Abfahrt dabei ist. 3. Kommt auf die Gegend an. Wenn bekannte Tour dann Bergfex App. Sonst Karte mit Hangneigungslayer. 4. ...schau ich auf Karten und erkundige mich im Netz ob Leute das schon gemacht haben. 5. ...aktuelle Tourenführer die ich habe, in welche Form auch immer, ob das jetzt Papier oder elektronisch ist. 6. Dann überlegen ich mir eine Tour von den wenigen die ich eh kenne, könnte das passe, ist das zu Steil für die Warnstufe, passt die Hanglage. 7. Ich habe da diese Outdoor-Active App, die ist eh vom Alpenverein. Soweit ich gesehen hab kann man die Hangneigung in Farbabstufungen anzeigen. 8. Und dann schau ich mir an, ob ich die Tour, die ich am morgigen Tag machen möchte, machen kann. 9. ...digitales Kartenwerk mit darübergelegten Geländeneigungskodierungen. 10. Für Österreich benutze ich die Bundesamtskarten und da hat sich digital am angenehmsten herausgestellt die Bergfex App.
Reduction Method	<ol style="list-style-type: none"> 1. Ich habe aber auch schon auf Skitourenguru zurückgegriffen, wenn es Touren sind die ich nicht kenne. 2. ...da dann auch Nord/Süd je nachdem, was im Detail dann für eine Hauptgefahr herrscht und lass das einfließen in die Wahl der Tour. 3. Und seit neuestem verwende ich auch dieses Skitourenguru, als begleitendes Instrument. 4. Ich schau welche sind die exponierten Hanglagen, welche Himmelsrichtungen. 5. ...dort heißt es genau lesen, zum einen gibt es die allgemeine Warnstufe die da immer vergeben wird, was mich aber auch interessiert sind die Nebensätze und auch das zu erwartende Wetter. 6. Entweder nach Munter mit der klassischen Risikoreduktion oder mit Stop-or-Go... 7. Dann schau ich wo sind kritische Stellen auf der Route. Wann erwartet man Tagesgang, wann muss man spätestens dort sein um nicht von der Nassschneeproblematik betroffen zu sein.
Weather Report	<ol style="list-style-type: none"> 1. ...Wetter war und in welche Himmelsrichtung es sich Lawinentechnisch bewegt 2. Windy oder da gibt es ja vom ZAMG diese SnowGrid Analyse und schau mal wo überhaupt eine schöne Schneemenge 3. ...Bergfex Wetter [...] Touren eher nur bei Schönwetter. 4. Dann schau ich mir das Wetter an, ... 5. Beim Wetter arbeite ich mit dem ZAMG Wetterbericht. 6. ...die ganze Saison über Schnee, Wind und Wetter in Beobachtung. 7. ...dass ich mir mal die Stationsdaten anschau. Von Wetterstationen wo man die Daten sieht wie Neuschnee, Temperaturverlauf in den letzten Tagen.

Reduction Methods	
Stop-or-Go	<ol style="list-style-type: none"> 1. Stop-or-Go kenne ich ein bisschen besser 2. Das Stop-or-Go ist mir ein Begriff. 3. Stop-or-Go ist aus Lawinenkurs bekannt ... 4. Natürlich, ich hab da [...] am meisten mit dem Stop-or-Go zu tun 5. Ja Stop-or-Go. 6. Ja, Stop-or-Go findet Anwendung
3x3	<ol style="list-style-type: none"> 1. Wenn ich unsicher bin, benutze ich auch mal das 3x3. Also wenn ich das Gefühl habe es ist grenzwertig, benutze ich gern das 3x3 um zu wissen wie grenzwertig es ist. 2. ... oder 3x3 in der Schweiz, es kommt eh immer das selbe heraus.
SnowCard	<ol style="list-style-type: none"> 1. Egal wie es heißt, ob es jetzt die SnowCard ist ... 2.SnowCard weiß ich dass existiert, die verwende ich aber nicht.

On-Site Checks	
Weather	<ol style="list-style-type: none"> 1. Ich schaue vor Ort ob das Wetter dem entspricht was der Wetterbericht vorhergesagt hat 2. Außer es ist dann so dass vor Ort ein Nebelbruch ist, das kannst du vielleicht nicht so vorhersagen. Dann würde ich es vielleicht nochmal abbrechen. Den Wetterbericht checke ich natürlich auch noch nicht nur den LLB. Damit ich sicher bin dass die Sicht okay ist und ich sicher bin dass ich nicht im Schneetreiben lande oder so. Das Bergwetter vom ORF ist da nicht so schlecht. 3. Dann den Wetterbericht und, immer wenn es sie gibt, auch die Stationsdaten ein paar Tage in die Vergangenheit. Wenn sich dann rausstellt es ist zu riskant dann wird man nicht hingehen.
High-Risk Areas	<ol style="list-style-type: none"> 1. ... ob ich irgendwelche Gefahrenzeichen sehe, also Triebsschnee, Windverwehungen, sowas. 2. Ich denk mir auch oft im Vorhinein schon das ist halt ein kurzes Stück. Wenn ein paar Meter dann sehr steil sind, dann denke ich mir fahre ich hin und schau es mir an, wenn es dann nicht geht fahre ich es nicht. 3. Den Aufstieg plane ich im Vorhinein detaillierter, in Bezug auf Sicherheit. Die Abfahrt überprüfe ich vor Ort genauer. 4. Und natürlich schaut man sich vor Ort dann die Verhältnisse an und entscheidet dann kurzfristig: fährt man vielleicht doch das oder vielleicht doch das nicht. 5. Ist die Tour grundsätzlich möglich und wo sind die riskanten Punkte. 6. Wenn man aber einen Grenzfall hat, wo es eine Stelle gibt, die potentiell riskant ist weil der Hang zu steil ist, dann ist das etwas das man vor Ort beurteilen müsste.

Information Content (positive)	
2D	3D
Da nehme ich lieber eine 2D Karte die mir die Höhenlinien und Farben für die Hangneigung einzeichnet.	Weil man von der Seite reinschauen kann, weil man es besser drehen kann und sofort erkennt ob es wo bergauf oder bergab geht. Weil man die Hangneigung schön sieht.
Weil es mehr Information beinhaltet für mich.	Also eigentlich hat mir die 3D besser gefallen weil das sieht man genau wo der Wald aufhört
Leichter tue ich mir mit den Höchenschichtlinien als das jetzt.	Dieses Zusammenspiel Lawinenwarnstufe mit Steilheit und einfärben finde ich eine coole Geschichte.
Ich mein gut auf einer 2D, wenn die Höchenschichtlinien dicht liegen, erkennt man auch die Hangneigung gut.	Wobei das 3D Bild ist schon interessant weil man das besser visualisiert hat als bei einer 2D Karte.
	Mit dem Einfärben vom umgebenden Gelände ist das sicher eine gute Zusatzinformation.
	Die 3D Geschichte macht schon was her, weil man wirklich visualisiert hat, wo Wiesen sind und wo Bäume stehen.
4	6
Information Content (negative)	
2D	3D
Ich fasse kurz zusammen: um planen zu können brauch man so viele Informationen wie möglich. Es hat in beiden Szenarien Information gefehlt, etwa Tourenbeschreibungen, die ja auch oft Information birgt.	Ich fasse kurz zusammen: um planen zu können brauch man so viele Informationen wie möglich. Es hat in beiden Szenarien Information gefehlt, etwa Tourenbeschreibungen, die ja auch oft Information birgt.
bei der anderen [2D] war ja kein Naturbild hinterlegt.	Was für mich ungewohnt ist sind diese Kartenbilder.
wo der Wald aufhört, das sieht man bei der anderen [2D] nicht wirklich.	Ich kann mir den Berg vorstellen, ich brauche ihn nicht visualisiert.
	Was mir aufgefallen ist, ist dass mir die Himmelsrichtung verloren geht.
3	4

Risk Encoding (positive)	
2D	3D
Viel leichter habe ich mir getan bei den Aufstellungen wo das Geländemodell mit Höhenlinien und die entsprechende Farbcodierung der Neigungen drinnen war.	Dass die Windrose komplett abgebildet ist und das Risiko je nach Exposition angepasst wird finde ich für uns heutzutage wo man sich eh nicht mehr anschauen will, sondern lieber die Information gleich sofort hat eine coole Geschichte.
Bei der ersten [2D] Karten hatte ich natürlich das Gefühl es wirkt für mich einfacher, weil ich weiß bei der Hangneigung muss ich aufpassen habe ich das Gefühl ich habe mehr Kontrolle oder habe das Gefühl mehr zu verstehen.	Grundsätzlich ist so eine Visualisierung schon cool. Ich bin halt jetzt was anders gewohnt.
Das Overlay mit der Hangneigung finde ich eigentlich sehr praktisch.	Ich würde den SnowCard-Layer zusätzlich verwenden. Wenn ich jetzt sehe hier ist eine Schlüsselstelle, dann würde ich die SnowCard drüberlegen.
	Wobei natürlich das mit der Risikobewertung so wie es der Skitourenguru auch macht eine Gewisse Sensibilität hervorruft. Dort sagt mir das Programm schon ich muss aufpassen dann schau ich halt besonders gut.
3	4
Risk Encoding (negative)	
2D	3D
	Ich zitieren nur den Günther Schudlach vom Skitourenguru, der die Befürchtung hat, dass durch seine Erfindung dann keiner mehr selber nachdenkt sondern nur noch: dort ist es rot, dort orange, dort grün und dann nicht mehr selber nachdenkt.
	Allerdings muss man dann immer zurückrechnen, um die Neigung schätzen zu können. Und so kann ich mit immer konstanter Farbcodierung mein Wissen anwenden.
0	2

Trust (positive)	
2D	3D
	Angenommen ich hätte beides zur Verfügung ich würde schon die 3D Karte bevorzugen. Weil mir von der Logik her klar ist dass ich da mehr Sicherheit bekomme.
	Ich bin relativ sicher, dass die 3D Kartenvisualisierung die die Warnstufe einbezieht, dass das sicher ist für mich und dass ich der Maschine mehr vertrauen sollte.
	Ich würde natürlich die 3D Darstellung bevorzugen, weil ich glaub, dass sie mehr Sicherheit bietet.
0	3
Trust (negative)	
2D	3D
Die 2D Version schaut einfacher aus aber es fehlen Informationen, man klammert sich dann an ein, zwei Sachen fest, die man intus hat.	Wenn ich nur nach diesen Risikobewertungen gehe, schalte ich irgendwann das Denken aus.
	Ja ich habe das Gefühl bei dem 3D Kartentyp, der sagt mir das ist es gefährlich, da ist es rot. Warum kann ich jetzt selbst nicht nachvollziehen. Das kann ich jetzt glauben oder nicht.
	Ich sehe das ein bisschen als Gefahr, als Tool ist es sehr cool aber für den Nutzer könnte es trügerisch sein wenn man sich hundertprozentig darauf verlässt und sagt das ist es weiß deswegen fahre ich da, ohne zu schauen.
	Das führt natürlich möglicherweise zu einer höheren Akzeptanz von Risiko.
	Wenn man immer nur ganz schnell reinschaut und dann blind dem System vertraut ist das auch nicht gut.
	Mir ist schon klar, dass ich dieser Visualisierung mehr vertrauen sollte aber vom Gefühl her sträube ich mich dagegen.
1	6